

Era of Big Data Processing: A New Approach via Tensor Networks and Tensor Decompositions

Andrzej CICHOCKI

RIKEN Brain Science Institute, Japan

and Systems Research Institute of the Polish Academy of Science, Poland

a.cichocki@riken.jp

Part of this work was presented on the International Workshop on Smart Info-Media Systems in Asia, (invited talk - SISA-2013) Sept.30–Oct.2, 2013, Nagoya, Japan

Abstract—Modern applications such as computational neuroscience, neuroinformatics and pattern/image recognition generate massive amounts of multidimensional data with multiple aspects and high dimensionality. Big data require novel technologies to efficiently process massive datasets within tolerable elapsed times. Such a new emerging technology for multidimensional big data is a multiway analysis via tensor networks (TNs) and tensor decompositions (TDs) which decompose tensors to sets of factor (component) matrices and low-order (core) tensors. Tensors (i.e., multiway arrays) provide a natural and compact representation for such massive multidimensional data via suitable low-rank approximations. Dynamic tensor analysis allows us to discover meaningful hidden structures of complex data and perform generalizations by capturing multi-linear and multi-aspect relationships. We will discuss some emerging TN models, their mathematical and graphical descriptions and associated learning algorithms for large-scale TDs and TNs, with many potential applications including: Anomaly detection, feature extraction, classification, cluster analysis, data fusion and integration, pattern recognition, predictive modeling, regression, time series analysis and multiway component analysis.

Keywords: Large-scale HOSVD, Hierarchical Tucker (HT) model, low-rank tensor approximations (LRA), tensor train (TT) decompositions, Matrix Product States (MPS), Matrix Product Operator (MPO), DMRG, Strong Kronecker Product (SKP) representation of tensor networks.

I. Introduction and Motivations

Big Data consists of multidimensional, multi-modal data-sets that are so huge and complex that they can not be easily stored or processed by using standard computers. Big data has not only big Volume but also another specific “V” features (see Fig. 1). High Volume implies the need for algorithms that are scalable; High Velocity address the challenges related to process data in near real-time, or virtually real-time; High Veracity demands robust and predictive algorithms for noisy, incomplete or inconsistent data, and finally, high Variety may require integration across different kind of data, e.g., neuroimages, time series, spiking trains, genetic and behavior data. Many challenging problems for big data

are related to capture, manage, search, visualize, cluster, classify, assimilate, merge, and process the data within a tolerable elapsed time, hence demanding new innovative solutions and technologies. Such emerging technology is Tensor Decompositions (TDs) and Tensor Networks (TNs) via low-rank matrix/tensor approximations. The challenge is how to analyze large-scale, multiway data sets. Data explosion creates deep research challenges that require new scalable, TD and TN algorithms.

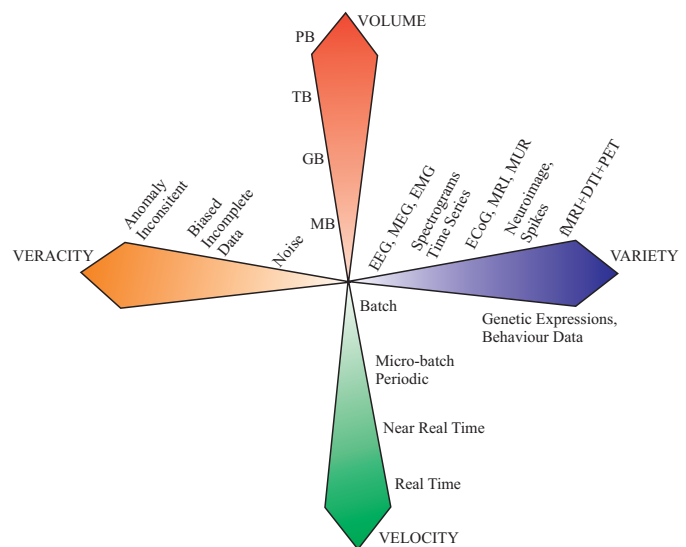


Figure 1: Illustration of Big Data analysis for neuroscience data, which involves analysis of multi-modal, multi-subjects neuroimages, spectrograms, time series, genetic and behavior data. Brain data are recorded by electroencephalography (EEG), electrocorticography (ECoG), magnetoencephalography (MEG), fMRI, DTI, PET, Multi Unit Recording (MUR). One of the challenge in computational and system neuroscience is to make fusion (assimilation) of such data and to understand the relationships among them for perception, cognition and human emotions. Four “V”s of big data: Volume - scale of data, Variety - different forms of data, Veracity - uncertainty of data, and Velocity - analysis of streaming data.

Tensors are adopted in diverse branches of science

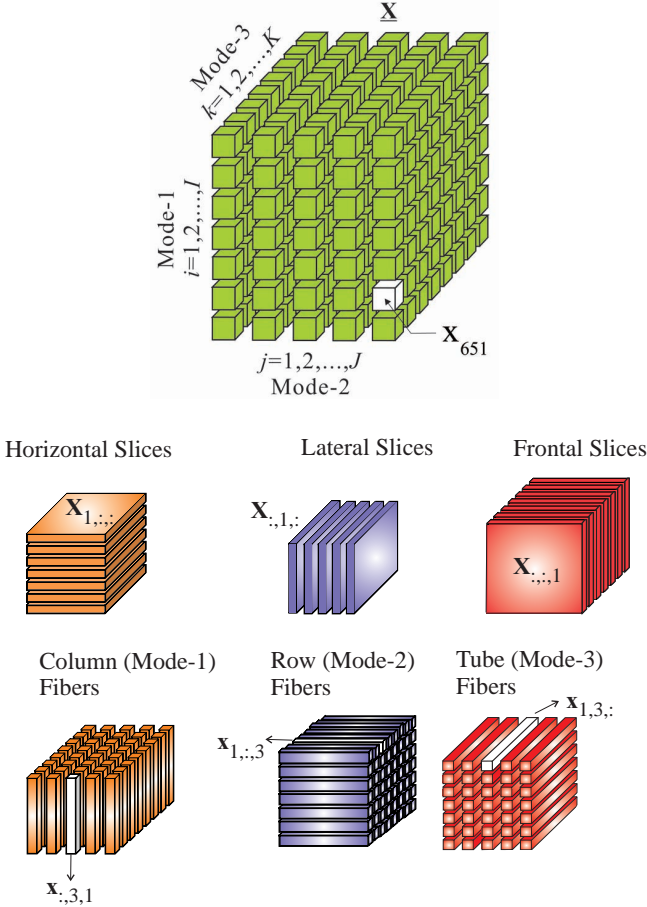


Figure 2: A 3rd-order tensor $\mathbf{X} \in \mathbb{R}^{I \times J \times K}$, with entries $x_{i,j,k} = \mathbf{X}(i,j,k)$ and its sub-tensors: Slices and fibers. All fibers are treated as column vectors.

data analysis such as signal and image processing [1]–[4], Psychometric, Chemometrics, Biometric, Quantum Physics/Information, and Quantum Chemistry [5]–[7]. Modern scientific areas such as bioinformatics or computational neuroscience generate massive amounts of data collected in various forms of large-scale, sparse tabulars, graphs or networks with multiple aspects and high dimensionality. Tensors, which are multi-dimensional generalizations of matrices (see Fig. 2 and Fig. 3), provide often a useful representation for such data. Tensor decompositions (TDs) decompose data tensors in factor matrices, while tensor networks (TNs) decompose higher-order tensors into lower-order tensors. We will show that TDs and TNs provide natural extensions of blind source separation (BSS) and 2-way (matrix) Component Analysis (2-way CA) to multi-way component analysis (MWCA) methods. TD and TN algorithms are suitable for dimensionality reduction and they can handle missing values, and noisy data. Moreover, they are potentially useful for analysis of linked (coupled) block of tensors with millions and even billions of non-zero entries, using the map-reduce paradigm, as well as out core approaches [8]–[10]. Furthermore, multidimensional data can often be represented by linked multi-

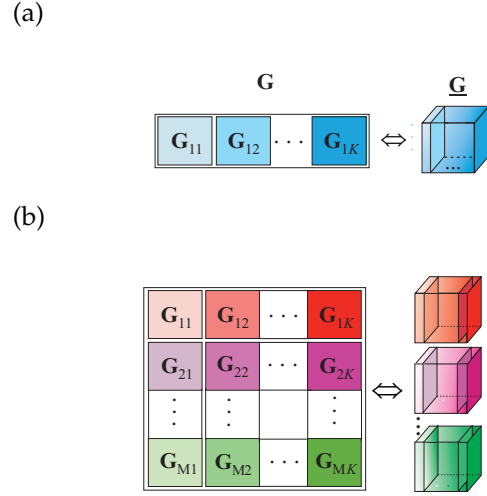


Figure 3: Block matrices and their representations by (a) a 3rd-order tensor and (b) a 4th-order tensor.

block tensors which can be decomposed to common (or correlated) and distinctive (uncorrelated) components. The effective analysis of coupled tensors requires the development of new models and associated algorithms that can identify the core relations that exist among the different tensor modes, and scale to extremely large datasets. Our motivation and objective is to develop suitable models and algorithms for linked low-rank tensor approximations (TAs), and associated scalable software to make such analysis possible.

Review and tutorial papers [2], [4], [11]–[13] and books [1], [5], [6] dealing with TDs already exist, however, they typically focus on standard TDs and/or do not provide explicit links to big data processing topics and do not explore natural connections with emerging areas including multi-block coupled tensor analysis and tensor networks. This paper extends beyond the standard TD models and aims to elucidate the power and flexibility of TNs in the analysis of multi-dimensional, multi-modal, and multi-block data, together with their role as a mathematical backbone for the discovery of hidden structures in large-scale data [1], [2], [4].

Motivations - Why low-rank tensor approximations?

A wealth of literature on (2-way) component analysis (CA) and BSS exists, especially on Principal Component Analysis (PCA), Independent Component Analysis (ICA), Sparse Component Analysis (SCA), Nonnegative Matrix Factorizations (NMF), and Morphological Component Analysis (MCA) [1], [14], [15]. These techniques are maturing, and are promising tools for blind source separation (BSS), dimensionality reduction, feature extraction, clustering, classification, and visualization [1], [15].

The “flattened view” provided by 2-way CA and matrix factorizations (PCA/SVD, NMF, SCA, MoCA) may be inappropriate for large classes of real-world data which exhibit multiple couplings and cross-correlations. In this context, higher-order tensor networks give us the

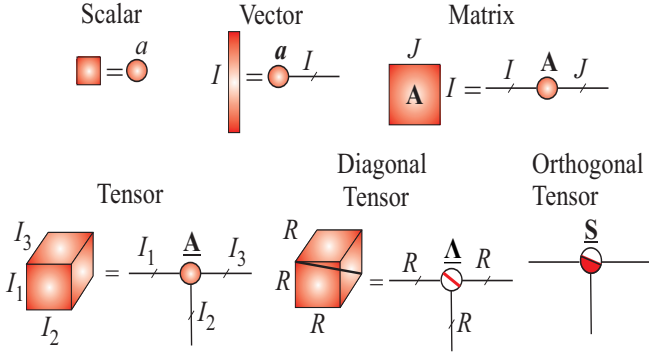


Figure 4: Basic symbols of tensor network diagrams.

TABLE I: Basic tensor notation and symbols. A tensor are denoted by underline bold capital letters, matrices by uppercase bold letters, vectors by lowercase boldface letters and scalars by lowercase letters.

$\underline{\mathbf{X}} \in \mathbb{R}^{I_1 \times I_2 \times \dots \times I_N}$	Nth-order tensor of size $I_1 \times I_2 \times \dots \times I_N$
$\underline{\mathbf{G}}, \underline{\mathbf{G}}_r, \underline{\mathbf{G}}_{\mathbf{X}}, \underline{\mathbf{G}}_{\mathbf{Y}}, \underline{\mathbf{S}}$	core tensors
$\underline{\mathbf{A}} \in \mathbb{R}^{R \times R \times \dots \times R}$	diagonal core tensor with nonzero λ_r entries on diagonal
$\mathbf{A} = [\mathbf{a}_1, \mathbf{a}_2, \dots, \mathbf{a}_R] \in \mathbb{R}^{I \times R}$	matrix with column vectors $\mathbf{a}_r \in \mathbb{R}^I$ and entries a_{ir}
$\mathbf{A}, \mathbf{B}, \mathbf{C}, \mathbf{B}^{(n)}, \mathbf{U}^{(n)}$	component matrices
$\mathbf{i} = [i_1, i_2, \dots, i_N]$	vector of indices
$\mathbf{X}_{(n)} \in \mathbb{R}^{I_n \times I_1 \dots I_{n-1} I_{n+1} \dots I_N}$	mode- n unfolding of $\underline{\mathbf{X}}$
$\mathbf{x}_{:,i_2,i_3,\dots,i_N}$	mode-1 fiber of $\underline{\mathbf{X}}$ obtained by fixing all but one index
$\mathbf{X}_{:,i_3,\dots,i_N}$	tensor slice of $\underline{\mathbf{X}}$ obtained by fixing all but two indices
$\underline{\mathbf{X}}_{:,i_3,i_4,\dots,i_N}$	subtensor of $\underline{\mathbf{X}}$ in which several indices are fixed
$\mathbf{x} = \text{vec}(\underline{\mathbf{X}})$	vectorization of $\underline{\mathbf{X}}$
$\text{diag}\{\bullet\}$	diagonal matrix

opportunity to develop more sophisticated models performing distributed computing and capturing multiple interactions and couplings, instead of standard pairwise interactions. In other words, to discover hidden components within multiway data the analysis tools should account for intrinsic multi-dimensional distributed patterns present in the data.

II. Basic Tensor Operations

A higher-order tensor can be interpreted as a multiway array, as illustrated graphically in Figs. 2, 3 and 4. Our adopted convenience is that tensors are denoted by bold

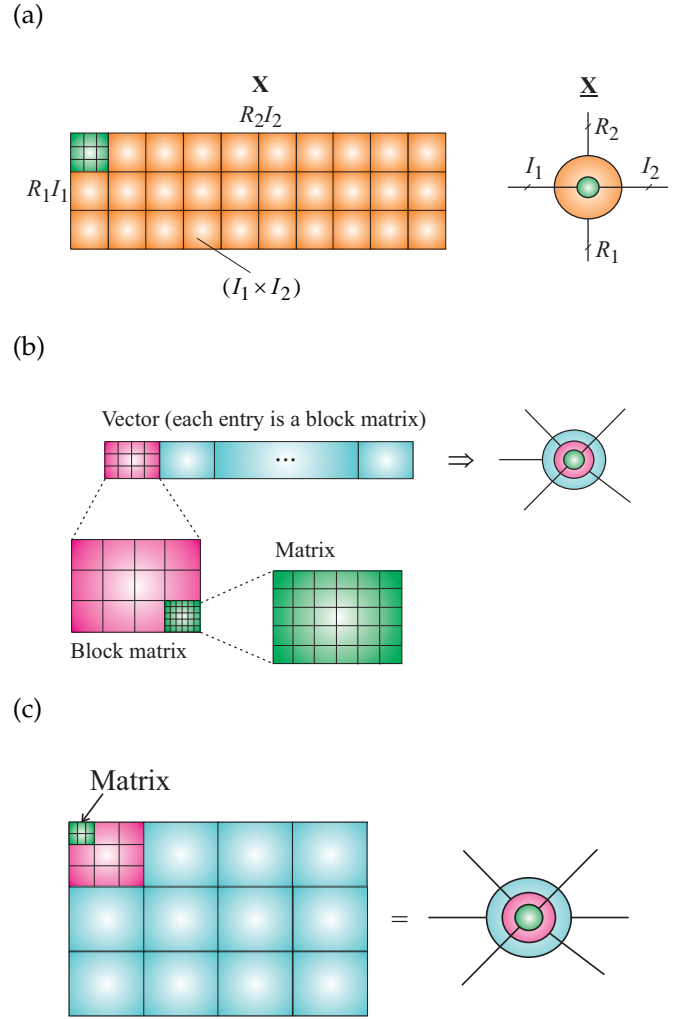


Figure 5: Hierarchical block matrices and their representations as tensors: (a) a 4th-order tensor for a block matrix $\underline{\mathbf{X}} \in \mathbb{R}^{R_1 I_1 \times R_2 I_2}$, with blocks matrices $\mathbf{X}_{r_1, r_2} \in \mathbb{R}^{I_1 \times I_2}$, (b) 5th-order tensor and (c) 6th-order tensor.

underlined capital letters, e.g., $\underline{\mathbf{X}} \in \mathbb{R}^{I_1 \times I_2 \times \dots \times I_N}$, and that all data are real-valued. The order of a tensor is the number of its “modes”, “ways” or “dimensions”, which can include space, time, frequency, trials, classes, and dictionaries. Matrices (2nd-order tensors) are denoted by boldface capital letters, e.g., \mathbf{X} , and vectors (1st-order tensors) by boldface lowercase letters; for instance the columns of the matrix $\mathbf{A} = [\mathbf{a}_1, \mathbf{a}_2, \dots, \mathbf{a}_R] \in \mathbb{R}^{I \times R}$ are denoted by \mathbf{a}_r and elements of a matrix (scalars) are denoted by lowercase letters, e.g., a_{ir} (see Table I).

TNs and TDs can be represented by tensor network diagrams in which tensors are represented graphically by nodes or any shapes (e.g., circles, spheres, triangular, squares, ellipses) and each outgoing edge (line) emerging from a shape represents a mode (a way, dimension, indices) (see Fig. 4) Tensor network diagrams are very helpful in visualizing tensor decompositions and their mathematical (multilinear) operations.

It should be noted that block matrices and hierarchical block matrices can be represented by tensors. For

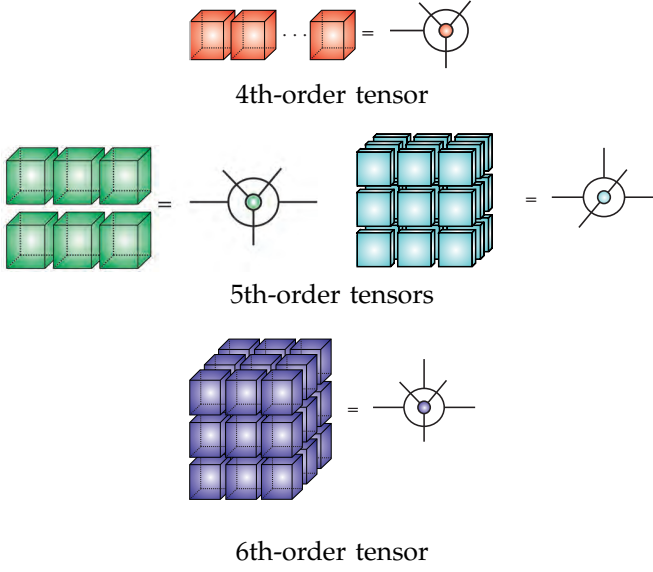


Figure 6: Graphical representations and symbols for higher-order block tensors. Each block represents a 3rd-order tensor or 2nd-order tensor.

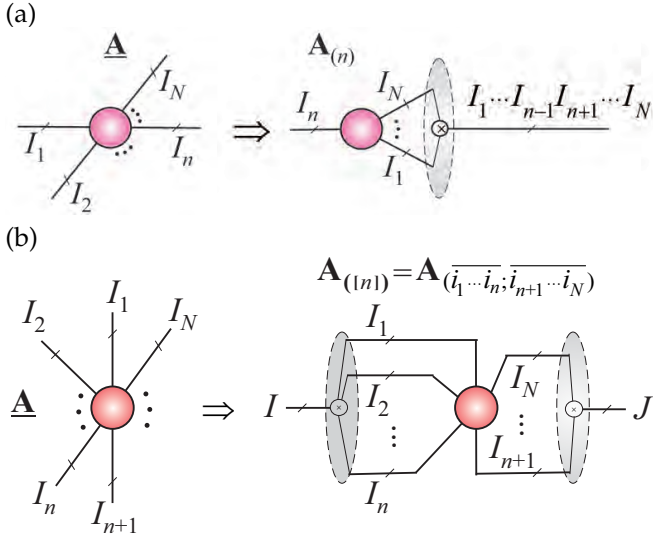


Figure 7: (a) Graphical representation of the basic mode- n unfolding (matricization, flattening) $\mathbf{A}_{(n)} \in \mathbb{R}^{I_n \times I_1 \times \dots \times I_{n-1} \times I_{n+1} \times \dots \times I_N}$ for an N th-order tensor $\mathbf{A} \in \mathbb{R}^{I_1 \times I_2 \times \dots \times I_N}$. (b) More general unfolding of the N th-order tensor into a matrix $\mathbf{A}_{([n])} = \mathbf{A}_{(\overline{i_1 \dots i_n}; \overline{i_{n+1} \dots i_N})} \in \mathbb{R}^{I_1 I_2 \dots I_n \times I_{n+1} \dots I_N}$. All entries of an unfolded tensor are arranged in a specific order, typically in a reverse lexicographical order. In more general case, let $\mathbf{r} = \{m_1, m_2, \dots, m_R\} \subset \{1, 2, \dots, N\}$ be the row indices and $\mathbf{c} = \{n_1, n_2, \dots, n_C\} \subset \{1, 2, \dots, N\} - \mathbf{r}$ be the column indices, then the mode- (\mathbf{r}, \mathbf{c}) unfolding of \mathbf{A} is denoted as $\mathbf{A}_{(\mathbf{r}, \mathbf{c})} \in \mathbb{R}^{I_{m_1} I_{m_2} \dots I_{m_R} \times I_{n_1} I_{n_2} \dots I_{n_C}}$.

example, 3rd-order and 4th-order tensors that can be represented by block matrices as illustrated on Fig. 3 and all algebraic operations can be performed on block matrices. Analogously, higher-order tensors can be represented as illustrated in Fig. 5 and Fig. 6. Subtensors are formed when a subset of indices is fixed. Of particular interest are *fibers*, defined by fixing every index but

TABLE II: Basic tensor/matrix operations.

$\underline{\mathbf{C}} = \underline{\mathbf{A}} \times_n \mathbf{B}$	mode- n product of $\underline{\mathbf{A}} \in \mathbb{R}^{I_1 \times I_2 \times \dots \times I_N}$ and $\mathbf{B} \in \mathbb{R}^{J_n \times I_n}$ yields $\underline{\mathbf{C}} \in \mathbb{R}^{I_1 \times \dots \times I_{n-1} \times J_n \times I_{n+1} \times \dots \times I_N}$, with entries $c_{i_1, \dots, i_{n-1}, j, i_{n+1}, \dots, i_N} = \sum_{i_n=1}^{I_n} a_{i_1, \dots, i_{n-1}, i_n, i_{n+1}, \dots, i_N} b_{j, i_n}$, or equivalently $\mathbf{C}_{(n)} = \mathbf{B} \mathbf{A}_{(n)}$
$\underline{\mathbf{C}} = \llbracket \underline{\mathbf{A}}; \mathbf{B}^{(1)}, \dots, \mathbf{B}^{(N)} \rrbracket = ((\underline{\mathbf{A}} \times_1 \mathbf{B}^{(1)}) \times_2 \mathbf{B}^{(2)}) \times_3 \dots \times_N \mathbf{B}^{(N)}$	
$\underline{\mathbf{C}} = \underline{\mathbf{A}} \circ \underline{\mathbf{B}}$	tensor or outer product of $\underline{\mathbf{A}} \in \mathbb{R}^{I_1 \times I_2 \times \dots \times I_N}$ and $\underline{\mathbf{B}} \in \mathbb{R}^{J_1 \times J_2 \times \dots \times J_M}$ yields $(N+M)$ th-order tensor $\underline{\mathbf{C}}$, with entries $c_{i_1, \dots, i_N, j_1, \dots, j_M} = a_{i_1, \dots, i_N} b_{j_1, \dots, j_M}$
$\mathbf{X} = \mathbf{a} \circ \mathbf{b} \circ \mathbf{c} \in \mathbb{R}^{I \times J \times K}$	tensor or outer product of vectors forms a rank-1 tensor with entries $x_{ijk} = a_i b_j c_k$
$\mathbf{A}^T, \mathbf{A}^{-1}, \mathbf{A}^\dagger$	transpose, inverse and Moore-Penrose pseudo-inverse of \mathbf{A}
$\underline{\mathbf{C}} = \underline{\mathbf{A}} \otimes \underline{\mathbf{B}}$	Kronecker product of $\underline{\mathbf{A}} \in \mathbb{R}^{I_1 \times I_2 \times \dots \times I_N}$ and $\underline{\mathbf{B}} \in \mathbb{R}^{J_1 \times J_2 \times \dots \times J_N}$ yields $\underline{\mathbf{C}} \in \mathbb{R}^{I_1 J_1 \times \dots \times I_N J_N}$, with entries $c_{i_1 \otimes j_1, \dots, i_N \otimes j_N} = a_{i_1, \dots, i_N} b_{j_1, \dots, j_N}$, where $i_n \otimes j_n = j_n + (i_n - 1)J_n$
$\mathbf{C} = \mathbf{A} \odot \mathbf{B}$	Khatri-Rao product of $\mathbf{A} \in \mathbb{R}^{I \times J}$ and $\mathbf{B} \in \mathbb{R}^{K \times J}$, with $\mathbf{c}_j = \mathbf{a}_j \otimes \mathbf{b}_j$

one, and *tensor slices* which are two-dimensional sections (matrices) of a tensor, obtained by fixing all the indices but two (see Fig. 2). A matrix has two modes: rows and columns, while an N th-order tensor has N modes.

The process of unfolding (see Fig. 7) flattens a tensor into a matrix. In the simplest scenario, mode- n unfolding (matricization, flattening) of the tensor $\underline{\mathbf{A}} \in \mathbb{R}^{I_1 \times I_2 \times \dots \times I_N}$ yields a matrix $\mathbf{A}_{(n)} \in \mathbb{R}^{I_n \times (I_1 \times \dots \times I_{n-1} \times I_{n+1} \times \dots \times I_N)}$, with entries $a_{i_n, (j_1, \dots, j_{n-1}, j_{n+1}, \dots, j_N)}$ such that remaining indices $(i_1, \dots, i_{n-1}, i_{n+1}, \dots, i_N)$ are arranged in a specific order, e.g., in a reverse lexicographical order [4]. In tensor networks we use, typically a generalized mode- $([n])$ unfolding as illustrated in Fig. 7 (b).

By a multi-index $i = \overline{i_1, i_2, \dots, i_N}$ we denote an index which takes all possible combination of values of i_1, i_2, \dots, i_N , for $i_n = 1, 2, \dots, I_n$ we have $\overline{i_1, i_2, \dots, i_N} = i_1 + (i_2 - 1)I_1 + \dots + (i_N - 1)I_1 I_2 \dots I_{N-1}$.

The most common types of tensor multiplications are denoted by: \otimes for the Kronecker, \odot for the Khatri-Rao, \circledast for the Hadamard (componentwise), \circ for the outer and \times_n for the mode- n products (see Table II).

The mode- n product of a tensor $\underline{\mathbf{A}} \in \mathbb{R}^{I_1 \times \dots \times I_N}$ by a vector $\mathbf{b} \in \mathbb{R}^{I_n}$ is defined as a tensor $\underline{\mathbf{C}} = \underline{\mathbf{A}} \times_n \mathbf{b}^T \in \mathbb{R}^{I_1 \times \dots \times I_{n-1} \times I_{n+1} \times \dots \times I_N}$, with entries $c_{i_1, \dots, i_{n-1}, i_{n+1}, \dots, i_N} = \sum_{i_n=1}^{I_n} (a_{i_1, i_2, \dots, i_N}) b_{i_n}$, while a mode- n product of the

tensor $\underline{\mathbf{A}} \in \mathbb{R}^{I_1 \times \dots \times I_N}$ by a matrix $\mathbf{B} \in \mathbb{R}^{J \times I_n}$ is the tensor $\underline{\mathbf{C}} = \underline{\mathbf{A}} \times_n \mathbf{B} \in \mathbb{R}^{I_1 \times \dots \times I_{n-1} \times J \times I_{n+1} \times \dots \times I_N}$, with entries $c_{i_1, i_2, \dots, i_{n-1}, j, i_{n+1}, \dots, i_N} = \sum_{i_n=1}^{I_n} a_{i_1, i_2, \dots, i_n} b_{j, i_n}$. This can also be expressed in a matrix form as $\mathbf{C}_{(n)} = \mathbf{B} \mathbf{A}_{(n)}$ (see Fig. 8), which allows to employ fast matrix by vector and matrix by matrix multiplications for very large scale problems.

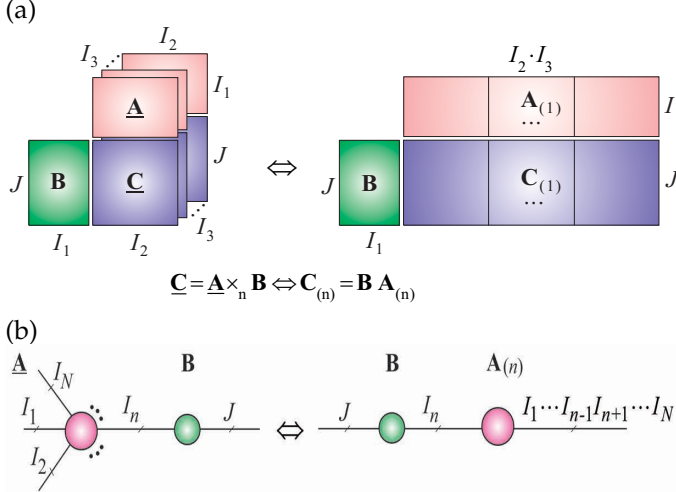


Figure 8: (a) Multilinear mode-1 product of a 3rd-order tensor $\underline{\mathbf{A}} \in \mathbb{R}^{I_1 \times I_2 \times I_3}$ and a factor (component) matrix $\mathbf{B} \in \mathbb{R}^{J \times I_1}$ yields a tensor $\underline{\mathbf{C}} = \underline{\mathbf{A}} \times_1 \mathbf{B} \in \mathbb{R}^{J \times I_2 \times I_3}$. This is equivalent to simple matrix multiplication formula $\mathbf{C}_{(1)} = \mathbf{B} \mathbf{A}_{(1)}$. (b) Multilinear mode- n product an N th-order tensor and a factor matrix $\mathbf{B} \in \mathbb{R}^{J \times I_n}$.

If we take all the modes, then we have a full multilinear product of a tensor and a set of matrices is compactly written as [4] (see Fig. 9 (a)):

$$\begin{aligned} \underline{\mathbf{C}} &= \underline{\mathbf{G}} \times_1 \mathbf{B}^{(1)} \times_2 \mathbf{B}^{(2)} \dots \times_N \mathbf{B}^{(N)} \\ &= \llbracket \underline{\mathbf{G}}; \mathbf{B}^{(1)}, \mathbf{B}^{(2)}, \dots, \mathbf{B}^{(N)} \rrbracket. \end{aligned} \quad (1)$$

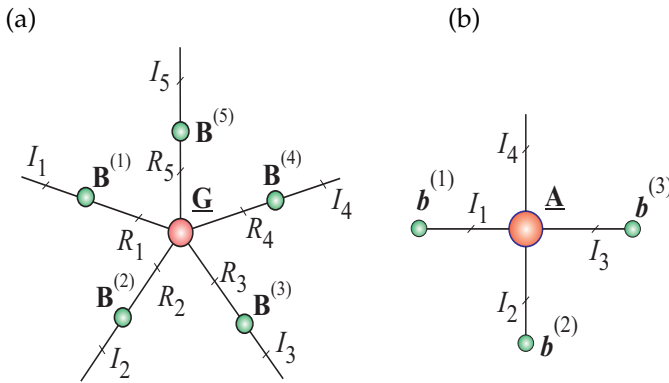


Figure 9: (a) Multilinear full product of tensor (Tucker decomposition) $\underline{\mathbf{G}} \in \mathbb{R}^{R_1 \times R_2 \times \dots \times R_5}$ and factor (component) matrices $\mathbf{B}^{(n)} \in \mathbb{R}^{I_n \times R_n}$ ($n = 1, 2, \dots, 5$) yields the Tucker tensor decomposition $\underline{\mathbf{C}} = \underline{\mathbf{G}} \times_1 \mathbf{B}^{(1)} \times_2 \mathbf{B}^{(2)} \times_3 \dots \times_5 \mathbf{B}^{(5)} \in \mathbb{R}^{I_1 \times I_2 \times \dots \times I_5}$. (b) Multilinear product of tensor $\underline{\mathbf{A}} \in \mathbb{R}^{I_1 \times I_2 \times \dots \times I_4}$ and vectors $\mathbf{b}_n \in \mathbb{R}^{I_n}$ ($n = 1, 2, 3$) yields a vector $\mathbf{c} = \underline{\mathbf{A}} \times_1 \mathbf{b}^{(1)T} \times_2 \mathbf{b}^{(2)T} \times_3 \mathbf{b}^{(3)T} \in \mathbb{R}^{I_4}$.

In a similar way to mode- n multilinear product, we can define the mode- $(\overset{m}{n})$ product of two

tensors (tensor contraction) $\underline{\mathbf{A}} \in \mathbb{R}^{I_1 \times I_2 \times \dots \times I_N}$ and $\underline{\mathbf{B}} \in \mathbb{R}^{I_1 \times I_2 \times \dots \times I_M}$, with common modes $I_n = I_m$ that produces a $(N + M - 2)$ -order tensor $\underline{\mathbf{C}} \in \mathbb{R}^{I_1 \times \dots \times I_{n-1} \times I_{n+1} \times \dots \times I_N \times I_1 \times \dots \times I_{m-1} \times I_{m+1} \times \dots \times I_M}$:

$$\underline{\mathbf{C}} = \underline{\mathbf{A}} \times_n^m \underline{\mathbf{B}}, \quad (2)$$

with entries $c_{i_1, \dots, i_{n-1}, i_{n+1}, \dots, i_N, j_1, \dots, j_{m-1}, j_{m+1}, \dots, j_M} = \sum_{i_n=1}^{I_n} a_{i_1, \dots, i_{n-1}, i_n, i_{n+1}, \dots, i_N} b_{j_1, \dots, j_{m-1}, i_n, j_{m+1}, \dots, j_M}$ (see Fig. 10 (a)). If not confused a super- or sub-index m, n can be neglected. For example, the multilinear product of the tensors $\underline{\mathbf{A}} \in \mathbb{R}^{I_1 \times I_2 \times \dots \times I_N}$ and $\underline{\mathbf{B}} \in \mathbb{R}^{I_1 \times I_2 \times \dots \times I_M}$, with a common modes $I_1 = I_2$ can be written as

$$\underline{\mathbf{C}} = \underline{\mathbf{A}} \times_1^2 \underline{\mathbf{B}} = \underline{\mathbf{A}} \times_2^2 \underline{\mathbf{B}} \in \mathbb{R}^{I_2 \times I_3 \times \dots \times I_N \times I_1 \times I_3 \times \dots \times I_M}, \quad (3)$$

with entries: $c_{i_2, i_3, \dots, i_N, j_1, j_3, \dots, j_M} = \sum_{i_1=1}^{I_1} a_{i_1, i_2, \dots, i_N} b_{j_1, i_2, j_3, \dots, j_M}$.

This operation can be considered as a contraction of two tensors in single common mode. Tensors can be contracted in several modes or even in all modes as illustrated in Fig. 10.

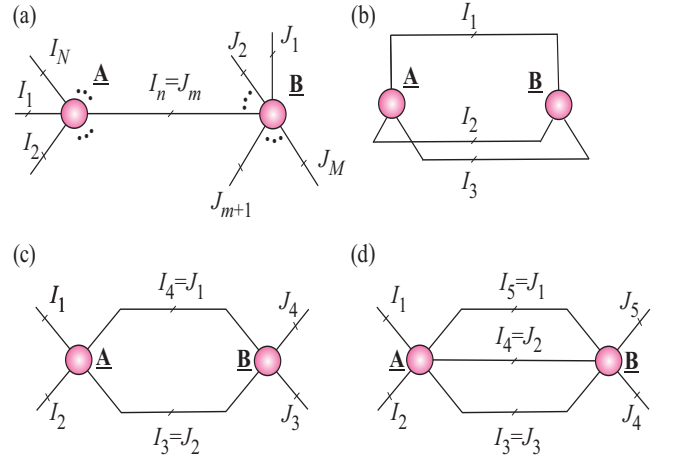


Figure 10: Examples of tensor contractions: (a) Multilinear product of two tensors is denoted as $\underline{\mathbf{C}} = \underline{\mathbf{A}} \times_n^m \underline{\mathbf{B}}$. (b) Inner product of two 3rd-order tensors yields $c = \langle \underline{\mathbf{A}}, \underline{\mathbf{B}} \rangle = \underline{\mathbf{A}} \times_{1,2,3}^{1,2,3} \underline{\mathbf{B}} = \underline{\mathbf{A}} \times \underline{\mathbf{B}} = \sum_{i_1, i_2, i_3} a_{i_1, i_2, i_3} b_{i_1, i_2, i_3}$. (c) Tensor contraction of two 4th-order tensors yields $\underline{\mathbf{C}} = \underline{\mathbf{A}} \times_{4,3}^{1,2} \underline{\mathbf{B}} \in \mathbb{R}^{I_1 \times I_2 \times I_3 \times I_4}$, with entries $c_{i_1, i_2, j_3, j_4} = \sum_{i_3, i_4} a_{i_1, i_2, i_3, i_4} b_{i_4, i_3, j_3, j_4}$. (d) Tensor contraction of two 5th-order tensors yields 4th-order tensor $\underline{\mathbf{C}} = \underline{\mathbf{A}} \times_{3,4,5}^{1,2,3} \underline{\mathbf{B}} \in \mathbb{R}^{I_1 \times I_2 \times I_4 \times I_5}$, with entries $c_{i_1, i_2, j_4, j_5} = \sum_{i_3, i_4, i_5} a_{i_1, i_2, i_3, i_4, i_5} b_{i_5, i_4, i_3, j_4, j_5}$.

Remark: If we use contraction for more than two tensors the order has to be specified (defined) as follows: $\underline{\mathbf{A}} \times_a^b \underline{\mathbf{B}} \times_c^d \underline{\mathbf{C}} = \underline{\mathbf{A}} \times_a^b (\underline{\mathbf{B}} \times_c^d \underline{\mathbf{C}})$ for $b < c$. Note that for multiplications of matrices and vectors this notation implies that $\mathbf{A} \times_1^2 \mathbf{B} = \mathbf{A} \mathbf{B}$, $\mathbf{A} \times_2^2 \mathbf{B} = \mathbf{A} \mathbf{B}^T$, $\mathbf{A} \times_{1,2}^{1,2} \mathbf{B} = \langle \mathbf{A}, \mathbf{B} \rangle$, and $\mathbf{A} \times_1^1 \mathbf{x} = \mathbf{A} \times_2 \mathbf{x} = \mathbf{A} \mathbf{x}$.

The outer or tensor product $\underline{\mathbf{C}} = \underline{\mathbf{A}} \circ \underline{\mathbf{B}}$ of the tensors $\underline{\mathbf{A}} \in \mathbb{R}^{I_1 \times \dots \times I_N}$ and $\underline{\mathbf{B}} \in \mathbb{R}^{J_1 \times \dots \times J_M}$ is the tensor $\underline{\mathbf{C}} \in \mathbb{R}^{I_1 \times \dots \times I_N \times J_1 \times \dots \times J_M}$, with entries $c_{i_1, \dots, i_N, j_1, \dots, j_M} = a_{i_1, \dots, i_N} b_{j_1, \dots, j_M}$. Specifically, the outer product of two nonzero vectors $\mathbf{a} \in \mathbb{R}^I$, $\mathbf{b} \in \mathbb{R}^J$ produces a rank-1 matrix $\mathbf{X} = \mathbf{a} \circ \mathbf{b} = \mathbf{a} \mathbf{b}^T \in \mathbb{R}^{I \times J}$ and the outer product of three nonzero vectors: $\mathbf{a} \in \mathbb{R}^I$, $\mathbf{b} \in \mathbb{R}^J$

and $c \in \mathbb{R}^K$ produces a 3rd-order rank-1 tensor: $\underline{\mathbf{X}} = \mathbf{a} \circ \mathbf{b} \circ \mathbf{c} \in \mathbb{R}^{I \times J \times K}$, whose entries are $x_{ijk} = a_i b_j c_k$. A tensor $\underline{\mathbf{X}} \in \mathbb{R}^{I_1 \times I_2 \times \dots \times I_N}$ is said to be rank-1 if it can be expressed exactly as $\underline{\mathbf{X}} = \mathbf{b}_1 \circ \mathbf{b}_2 \circ \dots \circ \mathbf{b}_N$, with entries $x_{i_1, i_2, \dots, i_N} = b_{i_1} b_{i_2} \dots b_{i_N}$, where $\mathbf{b}_n \in \mathbb{R}^{I_n}$ are nonzero vectors. We refer to [1], [4] for more detail regarding the basic notations and tensor operations.

III. Tensor Networks

A tensor network aims to decompose a higher-order tensor into a set of lower-order tensors (typically, 2nd (matrices) and 3rd-order tensors called cores or components) which are sparsely interconnected. In other words, in the contrast to TDs, TNs decompose the data tensors not only into factor matrices but rather into other low-order tensors. Recently, the curse of dimensionality for higher-order tensors has been considerably alleviated or even completely avoided through the concept of tensor networks (TN) [16], [17]. A TN can be represented by a set of shapes or nodes interconnected by lines. The lines (leads, branches, edges) connecting tensors between each other correspond to contracted modes, whereas lines that do not go from one tensor to another correspond to open (physical) modes in the TN (see Fig. 11).

An edge connecting two nodes indicates a contraction of the respective tensors in the associated pair of modes as illustrated in Fig. 10. In contrast to classical graphs in tensor network diagrams do not need connect two nodes, but may be connected to only one node. Each such free (dangling) edge corresponds to a mode, that is not contracted and, hence, the order of the entire tensor network is given by the number of free edges (called often physical indices). A tensor network may not contain any loops, i.e., any edges connecting a node with itself. Some examples of tensor network diagrams are given in Fig. 11.

If a tensor network is a tree, i.e., it does not contain any cycle, each of its edges splits the modes of the data tensor into two groups, which is related to the suitable matricization of the tensor. If, in such a tree tensor network, all nodes have degree 3 or less, it corresponds to an Hierarchical Tucker (HT) decomposition shown in Fig. 11 and Fig. 12 (a). The HT decomposition has been first introduced in scientific computing by Hackbush and Kuhn and further developed by Grasedyck, Kressner and Tobler [7], [18]–[20]. Note that for 6th-order, there are 2 such tensor networks (see Fig. 12 (b)), and for 10th-order there are 11 possible HT decompositions [18].

A simple approach to reduce the size of core tensors is to apply distributed tensor networks (DTNs), which consists in two kinds of cores (nodes): Internal cores (nodes) which have no free edges and external cores (nodes) which have free edges representing physical indices of a data tensor as illustrated in Figs. 12 and 13. The main idea in the case of the Tucker model, is that a core tensor is replaced by distributed sparsely interconnected cores of lower-order, resulting in Hierarchical Tucker

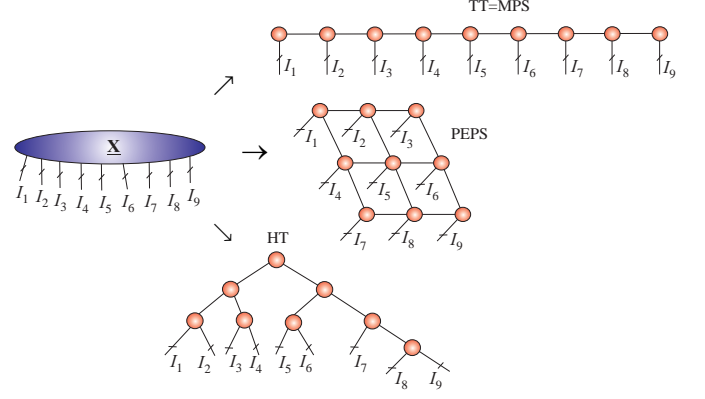


Figure 11: Examples of tensor networks. Illustration of decomposition of 9th-order tensor $\underline{\mathbf{X}} \in \mathbb{R}^{I_1 \times I_2 \times \dots \times I_9}$ into different kinds of tensor networks (TNs): Tensor Train (TT) which is equivalent to the Matrix Product State (MPS) (with open boundary conditions (OBC)), the Projected Entangled-Pair State (PEPS) called also Tensor Product States (TPS) and Hierarchical Tucker (HT) decomposition, which equivalent to the Tree-Tensor Network State (TTNS). In general, the objective is to decompose a high-order tensor into sparsely connected low-order and low-rank tensors, typically, 2nd-order, 3rd-order and/or 4th-order tensors, called cores.

(HT) network in which only some cores are connected (associated) directly with factor matrices [7], [19], [20].

For some very high-order data tensors it has been observed that the sizes R_n (dimensions) of cores increase rapidly with the order of the tensor and/or increasing accuracy of approximation for any choice of tensor network, that is, a tree (including TT and HT decompositions) [18]. For such cases, the Projected Entangled-Pair State (PEPS) or the Multi-scale Entanglement Renormalization Ansatz (MERA) tensor networks can be used which contains cycles, but have hierarchical structures (see Fig. 13). For the PEPS and MERA TNs the ranks can be kept considerably smaller, at the cost of employing 5th and 4th-order cores and consequently a higher computational complexity w.r.t. tensor contractions. The main advantage of PEPS and MERA is that the size of each core tensor in the internal tensor network structure is usually much smaller than the cores in TT/HT decompositions, so consequently the total number of parameters can be reduced. However, it should be noted that the contraction of the resulting tensor network becomes more difficult when compared to the basic tree structures represented by TT and HT models. This is due to the fact that the PEPS and MERA tensor networks contain loops.

IV. Basic Tensor Decompositions and their Representation via Tensor Networks Diagrams

The main objective of tensor decomposition is to decompose a data tensor into physically interpretable or meaningful factor matrices and a single core tensor which indicate links between components (vectors of factor matrices) in different modes.

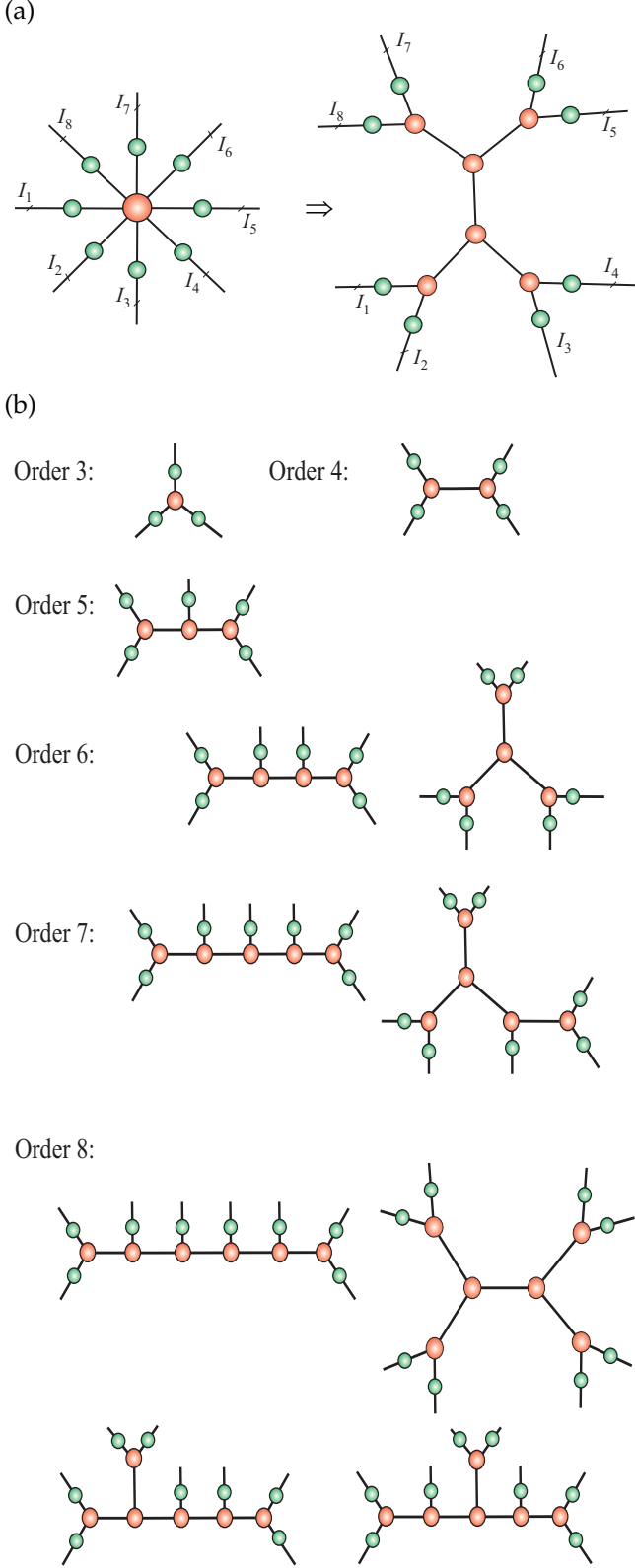


Figure 12: (a) The standard Tucker decomposition and its transformation into Hierarchical Tucker (HT) model for 8th-order tensor using interconnected 3rd-order core tensors. (b) Various exemplary structure HT/TT models for different order of data tensors. Green circles indicate factor matrices while red circles indicate cores.

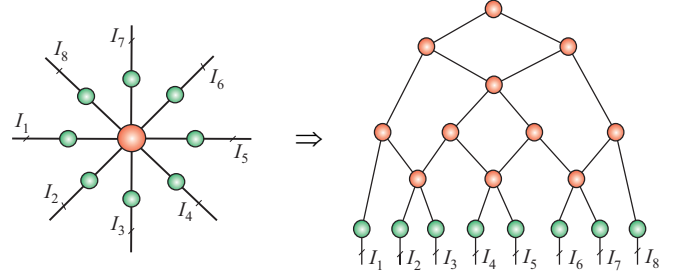


Figure 13: Alternative distributed representation of 8th-order Tucker decomposition where a core tensor is replaced by MERA (Multi-scale Entanglement Renormalization Ansatz) tensor network which employs 3rd-order and 4th-order core tensors. For some data-sets, the advantage of such model is relatively low size (dimensions) of the distributed cores.

A. Constrained Matrix Factorizations and Decompositions – Two-Way Component Analysis

Two-way Component Analysis (2-way CA) exploits *a priori* knowledge about different characteristics, features or morphology of components (or source signals) [1], [21] to find the hidden components thorough constrained matrix factorizations of the form

$$\mathbf{X} = \mathbf{A}\mathbf{B}^T + \mathbf{E} = \sum_{r=1}^R \mathbf{a}_r \circ \mathbf{b}_r + \mathbf{E} = \sum_{r=1}^R \mathbf{a}_r \mathbf{b}_r^T + \mathbf{E}, \quad (4)$$

where the constraints imposed on factor matrices \mathbf{A} and/or \mathbf{B} include orthogonality, sparsity, statistical independence, nonnegativity or smoothness. The CA can be considered as a bilinear (2-way) factorization, where $\mathbf{X} \in \mathbb{R}^{I \times J}$ is a known matrix of observed data, $\mathbf{E} \in \mathbb{R}^{I \times J}$ represents residuals or noise, $\mathbf{A} = [\mathbf{a}_1, \mathbf{a}_2, \dots, \mathbf{a}_R] \in \mathbb{R}^{I \times R}$ is the unknown (usually full column rank) mixing matrix with R basis vectors $\mathbf{a}_r \in \mathbb{R}^I$, and $\mathbf{B} = [\mathbf{b}_1, \mathbf{b}_2, \dots, \mathbf{b}_R] \in \mathbb{R}^{J \times R}$ is the matrix of unknown components (factors, latent variables, sources).

Two-way component analysis (CA) refers to a class of signal processing techniques that decompose or encode superimposed or mixed signals into components with certain constraints or properties. The CA methods exploit *a priori* knowledge about the true nature or diversities of latent variables. By diversity, we refer to different characteristics, features or morphology of sources or hidden latent variables [21].

For example, the columns of the matrix \mathbf{B} that represent different data sources should be: as statistically independent as possible for ICA; as sparse as possible for SCA; take only nonnegative values for (NMF) [1], [14], [21].

Remark: Note that matrix factorizations have an inherent symmetry, Eq. (4) could be written as $\mathbf{X}^T \approx \mathbf{B}\mathbf{A}^T$, thus interchanging the roles of sources and mixing process.

Singular value decomposition (SVD) of the data matrix $\mathbf{X} \in \mathbb{R}^{I \times J}$ is a special case of the factorization in Eq. (4). It is exact and provides an explicit notion of the range and null space of the matrix \mathbf{X} (key issues in low-rank

approximation), and is given by

$$\mathbf{X} = \mathbf{U}\mathbf{\Sigma}\mathbf{V}^T = \sum_{r=1}^R \sigma_r \mathbf{u}_r \mathbf{v}_r^T = \sum_{r=1}^R \sigma_r \mathbf{u}_r \circ \mathbf{v}_r, \quad (5)$$

where \mathbf{U} and \mathbf{V} are column-wise orthonormal matrices and $\mathbf{\Sigma}$ is a diagonal matrix containing only nonnegative singular values σ_r .

Another virtue of component analysis comes from a representation of multiple-subject, multiple-task datasets by a set of data matrices \mathbf{X}_k , allowing us to perform simultaneous matrix factorizations:

$$\mathbf{X}_k \approx \mathbf{A}_k \mathbf{B}_k^T, \quad (k = 1, 2, \dots, K), \quad (6)$$

subject to various constraints. In the case of statistical independence constraints, the problem can be related to models of group ICA through suitable pre-processing, dimensionality reduction and post-processing procedures [22].

The field of CA is maturing and has generated efficient algorithms for 2-way component analysis (especially, for sparse/functional PCA/SVD, ICA, NMF and SCA) [1], [14], [23]. The rapidly emerging field of tensor decompositions is the next important step that naturally generalizes 2-way CA/BSS algorithms and paradigms. We proceed to show how constrained matrix factorizations and component analysis (CA) models can be naturally generalized to multilinear models using constrained tensor decompositions, such as the Canonical Polyadic Decomposition (CPD) and Tucker models, as illustrated in Figs. 14 and 15.

B. The Canonical Polyadic Decomposition (CPD)

The CPD (called also PARAFAC or CANDECOMP) factorizes an N th-order tensor $\mathbf{X} \in \mathbb{R}^{I_1 \times I_2 \times \dots \times I_N}$ into a linear combination of terms $\mathbf{b}_r^{(1)} \circ \mathbf{b}_r^{(2)} \circ \dots \circ \mathbf{b}_r^{(N)}$, which are rank-1 tensors, and is given by [24]–[26]

$$\begin{aligned} \mathbf{X} &\cong \sum_{r=1}^R \lambda_r \mathbf{b}_r^{(1)} \circ \mathbf{b}_r^{(2)} \circ \dots \circ \mathbf{b}_r^{(N)} \\ &= \underline{\mathbf{A}} \times_1 \mathbf{B}^{(1)} \times_2 \mathbf{B}^{(2)} \dots \times_N \mathbf{B}^{(N)} \\ &= \llbracket \underline{\mathbf{A}}; \mathbf{B}^{(1)}, \mathbf{B}^{(2)}, \dots, \mathbf{B}^{(N)} \rrbracket, \end{aligned} \quad (7)$$

where the only non-zero entries λ_r of the diagonal core tensor $\underline{\mathbf{G}} = \underline{\mathbf{A}} \in \mathbb{R}^{R \times R \times \dots \times R}$ are located on the main diagonal (see Fig. 14 for a 3rd-order and 4th-order tensors). Via the Khatri-Rao products the CPD can also be expressed in a matrix/vector form as:

$$\mathbf{X}_{(n)} \cong \mathbf{B}^{(n)} \mathbf{\Lambda} (\mathbf{B}^{(N)} \circ \dots \circ \mathbf{B}^{(n+1)} \circ \mathbf{B}^{(n-1)} \circ \dots \circ \mathbf{B}^{(1)})^T$$

$$\text{vec}(\mathbf{X}) \cong [\mathbf{B}^{(N)} \circ \mathbf{B}^{(N-1)} \circ \dots \circ \mathbf{B}^{(1)}] \boldsymbol{\lambda}, \quad (8)$$

where $\mathbf{B}^{(n)} = [\mathbf{b}_1^{(n)}, \mathbf{b}_2^{(n)}, \dots, \mathbf{b}_R^{(n)}] \in \mathbb{R}^{I_n \times R}$, $\boldsymbol{\lambda} = [\lambda_1, \lambda_2, \dots, \lambda_R]^T$ and $\mathbf{\Lambda} = \text{diag}\{\boldsymbol{\lambda}\}$ is a diagonal matrix.

The rank of tensor \mathbf{X} is defined as the smallest R for which CPD (7) holds exactly.

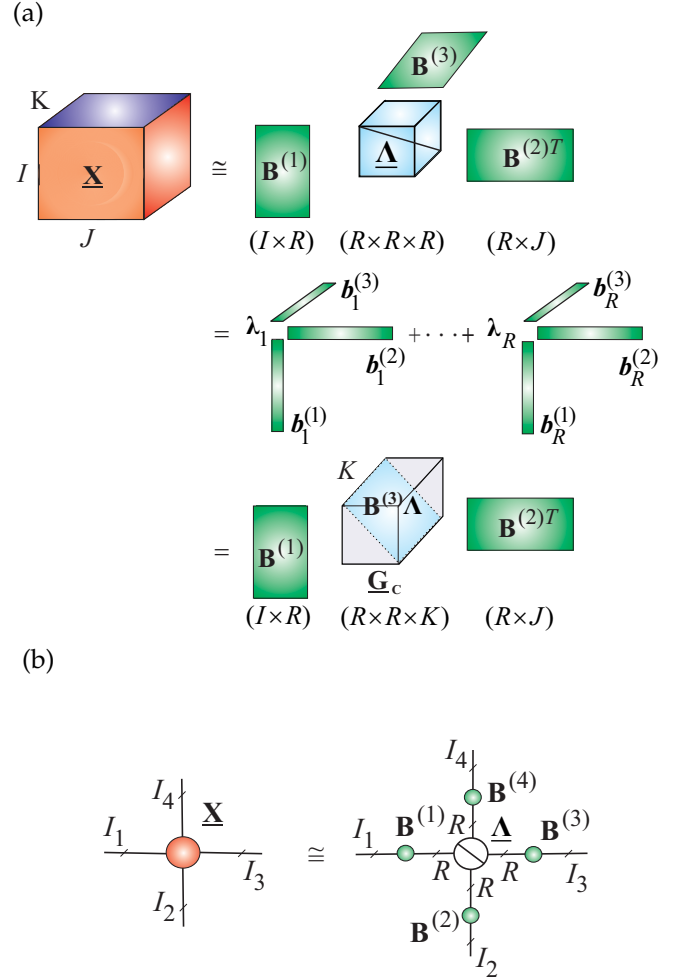


Figure 14: (a) The Canonical Polyadic Decomposition (CPD) of a 3rd-order tensor as: $\mathbf{X} \cong \underline{\mathbf{A}} \times_1 \mathbf{B}^{(1)} \times_2 \mathbf{B}^{(2)} \times_3 \mathbf{B}^{(3)} = \sum_{r=1}^R \lambda_r \mathbf{b}_r^{(1)} \circ \mathbf{b}_r^{(2)} \circ \mathbf{b}_r^{(3)} = \underline{\mathbf{G}}_c \times_1 \mathbf{B}^{(1)} \times_2 \mathbf{B}^{(2)}$ with $\underline{\mathbf{G}} = \underline{\mathbf{A}}$ and $\underline{\mathbf{G}}_c = \underline{\mathbf{A}} \times_3 \mathbf{B}^{(3)}$. (b) Diagram illustrating the CPD for a 4th-order tensor as: $\mathbf{X} \cong \underline{\mathbf{A}} \times_1 \mathbf{B}^{(1)} \times_2 \mathbf{B}^{(2)} \times_3 \mathbf{B}^{(3)} \times_4 \mathbf{B}^{(4)} = \sum_{r=1}^R \lambda_r \mathbf{b}_r^{(1)} \circ \mathbf{b}_r^{(2)} \circ \mathbf{b}_r^{(3)} \circ \mathbf{b}_r^{(4)}$. The objective of the CPD is to estimate the factor matrices $\mathbf{B}^{(n)}$ and a rank of tensor R , that is, the number of components R .

Algorithms to compute CPD. In the presence of noise in real world applications the CPD is rarely exact and has to be estimated by minimizing a suitable cost function, typically of the Least-Squares (LS) type in the form of the Frobenius norm $\|\mathbf{X} - \llbracket \underline{\mathbf{A}}; \mathbf{B}^{(1)}, \mathbf{B}^{(2)}, \dots, \mathbf{B}^{(N)} \rrbracket\|_F$, or using Least Absolute Error (LAE) criteria [27]. The Alternating Least Squares (ALS) algorithms [1], [11], [25], [28] minimize the LS cost function by optimizing individually each component matrix, while keeping the other component matrices fixed. For instance, assume that the diagonal matrix $\mathbf{\Lambda}$ in (8) has been absorbed in one of the component matrices; then, by taking advantage of the Khatri-Rao structure the component matrices

$\mathbf{B}^{(n)}$ can be updated sequentially as [4]

$$\mathbf{B}^{(n)} \leftarrow \mathbf{X}_{(n)} \left(\bigodot_{k \neq n} \mathbf{B}^{(k)} \right) \left(\bigotimes_{k \neq n} (\mathbf{B}^{(k)T} \mathbf{B}^{(k)}) \right)^{\dagger}, \quad (9)$$

which requires the computation of the pseudo-inverse of small $(R \times R)$ matrices.

The ALS is attractive for its simplicity and for well defined problems (not too many, well separated, not collinear components) and high SNR, the performance of ALS algorithms is often satisfactory. For ill-conditioned problems, more advanced algorithms exist, which typically exploit the rank-1 structure of the terms within CPD to perform efficient computation and storage of the Jacobian and Hessian of the cost function [29], [30].

Constraints. The CPD is usually unique by itself, and does not require constraints to impose uniqueness [31]. However, if components in one or more modes are known to be e.g., nonnegative, orthogonal, statistically independent or sparse, these constraints should be incorporated to relax uniqueness conditions. More importantly, constraints may increase the accuracy and stability of the CPD algorithms and facilitate better physical interpretability of components [32], [33].

C. The Tucker Decomposition

The Tucker decomposition can be expressed as follows [34]:

$$\begin{aligned} \mathbf{X} &\cong \sum_{r_1=1}^{R_1} \cdots \sum_{r_N=1}^{R_N} g_{r_1 r_2 \dots r_N} \left(\mathbf{b}_{r_1}^{(1)} \circ \mathbf{b}_{r_2}^{(2)} \circ \cdots \circ \mathbf{b}_{r_N}^{(N)} \right) \\ &= \mathbf{G} \times_1 \mathbf{B}^{(1)} \times_2 \mathbf{B}^{(2)} \cdots \times_N \mathbf{B}^{(N)} \\ &= [\mathbf{G}; \mathbf{B}^{(1)}, \mathbf{B}^{(2)}, \dots, \mathbf{B}^{(N)}]. \end{aligned} \quad (10)$$

where $\mathbf{X} \in \mathbb{R}^{I_1 \times I_2 \times \cdots \times I_N}$ is the given data tensor, $\mathbf{G} \in \mathbb{R}^{R_1 \times R_2 \times \cdots \times R_N}$ is the core tensor and $\mathbf{B}^{(n)} = [\mathbf{b}_1^{(n)}, \mathbf{b}_2^{(n)}, \dots, \mathbf{b}_{R_n}^{(n)}] \in \mathbb{R}^{I_n \times R_n}$ are the mode- n component matrices, $n = 1, 2, \dots, N$ (see Fig. 15). Using Kronecker products the decomposition in (10) can be expressed in a matrix and vector form as follows:

$$\begin{aligned} \mathbf{X}_{(n)} &\cong \mathbf{B}^{(n)} \mathbf{G}_{(n)} (\mathbf{B}^{(N)} \cdots \otimes \mathbf{B}^{(n+1)} \otimes \mathbf{B}^{(n-1)} \cdots \otimes \mathbf{B}^{(1)})^T \\ \text{vec}(\mathbf{X}) &\cong [\mathbf{B}^{(N)} \otimes \mathbf{B}^{(N-1)} \cdots \otimes \mathbf{B}^{(1)}] \text{vec}(\mathbf{G}). \end{aligned} \quad (11)$$

The core tensor (typically, $R_n < I_n$) models a potentially complex pattern of mutual interaction between the vectors (components) in different modes.

Multilinear rank. The N -tuple (R_1, R_2, \dots, R_N) is called the multilinear-rank of \mathbf{X} if the Tucker decomposition holds exactly.

Note that the CPD can be considered as a special case of the Tucker decomposition in which the core tensor has nonzero elements only on main diagonal. In contrast to the CPD the Tucker decomposition, in general, is non unique. However, constraints imposed on all factor matrices and/or core tensor can reduce the indeterminacies to only column-wise permutation and scaling [35].

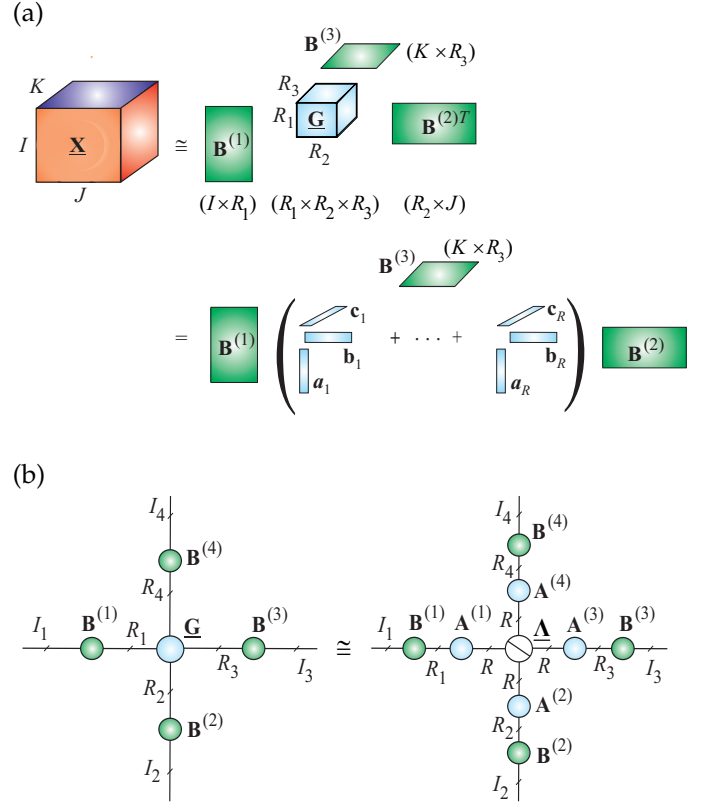


Figure 15: (a) Tucker decomposition of a 3rd-order tensor $\mathbf{X} \cong \mathbf{G} \times_1 \mathbf{B}^{(1)} \times_2 \mathbf{B}^{(2)} \times_3 \mathbf{B}^{(3)}$. The objective is to compute factor matrices $\mathbf{B}^{(n)}$ and core tensor \mathbf{G} . In some applications, in the second stage, the core tensor is approximately factorized using the CPD as $\mathbf{G} \cong \sum_{r=1}^R \mathbf{a}_r \circ \mathbf{b}_r \circ \mathbf{c}_r$. (b) Graphical representation of the Tucker and CP decompositions in two-stage procedure for a 4th-order tensor as: $\mathbf{X} \cong \mathbf{G} \times_1 \mathbf{B}^{(1)} \times_2 \mathbf{B}^{(2)} \cdots \times_4 \mathbf{B}^{(4)} = [\mathbf{G}; \mathbf{B}^{(1)}, \mathbf{B}^{(2)}, \mathbf{B}^{(3)}, \mathbf{B}^{(4)}] \cong (\mathbf{A} \times_1 \mathbf{A}^{(1)} \times_2 \mathbf{A}^{(2)} \cdots \times_4 \mathbf{A}^{(4)}) \times_1 \mathbf{B}^{(1)} \times_2 \mathbf{B}^{(2)} \cdots \times_4 \mathbf{B}^{(4)} = [\mathbf{A}; \mathbf{B}^{(1)} \mathbf{A}^{(1)}, \mathbf{B}^{(2)} \mathbf{A}^{(2)}, \mathbf{B}^{(3)} \mathbf{A}^{(3)}, \mathbf{B}^{(4)} \mathbf{A}^{(4)}]$.

D. Multiway Component Analysis Using Constrained Tucker Decompositions

A great success of 2-way component analysis (PCA, ICA, NMF, SCA) is largely due to the various constraints we can impose. Without constraints matrix factorization loses its most sense as the components are rather arbitrary and they do not have any physical meaning. There are various constraints that lead to all kinds of component analysis methods which are able give unique components with some desired physical meaning and properties and hence serve for different application purposes. Just similar to matrix factorization, unconstrained Tucker decompositions generally can only be served as multiway data compression as their results lack physical meaning. In the most practical applications we need to consider constrained Tucker decompositions which can provide multiple sets of essential unique components with desired physical interpretation and meaning. This is direct extension of 2-way component analysis and is referred to as multiway component analysis (MWCA) [2].

The MWCA based on Tucker- N model can be considered as a natural and simple extension of multilinear SVD and/or multilinear ICA in which we apply any efficient CA/BSS algorithms to each mode, which provides essential uniqueness [35].

There are two possible approaches to interpret and implement constrained Tucker decompositions for MWCA. (1) the columns of the component matrices $\mathbf{B}^{(n)}$ represent the desired latent variables, the core tensor \mathbf{G} has a role of “mixing process”, modeling the links among the components from different modes, while the data tensor \mathbf{X} represents a collection of 1-D or 2-D mixing signals; (2) the core tensor represents the desired (but hidden) N -dimensional signal (e.g., 3D MRI image or 4D video), while the component matrices represent mixing or filtering processes through e.g., time-frequency transformations or wavelet dictionaries [3].

The MWCA based on the Tucker- N model can be computed directly in two steps: (1) for $n = 1, 2, \dots, N$ perform model reduction and unfolding of data tensors sequentially and apply a suitable set of CA/BSS algorithms to reduced unfolding matrices $\tilde{\mathbf{X}}_{(n)}$, - in each mode we can apply different constraints and algorithms; (2) compute the core tensor using e.g., the inversion formula: $\hat{\mathbf{G}} = \mathbf{X} \times_1 \mathbf{B}^{(1)\dagger} \times_2 \mathbf{B}^{(2)\dagger} \dots \times_N \mathbf{B}^{(N)\dagger}$ [35]. This step is quite important because core tensors illuminate complex links among the multiple components in different modes [1].

V. Block-wise Tensor Decompositions for Very Large-Scale Data

Large-scale tensors cannot be processed by commonly used computers, since not only their size exceeds available working memory but also processing of huge data is very slow. The basic idea is to perform partition of a big data tensor into smaller blocks and perform tensor related operations block-wise using suitable tensor format (see Fig. 16). A data management system that divides the data tensor into blocks is an important approach both to process and to save large datasets. The method is based on a decomposition of the original tensor dataset into small blocks of the same-order tensors, which are approximated via TDs. Each block is approximated using low-rank reduced tensor decomposition e.g., CPD or a Tucker decomposition.

There are three important steps for such approach before we would be able to generate an output: First, an effective tensor representation should be chosen for the input dataset; second, the resulting tensor needs to be partitioned into sufficiently small blocks stored on distributed memory system, so that each block can fit into the main memory of a single machine; third, a suitable algorithm for TD needs to be adapted so that it can take the blocks of the original tensor, and still output the correct approximation as if the tensor for the original dataset had not been partitioned [8]–[10].

Converting the input data tensors from its original format into this block-structured tensor format is straight-

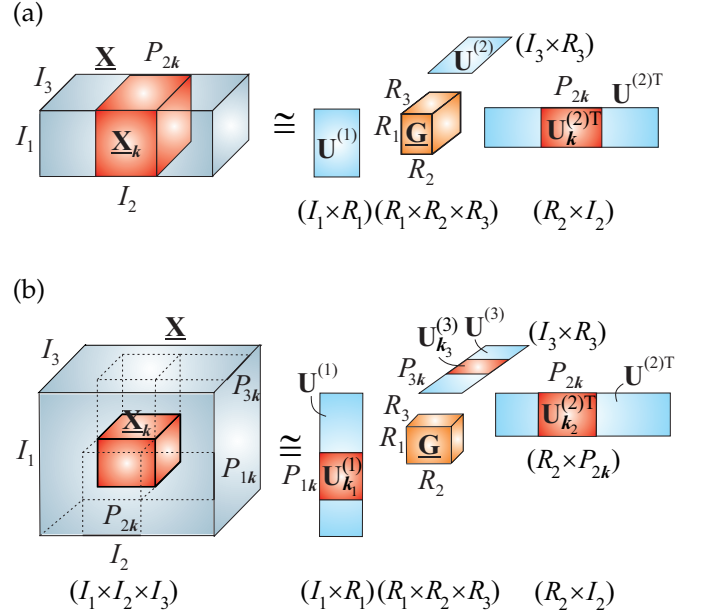


Figure 16: Conceptual models for performing the Tucker decomposition (HOSVD) for large-scale 3rd-order data tensors by dividing the tensors into blocks (a) along one largest dimension mode, with blocks $\mathbf{X}_k \cong \mathbf{G} \times_1 \mathbf{U}^{(1)} \times_2 \mathbf{U}_k^{(2)} \times_3 \mathbf{U}^{(3)}$, ($k = 1, 2, \dots, K$), and (b) along all modes with blocks $\mathbf{X}_k \cong \mathbf{G} \times_1 \mathbf{U}_{k_1}^{(1)} \times_2 \mathbf{U}_{k_2}^{(2)} \times_3 \mathbf{U}_{k_3}^{(3)}$. The models can be used for an anomaly detection by fixing a core tensor and some factor matrices and by monitoring the changes along one specific mode. First, we compute tensor decompositions for sampled (pre-selected) small blocks and in the next step we analyze changes in specific factor matrices $\mathbf{U}^{(n)}$.

forward, and needs to be performed as a preprocessing step. The resulting blocks should be saved into separate files on hard disks to allow efficient random or sequential access to all of blocks, which is required by most TD and TN algorithms.

We have successfully applied such techniques to CPD [10]. Experimental results indicate that our algorithms can not only process out-of-core data, but also achieve higher computation speed and performance than previous methods.

VI. Multilinear SVD (MLSVD) for Large Scale Problems

MultiLinear Singular Value Decomposition (MLSVD), called also higher-order SVD (HOSVD) is special form of the Tucker decomposition [36], [37], in which all factor matrices $\mathbf{B}^{(n)} = \mathbf{U}^{(n)} \in \mathbb{R}^{I_n \times I_m}$ are orthogonal and a core tensor $\mathbf{G} = \mathbf{S} \in \mathbb{R}^{I_1 \times I_2 \times \dots \times I_N}$ is all-orthogonal (see Fig. 17).

We say that the core tensor is all-orthogonal if it satisfies the following conditions:

(1) All orthogonality: Slices in each modes are mutually orthogonal, e.g., for a 3rd-order tensor

$$\langle \mathbf{S}_{:,k,:}, \mathbf{S}_{:,l,:} \rangle = 0, \quad \text{for } k \neq l, \quad (12)$$

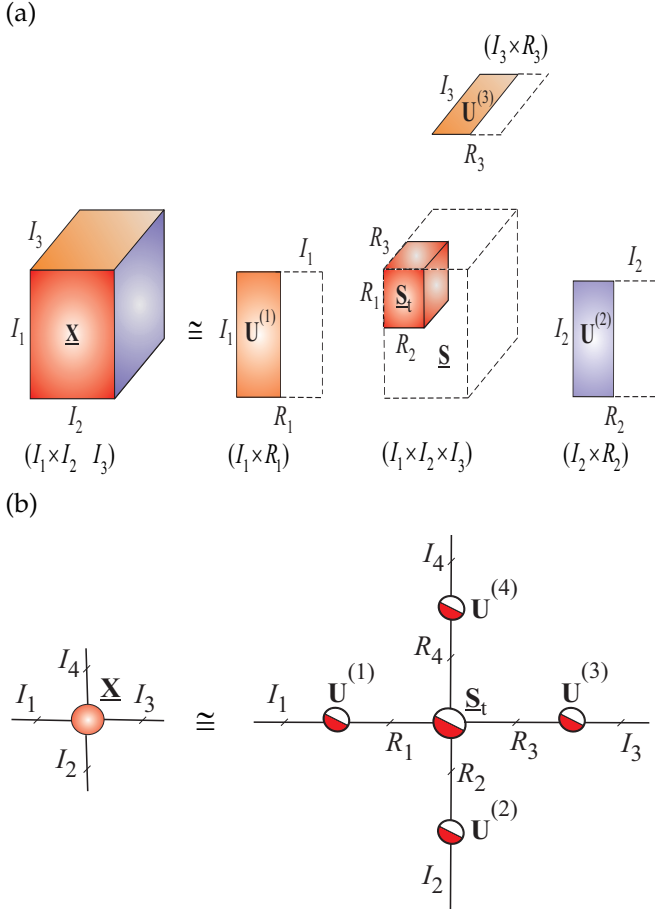


Figure 17: (a) Graphical illustration of the exact HOSVD and truncated (approximative) HOSVD for 3rd-order tensor as: $\mathbf{X} \cong \mathbf{S}_t \times_1 \mathbf{U}^{(1)} \times_2 \mathbf{U}^{(2)} \times_3 \mathbf{U}^{(3)}$ using a truncated SVD. (b) Graphical representation of the HOSVD for a 4th-order tensor $\mathbf{X} \cong \mathbf{S}_t \times_1 \mathbf{U}^{(1)} \times_2 \mathbf{U}^{(2)} \times_3 \mathbf{U}^{(3)} \times_4 \mathbf{U}^{(4)}$. All factor matrices $\mathbf{U}^{(n)}$ and a core tensor \mathbf{S}_t are orthogonal; due to orthogonality of the core tensor the HOSVD is unique for specific multilinear rank.

(2) Pseudo-diagonality: Frobenius norms of slices in each mode are decreasing in increasing of running index

$$\|\mathbf{S}_{:,k,:}\|_F \geq \|\mathbf{S}_{:,l,:}\|_F, \quad k \geq l. \quad (13)$$

These norms play a similar role as the singular values in the matrix SVD.

The orthogonal matrices $\mathbf{U}^{(n)}$ are in practice computed from the standard SVD or truncated SVD of unfolding mode- n matrices $\mathbf{X}_{(n)} = \mathbf{U}^{(n)} \mathbf{\Sigma}_n \mathbf{V}^{(n)T} \in \mathbb{R}^{I_n \times I_1 \cdots I_{n-1} I_{n+1} \cdots I_N}$. After obtaining the orthogonal matrices $\mathbf{U}^{(n)}$ of left singular vectors of $\mathbf{X}_{(n)}$, for each n , we can compute core tensor $\mathbf{G} = \mathbf{S}$ as

$$\mathbf{S} = \mathbf{X} \times_1 \mathbf{U}^{(1)T} \times_2 \mathbf{U}^{(2)T} \cdots \times_N \mathbf{U}^{(N)T}, \quad (14)$$

such that

$$\mathbf{X} = \mathbf{S} \times_1 \mathbf{U}^{(1)} \times_2 \mathbf{U}^{(2)} \cdots \times_N \mathbf{U}^{(N)}. \quad (15)$$

Due to orthogonality of the core tensor \mathbf{S} its slices are mutually orthogonal, this reduces to diagonality in the matrix case. In some applications we use modified HOSVD in which the SVD can be performed

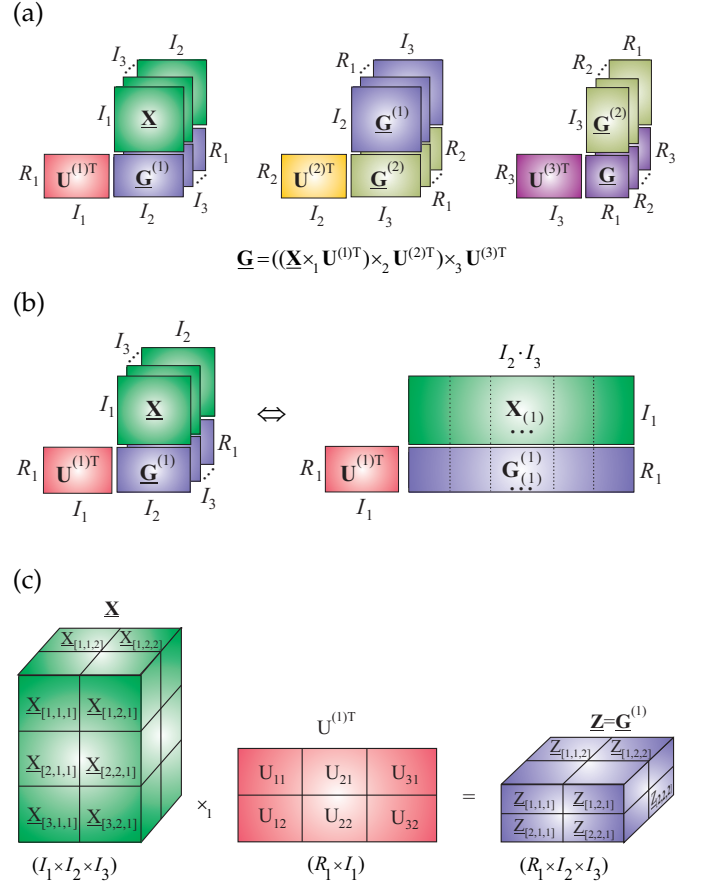


Figure 18: Illustration of the computation of a core tensor for the large-scale HOSVD: (a) using sequential computing of multilinear products $\mathbf{G} = \mathbf{S} = ((\mathbf{X} \times_1 \mathbf{U}^{(1)T}) \times_2 \mathbf{U}^{(2)T}) \times_3 \mathbf{U}^{(3)T}$, and (b) by applying fast and distributed implementation of matrix by matrix multiplications; (c) alternative method for very large-scale problems by applying divide and conquer approach, in which a data tensor \mathbf{X} and factor matrices $\mathbf{U}^{(n)T}$ are partitioned into suitable small blocks: Subtensors $\mathbf{X}_{[k_1,k_2,k_3]}$ and blocks matrices $\mathbf{U}_{[k_1,p_1]}^{(1)T}$, respectively. We compute the blocks of tensor $\mathbf{Z} = \mathbf{G}^{(1)} = \mathbf{X} \times_1 \mathbf{U}^{(1)T}$ as follows $\mathbf{Z}_{[q_1,k_2,k_3]} = \sum_{k_1=1}^{K_1} \mathbf{X}_{[k_1,k_2,k_3]} \times_1 \mathbf{U}_{[k_1,q_1]}^{(1)T}$ (see Eq. (18) for a general case.)

not on the unfolding mode- n matrices $\mathbf{X}_{(n)}$ but their transposes, i.e., $\mathbf{X}_{(n)}^T \cong \mathbf{V}^{(n)} \mathbf{\Sigma}_n \mathbf{U}^{(n)T}$. This leads to the modified HOSVD corresponding to Grassmann manifolds [38], which needs to compute very large (tall) factor orthogonal matrices $\mathbf{V}^{(n)} \in \mathbb{R}^{I_n \times I_n}$, where $I_n = \prod_{k \neq n} I_k = I_1 \cdots I_{n-1} I_{n+1} \cdots I_N$, and the core tensor $\tilde{\mathbf{S}} \in \mathbb{R}^{I_1 \times I_2 \times \cdots \times I_N}$ of the following model:

$$\mathbf{X} = \tilde{\mathbf{S}} \times_1 \mathbf{V}^{(1)T} \times_2 \mathbf{V}^{(2)T} \cdots \times_N \mathbf{V}^{(N)T}. \quad (16)$$

In practical applications the dimensions of unfolding matrices $\mathbf{X}_{(n)} \in \mathbb{R}^{I_n \times I_n}$ may be prohibitively large (with $I_n \gg I_n$), exceeding memory of standard computers. A truncated SVD of a large-scale unfolding matrix $\mathbf{X}_{(n)} = \mathbf{U}^{(n)} \mathbf{\Sigma}_n \mathbf{V}^{(n)T}$ is performed by partitioning it into Q slices, as $\mathbf{X}_{(n)} = [\mathbf{X}_{1,n}, \mathbf{X}_{2,n}, \dots, \mathbf{X}_{Q,n}] =$

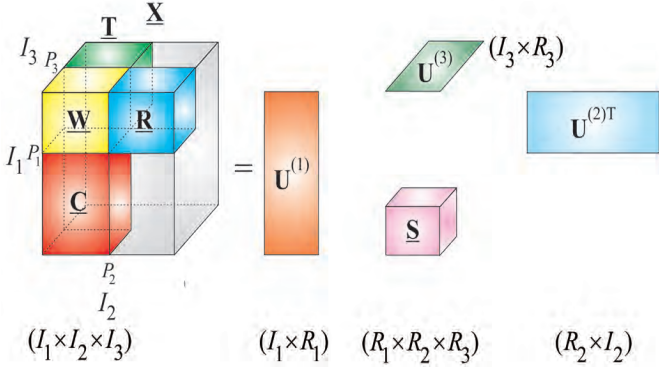


Figure 19: Alternative approach to computation of the HOSVD for very large data tensor, by exploiting multilinear low-rank approximation. The objective is to select such fibers (up to permutation of fibers) that the subtensor $\mathbf{W} \in \mathbb{R}^{P_1 \times P_2 \times P_3}$ with $P_n \geq R_n$ ($n = 1, 2, 3$) has the same multilinear rank $\{R_1, R_2, R_3\}$ as the whole huge data tensor \mathbf{X} , with $R_n \ll I_n$. Instead of unfolding of the whole data tensor we need to preform unfolding (and applying the standard SVD) for typically much smaller subtensors $\mathbf{X}^{(1)} = \mathbf{C} \in \mathbb{R}^{I_1 \times P_2 \times P_3}$, $\mathbf{X}^{(2)} = \mathbf{R} \in \mathbb{R}^{P_1 \times I_2 \times P_3}$, $\mathbf{X}^{(3)} = \mathbf{T} \in \mathbb{R}^{P_1 \times P_2 \times I_3}$, each in a single mode- n , ($n = 1, 2, 3$). This approach can be applied if data tensor has low multilinear rank approximation. For simplicity of illustration, we assumed that fibers are permuted in a such way that the first $(P_2 \times P_3)$ fibers in mode-1 was selected.

$\mathbf{U}^{(n)} \Sigma_n [\mathbf{V}_{1,n}^T, \mathbf{V}_{2,n}^T, \dots, \mathbf{V}_{Q,n}^T]$. Next, the orthogonal matrices $\mathbf{U}^{(n)}$ and the diagonal matrices Σ_n are obtained from eigenvalue decompositions $\mathbf{X}_{(n)} \mathbf{X}_{(n)}^T = \mathbf{U}^{(n)} \Sigma_n^2 \mathbf{U}^{(n)T} = \sum_q \mathbf{x}_{q,n} \mathbf{x}_{q,n}^T \in \mathbb{R}^{I_n \times I_n}$, allowing for the terms $\mathbf{V}_{q,n} = \mathbf{x}_{q,n}^T \mathbf{U}^{(n)} \Sigma_n^{-1}$ to be computed separately. This allows to optimize the size of the q -th slice $\mathbf{x}_{q,n} \in \mathbb{R}^{I_n \times (I_n/Q)}$ so as to match the available computer memory. Such a simple approach to compute matrices $\mathbf{U}^{(n)}$ and/or $\mathbf{V}^{(n)}$ does not require loading the entire unfolding matrices at once into computer memory, instead it accesses the dataset sequentially. Depending on computer's physical memory, the dimension I_n is typically less than 10,000, while there is no limit on the dimension $I_{\bar{n}} = \prod_{k \neq n} I_k$. Similar approaches can be applied to multilinear PCA, ICA, and NTF [10], [23], [39].

When a data tensor \mathbf{X} is very large and can not be stored in a memory of computer, then another challenge is to compute a core tensor $\mathbf{G} = \mathbf{S}$ by directly using the formula:

$$\mathbf{G} = \mathbf{X} \times_1 \mathbf{U}^{(1)T} \times_2 \mathbf{U}^{(2)T} \dots \times_n \mathbf{U}^{(n)T}, \quad (17)$$

which is generally performed sequentially as illustrated in Fig. 18 (a) and (b) [8], [9]. For very large tensor it is useful to divide the data tensor \mathbf{X} into small blocks $\mathbf{X}_{[k_1, k_2, \dots, k_N]}$ and store them on hard disks or distributed memory. In similar way, we can divide the orthogonal factor matrices $\mathbf{U}^{(n)T}$ into corresponding blocks matrices $\mathbf{U}_{[k_n, p_n]}^{(n)T}$ as illustrated in Fig. 18 (c) for a 3rd-order tensors [9]. In general case, we can compute blocks of resulting

tensor $\mathbf{G}^{(n)}$ sequentially or in parallel way as follows:

$$\mathbf{G}_{[k_1, k_2, \dots, k_N]}^{(n)} = \sum_{k_n=1}^{K_n} \mathbf{X}_{[k_1, k_2, \dots, k_n, \dots, k_N]} \times_n \mathbf{U}_{[k_n, q_n]}^{(n)T}. \quad (18)$$

If data tensor satisfies low-multilinear rank, that is, it has multilinear rank $\{R_1, R_2, \dots, R_N\}$ with $R_n \ll I_n$, $\forall n$, we can further alleviate the problem of dimensionality by first identifying a subtensor $\mathbf{W} \in \mathbb{R}^{P_1 \times P_2 \times \dots \times P_N}$ with $P_n \geq R_n$, using efficient CUR tensor decomposition [40]. Then the HOSVD can be computed from subtensors as illustrated in Fig. 19 for a 3rd-order tensor. This feature can be formulated in more general form as the following Proposition:

Proposition 1: If tensor $\mathbf{X} \in \mathbb{R}^{I_1 \times I_2 \times \dots \times I_N}$ has low multilinear rank $\{R_1, R_2, \dots, R_N\}$, with $R_n \leq I_n$, $\forall n$, then it can be fully reconstructed via the HOSVD using only N subtensors $\mathbf{X}^{(n)} \in \mathbb{R}^{P_1 \times \dots \times P_{n-1} \times I_n \times P_{n+1} \times \dots \times P_N}$, ($n = 1, 2, \dots, N$), under condition that subtensor $\mathbf{W} \in \mathbb{R}^{P_1 \times P_2 \times \dots \times P_N}$, with $P_n \geq R_n$, $\forall n$ has multilinear rank $\{R_1, R_2, \dots, R_N\}$.

In practice, we can compute the HOSVD for low-rank, large-scale data tensor in several steps. In the first step, we apply CUR FSTD decomposition [40] to identify close to optimal a subtensor $\mathbf{W} \in \mathbb{R}^{R_1 \times R_2 \times \dots \times R_N}$ (see the next section). In the next step, we apply the standard SVD for unfolding matrices $\mathbf{X}_{(n)}^{(n)}$ of subtensors $\mathbf{X}^{(n)}$ to compute the left orthogonal matrices $\tilde{\mathbf{U}}^{(n)} \in \mathbb{R}^{I_n \times R_n}$. In the next step, we compute an auxiliary core tensor $\mathbf{G} = \mathbf{W} \times_1 \mathbf{B}^{(1)} \dots \times_N \mathbf{B}^{(N)}$, where $\mathbf{B}^{(n)} \in \mathbb{R}^{R_n \times R_n}$ are inverses of the sub-matrices consisting the first R_n rows of the matrices $\tilde{\mathbf{U}}^{(n)}$. In the last step, we perform HOSVD decomposition of the relatively small core tensor as $\mathbf{G} = \mathbf{S} \times_1 \mathbf{Q}^{(1)} \dots \times_N \mathbf{Q}^{(N)}$, with $\mathbf{Q}^{(n)} \in \mathbb{R}^{R_n \times R_n}$ and then desired orthogonal matrices are computed as $\mathbf{U}^{(n)} = \tilde{\mathbf{U}}^{(n)} \mathbf{Q}^{(n)}$.

VII. CUR Tucker Decomposition for Dimensionality Reduction and Compression of Tensor Data

Note that instead of using the full tensor, we may compute an approximative tensor decomposition model from a limited number of entries (e.g., selected fibers, slices or subtensors). Such completion-type strategies have been developed for low-rank and low-multilinear-rank [41], [42]. An alternative approach is to apply CUR decomposition or Cross-Approximation by sampled fibers for the columns of factor matrices in a Tucker approximation [40], [43]. Furthermore, since large-scale tensors cannot be loaded explicitly in main memory, they usually reside in distributed storage by splitting tensors to smaller blocks. More drastic and promising approach is to apply tensor networks and represent big data by high-order tensors not explicitly but in compressed tensor formats (see next sections). Dimensionality reduction methods are based on the fundamental assumption that the large datasets are highly redundant and can be approximated by low-rank matrices and cores, allowing

for a significant reduction in computational complexity and to discover meaningful components while exhibiting marginal loss of information.

For very large-scale problems, so called CUR matrix decompositions can be employed for dimensionality reduction [40], [43]–[46]. By assuming that a sufficiently precise low-rank approximation exists, which implies that data has some internal structure or smoothness, the idea is to provide data representation through a linear combination of a few “meaningful” components, which are exact replicas of columns and rows of the original data matrix [47].

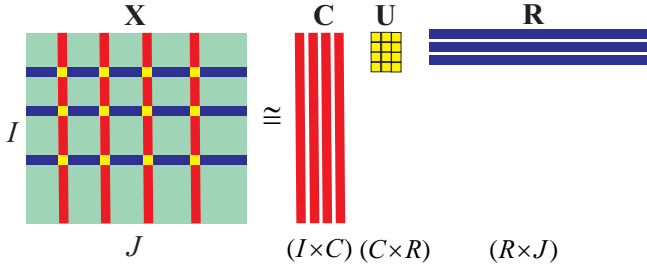


Figure 20: CUR decomposition for a huge matrix.

The CUR model, called also skeleton Cross-Approximation, decomposes a given data matrix $\mathbf{X} \in \mathbb{R}^{I \times J}$ as [44], [45] (see Fig. 20):

$$\mathbf{X} = \mathbf{C}\mathbf{U}\mathbf{R} + \mathbf{E}, \quad (19)$$

where $\mathbf{C} \in \mathbb{R}^{I \times C}$ is a matrix constructed from C suitably selected columns of data matrix \mathbf{X} , $\mathbf{R} \in \mathbb{R}^{R \times J}$ consists of R rows of \mathbf{X} , and the matrix $\mathbf{U} \in \mathbb{R}^{C \times R}$ is chosen to minimize the norm of the error $\mathbf{E} \in \mathbb{R}^{I \times J}$. Since typically, $C \ll J$ and $R \ll I$, the objective is to select rows and columns of \mathbf{X} such that the error cost function $\|\mathbf{E}\|_F^2$ is minimized; these columns and rows are chosen so as to exhibit high “statistical leverage” and provide the best low-rank fit to the data matrix. For a given set of columns (\mathbf{C}) and rows (\mathbf{R}), the optimal choice for the core matrix is $\mathbf{U} = \mathbf{C}^\dagger \mathbf{X} (\mathbf{R}^\dagger)^T$. This is not practical since it requires access to all the entries of \mathbf{X} , which is not feasible for large-scale data. A pragmatic choice for the core matrix would be $\mathbf{U} = \mathbf{W}^\dagger$, where the matrix $\mathbf{W} \in \mathbb{R}^{R \times C}$ is defined by the intersections of the selected rows and columns. It should be noted that, if $\text{rank}(\mathbf{X}) \leq C, R$, then the CUR approximation is exact. For the general case, it has been proven that, when the intersection sub-matrix \mathbf{W} is of maximum volume (the volume of a sub-matrix \mathbf{W} is defined as $|\det(\mathbf{W})|$), this approximation is close to the optimal SVD solution [45].

The concept of CUR decomposition has been successfully generalized to tensors. In [43] the matrix CUR decomposition was applied to one unfolded version of the tensor data, while in [40] a reconstruction formula of a tensor having a low rank Tucker approximation was proposed, termed the Fiber Sampling Tucker Decomposition (FSTD), which is a practical and fast technique. The latter takes into account the linear structure in all the

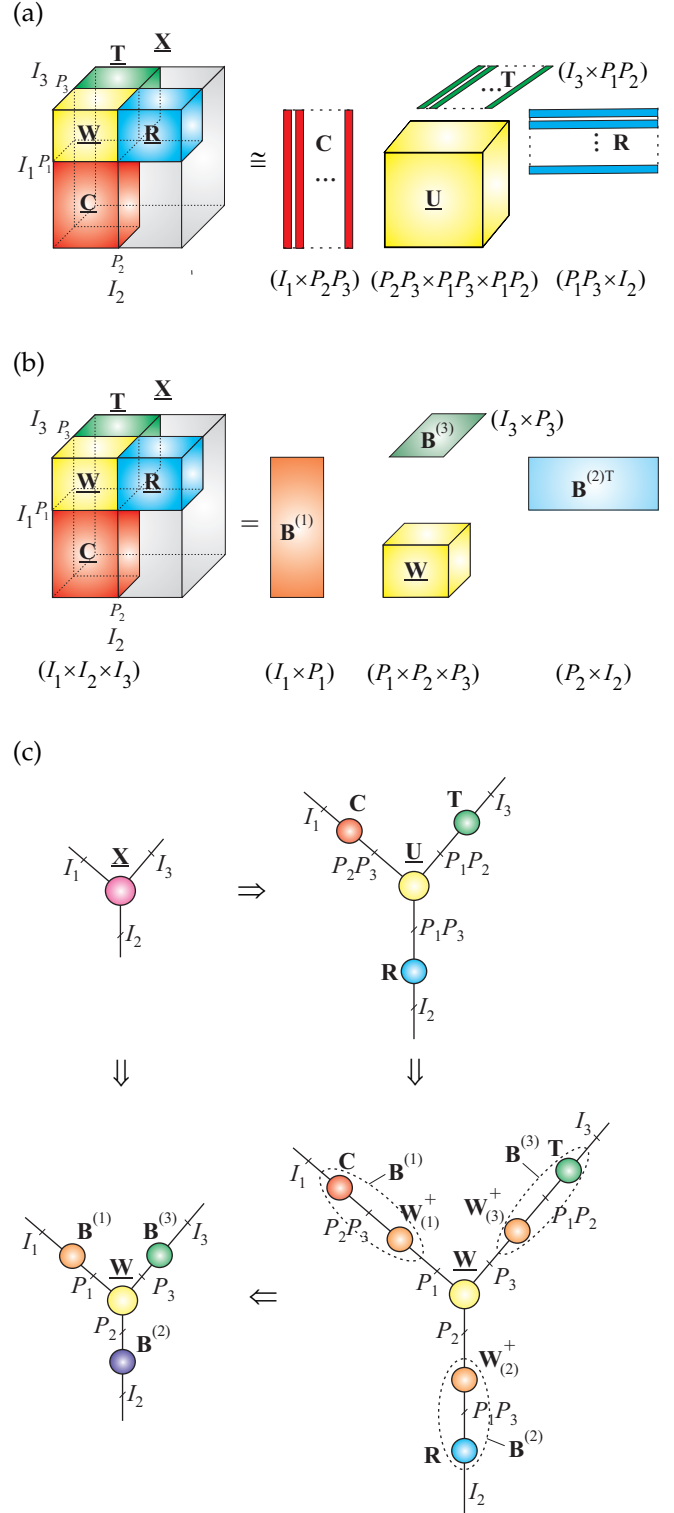


Figure 21: (a) CUR decomposition of a large 3rd-order tensor (for simplicity of illustration up to permutation of fibers) $\mathbf{X} \cong \mathbf{U} \times_1 \mathbf{C} \times_2 \mathbf{R} \times_3 \mathbf{T} = \llbracket \mathbf{U}; \mathbf{C}, \mathbf{R}, \mathbf{T} \rrbracket$, where $\mathbf{U} = \mathbf{W} \times_1 \mathbf{W}_{(1)}^\dagger \times_2 \mathbf{W}_{(2)}^\dagger \times_3 \mathbf{W}_{(3)}^\dagger = \llbracket \mathbf{W}; \mathbf{W}_{(1)}^\dagger, \mathbf{W}_{(2)}^\dagger, \mathbf{W}_{(3)}^\dagger \rrbracket$. (b) equivalent decomposition expressed via subtensor \mathbf{W} , (c) Tensor network diagram illustrating transformation from CUR Tucker format (a) to form (b) as: $\mathbf{X} \cong \mathbf{W} \times_1 \mathbf{B}^{(1)} \times_2 \mathbf{B}^{(2)} \times_3 \mathbf{B}^{(3)} = \llbracket \mathbf{W}; \mathbf{C}\mathbf{W}_{(1)}^\dagger, \mathbf{R}\mathbf{W}_{(2)}^\dagger, \mathbf{T}\mathbf{W}_{(3)}^\dagger \rrbracket$.

modes of the tensor simultaneously. Since real-life data have often good low multilinear rank approximations, FSTD provides such a low-rank Tucker decomposition that is directly expressed in terms of a relatively small number of fibers of the data tensor (see Fig. 21).

For a given 3rd-order tensor $\underline{\mathbf{X}} \in \mathbb{R}^{I_1 \times I_2 \times I_3}$ for which an exact rank- (R_1, R_2, R_3) Tucker representation exists, FSTD selects $P_n \geq R_n$ ($n = 1, 2, 3$) indices in each mode, which determine an intersection sub-tensor $\underline{\mathbf{W}} \in \mathbb{R}^{P_1 \times P_2 \times P_3}$ so that the following exact Tucker representation can be obtained:

$$\underline{\mathbf{X}} = [\underline{\mathbf{U}}; \underline{\mathbf{C}}, \underline{\mathbf{R}}, \underline{\mathbf{T}}], \quad (20)$$

in which the core tensor is computed as $\underline{\mathbf{U}} = \underline{\mathbf{G}} = [\underline{\mathbf{W}}; \underline{\mathbf{W}}_{(1)}^\dagger, \underline{\mathbf{W}}_{(2)}^\dagger, \underline{\mathbf{W}}_{(3)}^\dagger]$, and the factor matrices $\underline{\mathbf{C}} \in \mathbb{R}^{I_1 \times P_1}$, $\underline{\mathbf{R}} \in \mathbb{R}^{I_2 \times P_2}$, $\underline{\mathbf{T}} \in \mathbb{R}^{I_3 \times P_3}$ contain the fibers (columns, rows and tubes, respectively). This can also be written as a the Tucker representation:

$$\underline{\mathbf{X}} = [\underline{\mathbf{W}}; \underline{\mathbf{C}}\underline{\mathbf{W}}_{(1)}^\dagger, \underline{\mathbf{R}}\underline{\mathbf{W}}_{(2)}^\dagger, \underline{\mathbf{T}}\underline{\mathbf{W}}_{(3)}^\dagger]. \quad (21)$$

Observe that for $N = 2$ this model simplifies into the CUR matrix case, $\mathbf{X} = \mathbf{C}\mathbf{U}\mathbf{R}$, and the core matrix is $\underline{\mathbf{U}} = [\underline{\mathbf{W}}; \underline{\mathbf{W}}_{(1)}^\dagger, \underline{\mathbf{W}}_{(2)}^\dagger] = \underline{\mathbf{W}}^\dagger \underline{\mathbf{W}} \underline{\mathbf{W}}^\dagger = \underline{\mathbf{W}}^\dagger$.

In more general case for N th-order tensor can formulate the following Proposition [40]:

Proposition 2: If tensor $\underline{\mathbf{X}} \in \mathbb{R}^{I_1 \times I_2 \times \dots \times I_N}$ has low multilinear rank $\{R_1, R_2, \dots, R_N\}$, with $R_n \leq I_n$, $\forall n$, then it can be fully reconstructed via the CUR FSTD $\underline{\mathbf{X}} = [\underline{\mathbf{U}}; \underline{\mathbf{C}}^{(1)}, \underline{\mathbf{C}}^{(2)}, \dots, \underline{\mathbf{C}}^{(N)}]$, using only N factor matrices $\underline{\mathbf{C}}^{(n)} \in \mathbb{R}^{I_n \times P_n}$, ($n = 1, 2, \dots, N$), build up from fibers of the data tensor, and a core tensor $\underline{\mathbf{U}} = \underline{\mathbf{G}} = [\underline{\mathbf{W}}; \underline{\mathbf{W}}_{(1)}^\dagger, \underline{\mathbf{W}}_{(2)}^\dagger, \dots, \underline{\mathbf{W}}_{(N)}^\dagger]$ under condition that sub-tensor $\underline{\mathbf{W}} \in \mathbb{R}^{P_1 \times P_2 \times \dots \times P_N}$ with $P_n \geq R_n$, $\forall n$ has multilinear rank $\{R_1, R_2, \dots, R_N\}$.

An efficient strategy for the selection of suitable fibers, only requiring access to a partial (small) subset of entries of a data tensor through identifying the entries with maximum modulus within single fibers [40]. The indices are selected sequentially using a deflation approach making the FSTD algorithm suitable for very large-scale but relatively low-order tensors (including tensors with missing fibers or entries).

VIII. Analysis of Coupled Multi-Block Tensor Data – Linked Multiway Component Analysis (LMWCA)

Group analysis or multi-block data analysis aims to identify links between hidden components in data making it possible to analyze the correlation, variability and consistency of the components across multi-block data sets. This equips us with enhanced flexibility: Some components do not necessarily need to be orthogonal or statistically independent, and can be instead sparse, smooth or non-negative (e.g., for spectral components). Additional constraints can be used to reflect the spatial distributions, spectral, or temporal patterns [3].

Consider the analysis of multi-modal high-dimensional data collected under the same or very

similar conditions, for example, a set of EEG and MEG or fMRI signals recorded for different subjects over many trials and under the same experiment configuration and mental tasks. Such data share some common latent (hidden) components but can also have their own independent features. Therefore, it is quite important and necessary that they will be analyzed in a linked way instead of independently.

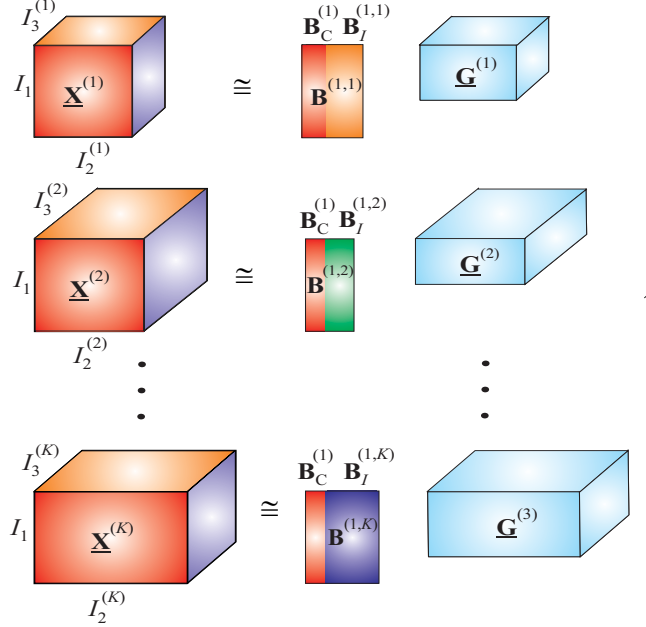


Figure 22: Linked Multiway Component Analysis (LMWCA) for coupled multi-block tensor data with different dimensions in each mode except of the first mode. The objective is to find the common components $\underline{\mathbf{B}}_C^{(1)} \in \mathbb{R}^{I_1 \times C_1}$, where $C_1 \leq R_1$ is the number of the common components in mode-1.

The linked multiway component analysis (LMWCA) for multi-block tensors data is formulated as a set of approximate joint Tucker-1 decompositions of a set of data tensors $\underline{\mathbf{X}}^{(k)} \in \mathbb{R}^{I_1^{(k)} \times I_2^{(k)} \times \dots \times I_N^{(k)}}$, with $I_1^{(k)} = I_1$, $\forall k$ ($k = 1, 2, \dots, K$) (see Fig. 22):

$$\underline{\mathbf{X}}^{(k)} = \underline{\mathbf{G}}^{(k)} \times_1 \underline{\mathbf{B}}^{(1,k)}, \quad (k = 1, 2, \dots, K) \quad (22)$$

where each factor (component) matrix $\underline{\mathbf{B}}^{(1,k)} = [\underline{\mathbf{B}}_C^{(1)}, \underline{\mathbf{B}}_I^{(1,k)}] \in \mathbb{R}^{I_1 \times R_n}$ has two sets of components: (1) Components $\underline{\mathbf{B}}_C^{(1)} \in \mathbb{R}^{I_1 \times C}$ (with $0 \leq C \leq R$), which are common for all available blocks and correspond to identical or maximally correlated components, and (2) components $\underline{\mathbf{B}}_I^{(1,k)} \in \mathbb{R}^{I_1 \times (R_1 - C_1)}$, which are different independent processes, for example, latent variables independent of excitations or stimuli/tasks. The objective is to estimate the common components $\underline{\mathbf{B}}_C^{(1)}$ and independent (distinctive) components $\underline{\mathbf{B}}_I^{(1,k)}$ (see Fig. 22) [3].

If $\underline{\mathbf{B}}^{(n,k)} = \underline{\mathbf{B}}_C^{(n)} \in \mathbb{R}^{I_n \times R_n}$ for a specific mode n (in our case $n = 1$), under additional assumption of the same dimension of tensors, then the problem simplifies to generalized Common Component Analysis or tensor

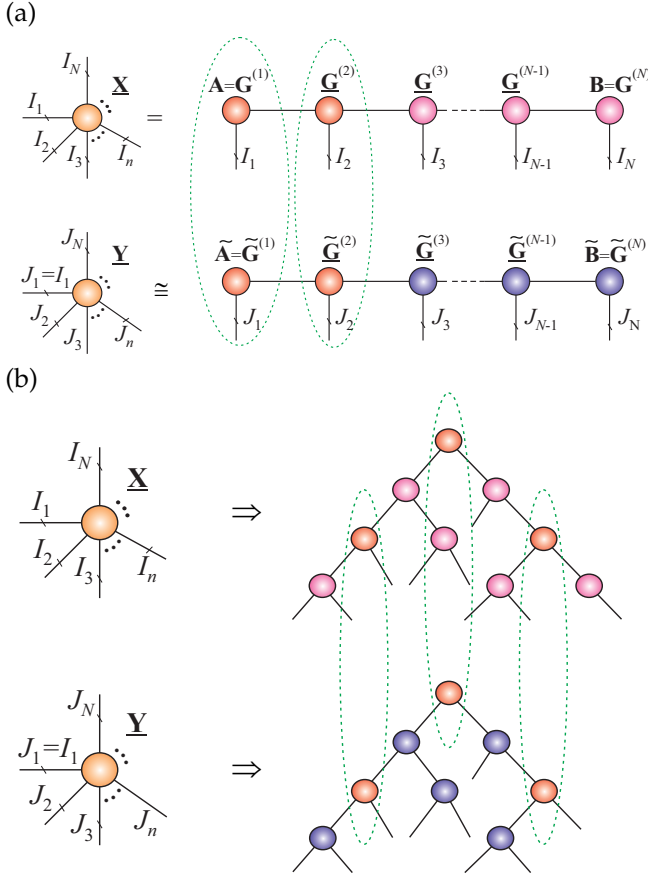


Figure 23: Conceptual models of generalized Linked Multiway Component Analysis (LMWCA) applied to tensor networks: The objective is to find core tensors which are maximally correlated for (a) Tensor Train and for (b) Tensor Tree States (Hierarchical Tucker).

Population Value Decomposition (PVD) [48]. This can be solved by concatenation all data tensors along one mode, and perform constrained Tucker or CP tensor decompositions (see [48]).

In a more general case, when $C_n < R_n$, we can unfold each data tensor $\mathbf{X}^{(k)}$ in common mode, and perform a set of linked and constrained matrix factorizations: $\mathbf{X}_{(1)}^{(k)} \cong \mathbf{B}_C^{(1)} \mathbf{A}_C^{(1,k)} + \mathbf{B}_I^{(1,k)} \mathbf{A}_I^{(1,k)}$ through solving constrained optimization problems:

$$\min \sum_{k=1}^K \|\mathbf{X}_{(1)}^{(k)} - \mathbf{B}_C^{(1)} \mathbf{A}_C^{(1,k)} - \mathbf{B}_I^{(1,k)} \mathbf{A}_I^{(1,k)}\|_F \quad (23)$$

$$+ f_1(\mathbf{B}_C^{(1)}), \text{ s.t. } \mathbf{B}_C^{(1)T} \mathbf{B}_I^{(1,k)} = \mathbf{0} \quad \forall k,$$

where f_1 are the penalty terms which impose additional constraints on common components $\mathbf{B}_C^{(1)}$, in order to extract as many as possible unique and desired components. In a special case of orthogonality constraints, the problem can be transformed to a generalized eigenvalue problem and solved by the power method [49]. The key point is to assume that common factor sub-matrices $\mathbf{B}_C^{(1)}$ are present in all multiple data blocks and hence reflect structurally complex (hidden) latent and intrinsic

links between them. In practice, the number of common components C_1 in each mode is unknown and should be estimated (see [49] for detail).

The linked multiway component analysis model provides a quite flexible and general framework and thus supplements currently available techniques for group ICA and feature extraction for multi-block data. The LWCA models are designed for blocks of K tensors, where dimensions naturally split into several different modalities (e.g., time, space and frequency). In this sense, a multi-block multiway CA attempts to estimate both common and independent or uncorrelated components, and is a natural extension of group ICA, PVD, and CCA/PLS methods (see [3], [49], [50] and references therein). The concept of the LMWCA can be generalized to tensor networks as illustrated in Fig. 23.

IX. Mathematical and Graphical Description of Tensor Trains (TT) Decompositions

In this section we discuss with more detail the Tensor Train (TT) decompositions which are the simplest tensor networks. Tensor train decompositions was introduced by Oseledets and Tyrtshnikov [17], [51] and can take various forms depending on the order of input data as illustrated in Fig. 24.

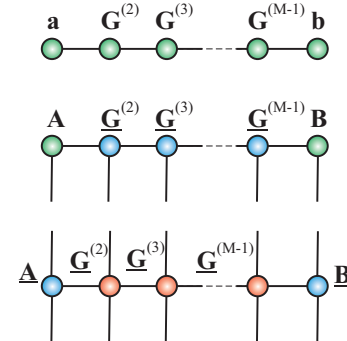


Figure 24: Various form of tensor train (TT) models: (Top) Scalar function can be expressed as $x = a^T \mathbf{G}^{(2)} \mathbf{G}^{(3)} \dots \mathbf{G}^{(M-1)} \mathbf{b}$, (middle) TT/MPS model of an M th-order data tensor (multidimensional vector) is expressed by 3rd-order tensors and two factor matrices as: $\mathbf{X} = \llbracket \mathbf{A}, \mathbf{G}^{(2)}, \mathbf{G}^{(3)}, \dots, \mathbf{G}^{(M-1)}, \mathbf{B} \rrbracket$; (bottom) TT/MPO model of $2M$ th-order data tensor (multidimensional matrix) can be expressed by the chain of 3rd-order and 4th-order cores as: $\mathbf{X} = \llbracket \mathbf{A}, \mathbf{G}^{(2)}, \mathbf{G}^{(3)}, \dots, \mathbf{G}^{(M-1)}, \mathbf{B} \rrbracket$.

The basic Tensor Train [17], [51], [52], called also Matrix Product State (MPS), in quantum physics [53]–[56] decomposes the higher-order tensor into set of 3rd-order core tensors and factor matrices as illustrated in more detail in Figure 27. In fact TT is equivalent to the MPS (i.e. TT/MPS) only if the MPS has the open boundary conditions [57], [58].

The tensor train (TT/MPS) for N th-order data tensor $\mathbf{X} \in \mathbb{R}^{I_1 \times I_2 \times \dots \times I_N}$ can be described in the various equivalent mathematical forms as follows:

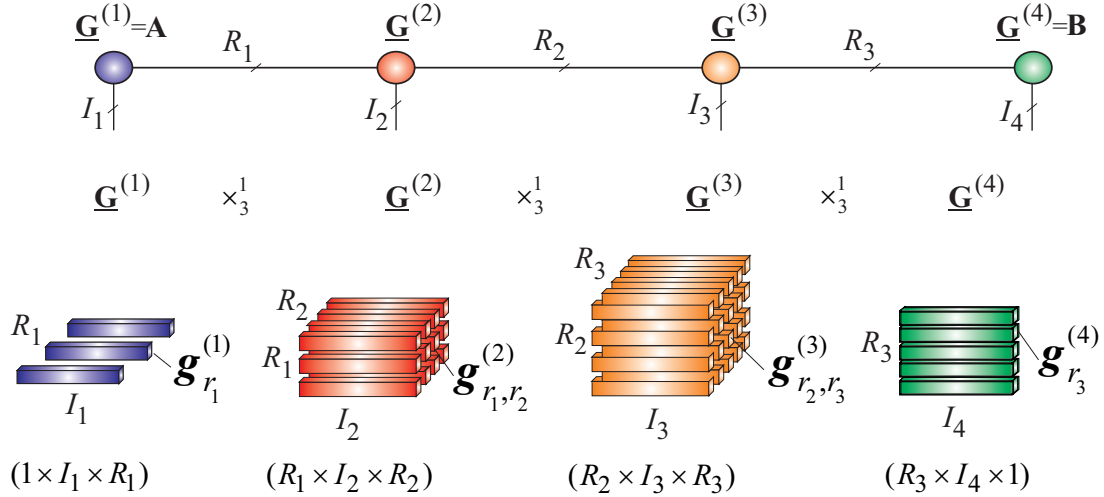


Figure 25: Illustration of the tensor train decomposition (TT/MPS) for a 4th-order tensor expressed via multilinear product of cores and the outer product of vectors (sum of rank-1 tensors) as: $\mathbf{X} \cong \mathbf{G}^{(1)} \times_3^1 \mathbf{G}^{(2)} \times_3^1 \mathbf{G}^{(3)} \times_3^1 \mathbf{G}^{(4)} = \sum_{r_1=1}^{R_1} \sum_{r_2=1}^{R_2} \sum_{r_3=1}^{R_3} (\mathbf{g}_{r_1}^{(1)} \circ \mathbf{g}_{r_2}^{(2)} \circ \mathbf{g}_{r_3}^{(3)} \circ \mathbf{g}_{r_4}^{(4)})$ (for $R_1 = 3, R_2 = 4, R_3 = 5; R_0 = R_4 = 1$). All vectors $\mathbf{g}_{r_{n-1}, r_n}^{(n)} \in \mathbb{R}^{I_n}$ are considered as the column vectors.

In a compact tensor form using multilinear products:

$$\begin{aligned} \mathbf{X} &\cong \mathbf{A} \times_2^1 \mathbf{G}^{(2)} \times_3^1 \mathbf{G}^{(3)} \times_3^1 \dots \times_3^1 \mathbf{G}^{(N-1)} \times_3^1 \mathbf{B} \\ &= [\mathbf{A}, \mathbf{G}^{(2)}, \mathbf{G}^{(3)}, \dots, \mathbf{G}^{(N-1)}, \mathbf{B}], \end{aligned} \quad (24)$$

where 3rd-order cores are defined as $\mathbf{G}^{(n)} \in \mathbb{R}^{R_{n-1} \times I_n \times R_n}$ for $n = 2, 3, \dots, N-1$ (see Fig. 25).

By employing the unfolding of cores $\mathbf{G}^{(n)}$ and suitable reshaping of matrices, we can obtain other very useful mathematical and graphical descriptions of the MPS, for example, as summation of rank-1 tensors using outer (tensor) product (similar to CPD, Tucker and PARATREE formats):

$$\mathbf{X} \cong \sum_{r_1, r_2, \dots, r_{N-1}=1}^{R_1, R_2, \dots, R_{N-1}} \mathbf{g}_{r_1}^{(1)} \circ \mathbf{g}_{r_1, r_2}^{(2)} \circ \mathbf{g}_{r_2, r_3}^{(3)} \circ \dots \circ \mathbf{g}_{r_{N-1}}^{(N)} \quad (25)$$

where $\mathbf{g}_{r_{n-1}, r_n}^{(n)} \in \mathbb{R}^{I_n}$ are column vectors of matrices $\mathbf{G}^{(n)} = [\mathbf{g}_{1,1}^{(n)}, \mathbf{g}_{2,1}^{(n)}, \dots, \mathbf{g}_{R_{n-1},1}^{(n)}, \mathbf{g}_{1,2}^{(n)}, \dots, \mathbf{g}_{R_{n-1},R_n}^{(n)}] \in \mathbb{R}^{I_n \times R_{n-1} \times R_n}$ ($n = 1, 2, \dots, N$), with $R_0 = R_N = 1$. Note that $\mathbf{g}_{r_1}^{(1)} = \mathbf{a}_{r_1}$ are columns of the matrix $\mathbf{A} = [\mathbf{a}_1, \mathbf{a}_2, \dots, \mathbf{a}_{R_1}] \in \mathbb{R}^{I_1 \times R_1}$, while $\mathbf{g}_{r_{N-1}}^{(N)} = \mathbf{b}_{r_{N-1}}$ are vector of the transpose factor matrix $\mathbf{B}^T = [\mathbf{b}_1, \mathbf{b}_2, \dots, \mathbf{b}_{R_{N-1}}] \in \mathbb{R}^{I_N \times R_{N-1}}$ (see Fig. 25). The minimal $(N-1)$ tuple $\{R_1, R_2, \dots, R_{N-1}\}$ is called TT-rank.

Alternatively, we can use the standard scalar form:

$$x_{i_1, i_2, \dots, i_N} \cong \sum_{r_1, r_2, \dots, r_{N-1}=1}^{R_1, R_2, \dots, R_{N-1}} g_{i_1, r_1}^{(1)} g_{r_1, i_2, r_2}^{(2)} g_{r_2, i_3, r_3}^{(3)} \dots g_{r_{N-1}, i_N}^{(N)} \quad (26)$$

or equivalently using slice representations (see Fig. 26):

$$\begin{aligned} x_{i_1, i_2, \dots, i_N} &\cong \mathbf{G}^{(1)}(i_1) \mathbf{G}^{(2)}(i_2) \dots \mathbf{G}^{(N)}(i_N) \\ &= \mathbf{g}^{(1)T}(i_1) \mathbf{G}^{(2)}(i_2) \dots \mathbf{g}^{(N)}(i_N), \end{aligned} \quad (27)$$

where slice matrices $\mathbf{G}^{(n)}(i_n) = \mathbf{G}^{(n)}(:, i_n, :) = \mathbf{G}_{R_{n-1}, R_n}^{(n)}(i_n) \in \mathbb{R}^{R_{n-1} \times R_n}$ (with $\mathbf{G}^{(1)}(i_1) = \mathbf{g}^{(1)T}(i_1) \in \mathbb{R}^{1 \times R_1}$ and $\mathbf{G}^{(N)}(i_N) = \mathbf{g}^{(N)}(i_N) \in \mathbb{R}^{R_{N-1} \times 1}$ are the lateral slices of the cores $\mathbf{G}^{(n)} \in \mathbb{R}^{R_{n-1} \times I_n \times R_n}$ for $n = 1, 2, \dots, N$ with $R_0 = R_N = 1$).

By representing the cores $\mathbf{G}^{(n)} \in \mathbb{R}^{R_{n-1} \times I_n \times R_n}$ by unfolding matrices $\tilde{\mathbf{G}}^{(n)} = (\mathbf{G}^{(n)})^T \in \mathbb{R}^{R_{n-1} I_n \times R_n}$ for $n = 1, 2, \dots, N$ with $R_0 = R_N = 1$ and considering them as block matrices with blocks $\mathbf{g}_{r_{n-1}, r_n}^{(n)} \in \mathbb{R}^{I_n \times 1}$, we can express the TT/MPS in the matrix form via strong Kronecker products (see Fig. 27 (c) and Fig. 28):

$$\mathbf{x}_{i_1, i_2, \dots, i_N} \cong \tilde{\mathbf{G}}^{(1)} | \otimes | \tilde{\mathbf{G}}^{(2)} | \otimes | \dots | \otimes | \tilde{\mathbf{G}}^{(N-1)} | \otimes | \tilde{\mathbf{G}}^{(N)}, \quad (28)$$

where the vector $\mathbf{x}_{i_1, i_2, \dots, i_N} = \mathbf{x}_{(1:N)} \in \mathbb{R}^{I_1 I_2 \dots I_N}$ denotes vectorization of the tensor \mathbf{X} in reverse lexicographical order of indices and $| \otimes |$ denotes strong Kronecker product (see Fig. 28 for definition).

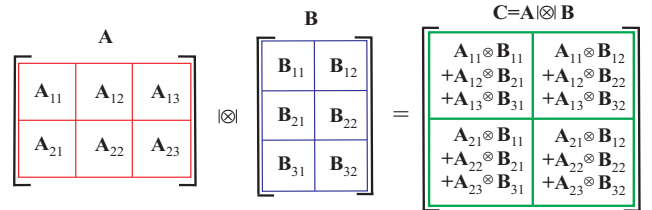


Figure 28: Illustration of definition of the strong Kronecker product for two block matrices. The strong Kronecker product of two block matrices $\mathbf{A} \in \mathbb{R}^{R_1 I_1 \times R_2 I_2}$ and $\mathbf{B} \in \mathbb{R}^{R_3 I_3 \times R_4 I_4}$ is defined as the block matrix $\mathbf{C} = \mathbf{A} | \otimes | \mathbf{B} = \sum_{r_2=1}^{R_2} \mathbf{A}_{r_1, r_2} \otimes \mathbf{B}_{r_2, r_3} \in \mathbb{R}^{R_1 I_1 I_3 \times R_3 I_2 I_4}$, where $\mathbf{A}_{r_1, r_2} \in \mathbb{R}^{I_1 \times I_2}$ and $\mathbf{B}_{r_2, r_3} \in \mathbb{R}^{I_3 \times I_4}$ are block matrices of \mathbf{A} and \mathbf{B} , respectively. In a similar way, we define a strong Kronecker product of two block tensors (see next section).

Another important model of TT, called also MPO (Ma-

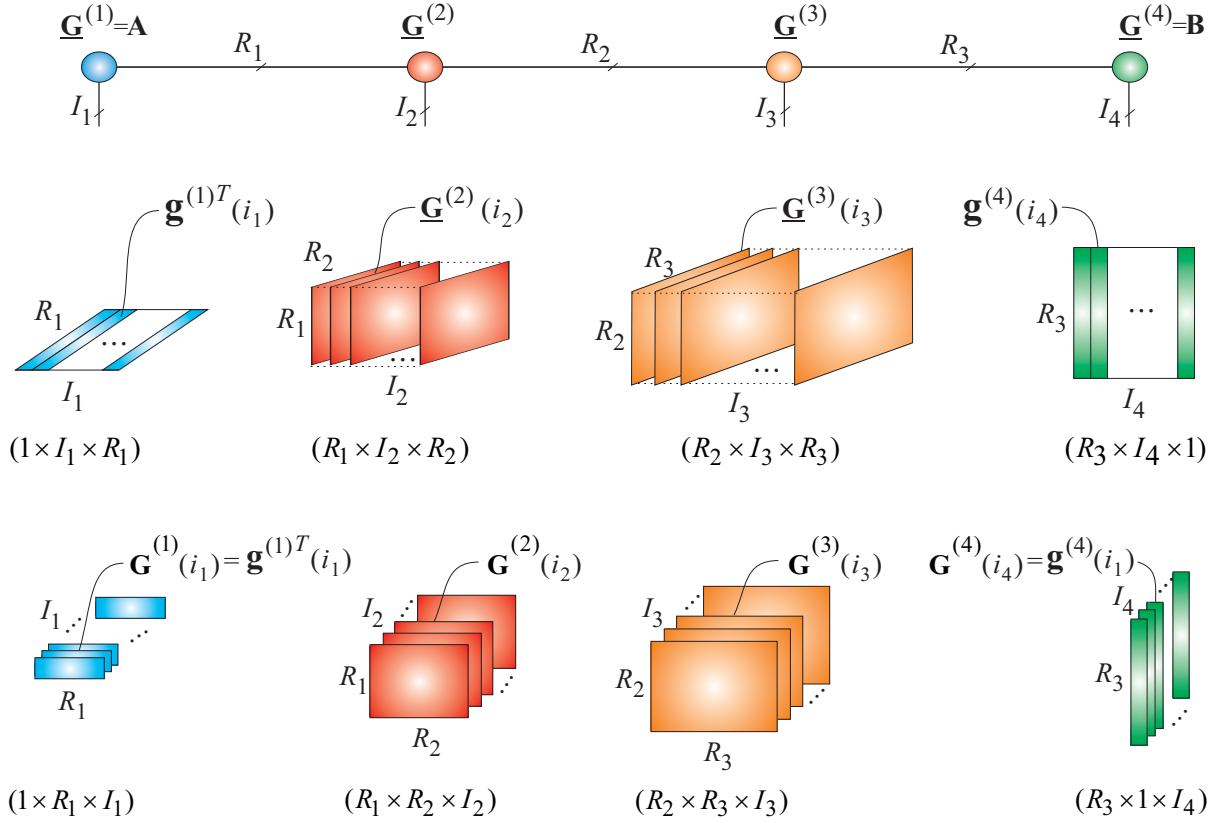


Figure 26: Illustration of tensor train decomposition (TT/MPS) of a 4th-order data tensor $\mathbf{X} \in \mathbb{R}^{I_1 \times I_2 \times I_3 \times I_4}$ represented in a scalar form via slice matrices as: $x_{i_1, i_2, i_3, i_4} \cong \mathbf{g}^{(1)T}(i_1) \mathbf{G}^{(2)}(i_2) \mathbf{G}^{(3)}(i_3) \mathbf{g}^{(4)}(i_4) = \sum_{r_1, r_2, r_3, r_4=1}^{R_1, R_2, R_3, R_4} g_{i_1, r_1}^{(1)} g_{r_1, i_2, r_2}^{(2)} g_{r_2, i_3, r_3}^{(3)} g_{r_3, i_4, r_4}^{(4)}$.

trix Product Operator with Open Boundary Conditions), consists of chain (train) of 3rd-order and 4th-order cores as illustrated in Fig. 29. Note that a 3rd-order tensor can be represented equivalently as a block (column or row) vector in which each element (block) is a matrix (lateral slice) of the tensor, while a 4th-order tensor can be represented equivalently as a block matrix. The TT/MPO model for $2N$ th-order tensor $\mathbf{X} \in \mathbb{R}^{I_1 \times I_2 \times \dots \times I_{2N}}$ can be described mathematically in the following general forms (see also Table III):

A) In the tensor compact form using multilinear products

$$\begin{aligned} \mathbf{X} &\cong \mathbf{G}^{(1)} \times_{I_1}^1 \mathbf{G}^{(2)} \times_{I_2}^1 \dots \times_{I_N}^1 \mathbf{G}^{(N)} \\ &= [\mathbf{G}^{(1)}, \mathbf{G}^{(2)}, \dots, \mathbf{G}^{(N)}], \end{aligned} \quad (29)$$

where the cores are defined as $\mathbf{G}^{(n)} \in \mathbb{R}^{R_{n-1} \times I_{2n-1} \times I_{2n} \times R_n}$, with $R_0 = R_N = 1$, ($n = 1, 2, \dots, N$).

B) Equivalently, we can use the standard (long and tedious) scalar form:

$$\begin{aligned} x_{i_1, i_2, \dots, i_{2N}} &\cong \sum_{r_1=1}^{R_1} \sum_{r_2=1}^{R_2} \dots \sum_{r_{N-1}=1}^{R_{N-1}} g_{i_1, i_2, r_1}^{(1)} g_{r_1, i_3, i_4, r_2}^{(2)} \dots \\ &\dots g_{r_{N-2}, i_{2N-3}, i_{2N-2}, r_{N-1}}^{(N-1)} g_{r_{N-1}, i_{2N-1}, i_{2N}}^{(N)}. \end{aligned} \quad (30)$$

C) Alternatively, using matrix representations of cores, the TT/MPO decomposition can be expressed by strong

Kronecker products (see Fig. 29):

$$\mathbf{X}_{(\overline{1,3,\dots,2N-1}; \overline{2,4,\dots,2N})} \cong \tilde{\mathbf{G}}^{(1)} \otimes \tilde{\mathbf{G}}^{(2)} \otimes \dots \otimes \tilde{\mathbf{G}}^{(N)}, \quad (31)$$

where $\mathbf{X}_{(\overline{1,3,\dots,2N-1}; \overline{2,4,\dots,2N})} \in \mathbb{R}^{I_1 I_3 \dots I_{2N-1} \times I_2 I_4 \dots I_{2N}}$ is unfolding matrix of \mathbf{X} in reverse lexicographical order of indices and $\tilde{\mathbf{G}}^{(n)} \in \mathbb{R}^{R_{n-1} I_{2n-1} \times R_n I_{2n}}$ are block matrices with blocks $\mathbf{G}_{r_{n-1}, r_n}^{(n)} \in \mathbb{R}^{I_{2n-1} \times I_{2n}}$ and the number of blocks $R_{n-1} \times R_n$. In the special case when ranks of the TT/MPO $R_n = 1$, $\forall n$ the strong Kronecker products simplify to the standard Kronecker products.

The Tensor Train (TT) format [51], can be interpreted as a special case of the HT [7], where all nodes of the underlying tensor network are aligned and where, moreover, the leaf matrices are assumed to be identities (and thus need not be stored). An advantage of the TT format is its simpler practical implementation using SVD or alternative low-rank matrix approximations, as no binary tree need be involved [17], [59] (see Figs. 30 and 31).

There are two different types of approaches to perform tensor approximation via TT [20]. A first class of methods is based on combining standard iterative algorithms, with a low-rank decompositions, such as SVD/QR or CUR or Cross-Approximations. Similar to the Tucker decomposition, the TT and HT decompositions are usually based on low rank approximation of generalized unfolding matrices $\mathbf{X}_{([n])}$, and a good approximation in a

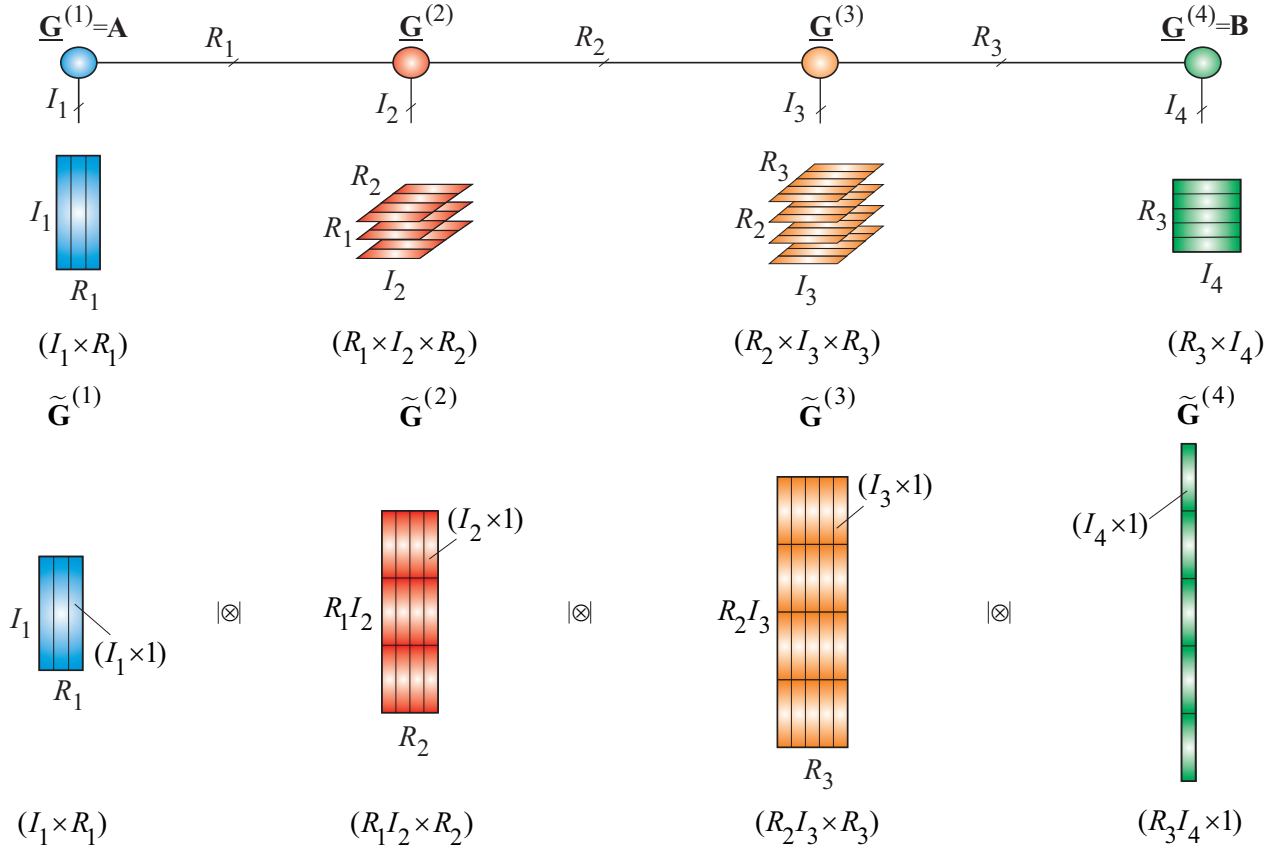


Figure 27: Alternative representation of the tensor train decomposition (TT/MPS) expressed via strong Kronecker products of block matrices in the form of a vector as: $\mathbf{x}_{i_1 i_2 i_3 i_4} \cong \tilde{\mathbf{G}}^{(1)} | \otimes | \tilde{\mathbf{G}}^{(2)} | \otimes | \tilde{\mathbf{G}}^{(3)} | \otimes | \tilde{\mathbf{G}}^{(4)} \in \mathbb{R}^{I_1 I_2 I_3 I_4}$, where block matrices are defined as $\tilde{\mathbf{G}}^{(n)} \in \mathbb{R}^{R_{n-1} I_n \times R_n}$, with block vectors $\mathbf{g}_{i_{n-1} i_n}^{(n)} \in \mathbb{R}^{I_n \times 1}$ for $n = 1, 2, 3, 4$ and $R_0 = R_4 = 1$. For an illustrative purpose, we assumed that $N = 4$, $R_1 = 3$, $R_2 = 4$ and $R_3 = 5$.

decomposition for a given TT/HT-rank can be obtained using the truncated SVDs of the unfolding matrices [51], [59].

In [46] Oseledets and Tyrtshnikov proposed for TT decomposition a new approximative formula in which a N th-order data tensor is interpolated using special form of Cross-Approximation, which is modification of CUR algorithm. The total number of entries and the complexity of the interpolation algorithm depend on the order of data tensor N linearly, so the developed algorithm does not suffer from the curse of dimensionality. The TT-Cross-Approximation is analog to the SVD/HOSVD like algorithms for TT/MPS, but uses the adaptive cross-approximation instead of the computational more expensive SVD.

A second class of algorithms based on optimizations of suitable designed cost functions, often with additional penalty or regularization terms, and applying various optimization techniques such as gradient descent, conjugate gradient, and Newton-like methods (see [20], [60] and references therein). Gradient descent methods leads often to the Alternating Least Squares (ALS) like algorithms, which can be improved in various ways [60], [61] (see Fig. 32).

One quite successful improvement for TNs (TT, HT) is called the DMRG method which join two neighboring factors (cores), optimize the resulting “superdose”, and split the result into separate factors by a low-rank matrix factorization [18], [57], [58], [60] (see Fig. 33).

Remark: In most optimization problems it is very convenient to present TT in a canonical form, in which all cores are left or right orthogonal [60], [62] (see also Fig. 32 and Fig. 33).

The N -order core tensor is called right-orthogonal if

$$\mathbf{G}_{(1)} \mathbf{G}_{(1)}^T = \mathbf{I}. \quad (32)$$

Analogously the N -order core tensor is called left orthogonal if

$$\mathbf{G}_{(N)} \mathbf{G}_{(N)}^T = \mathbf{I}. \quad (33)$$

In contrast, for the all-orthogonal core tensor we have $\mathbf{G}_{(n)} \mathbf{G}_{(n)}^T = \mathbf{I}, \forall n$.

TT-Rounding TT-rounding (also called truncation or recompression) [46] is post-processing procedure to reduce the TT ranks which in the first stage after applying low-rank matrix factorizations are usually not optimal with respect of desired approximation errors. The optimal computation of TT-tensor is generally impossible

TABLE III: Different forms of the Tensor Trains (TT): MPS and MPO (with open boundary conditions) representations of an N th-order tensor $\mathbf{X} \in \mathbb{R}^{I_1 \times I_1 \times \dots \times I_N}$ and a $2N$ th-order tensor $\mathbf{Y} \in \mathbb{R}^{I_1 \times I_1 \times \dots \times I_N \times J_1 \times J_2 \times \dots \times J_N}$, respectively. It is assumed that the TT rank is $\{R_1, R_2, \dots, R_{N-1}\}$, with $R_0 = R_N = 1$ ($r_0 = r_N = 1$).

TT/MPS	TT/MPO
Scalar (standard) Representations	
$x_{i_1, i_2, \dots, i_N} = \sum_{r_1, r_2, \dots, r_{N-1}=1}^{R_1, R_2, \dots, R_{N-1}} g_{i_1, r_1}^{(1)} g_{r_1, i_2, r_2}^{(2)} g_{r_2, i_3, r_3}^{(3)} \dots g_{r_{N-1}, i_N}^{(N)}$	$y_{i_1, j_1, i_2, j_2, \dots, i_N, j_N} = \sum_{r_1, r_2, \dots, r_{N-1}=1}^{R_1, R_2, \dots, R_{N-1}} g_{i_1, j_1, r_1}^{(1)} g_{r_1, i_2, j_2, r_2}^{(2)} \dots g_{r_{N-1}, i_N, j_N}^{(N)}$
$g_{r_{n-1}, i_n, r_n}^{(n)}$ entries of a 3rd-order core $\underline{\mathbf{G}}^{(n)} \in \mathbb{R}^{R_{n-1} \times I_n \times R_n}$	$g_{r_{n-1}, i_n, j_n, r_n}^{(n)}$ entries of a 4th-order core $\underline{\mathbf{G}}^{(n)} \in \mathbb{R}^{R_{n-1} \times I_n \times J_n \times R_n}$
Slice Representations	
$x_{i_1, i_2, \dots, i_N} = \mathbf{G}^{(1)}(i_1) \mathbf{G}^{(2)}(i_2) \dots \mathbf{G}^{(N-1)}(i_{N-1}) \mathbf{G}^{(N)}(i_N)$	$y_{i_1, j_1, i_2, j_2, \dots, i_N, j_N} = \mathbf{G}^{(1)}(i_1, j_1) \mathbf{G}^{(2)}(i_2, j_2) \dots \mathbf{G}^{(N)}(i_N, j_N)$
$\mathbf{G}^{(n)}(i_n) \in \mathbb{R}^{R_{n-1} \times R_n}$ lateral slices of cores $\underline{\mathbf{G}}^{(n)}$	$\mathbf{G}^{(n)}(i_n, j_n) \in \mathbb{R}^{R_{n-1} \times R_n}$ slices of cores $\underline{\mathbf{G}}^{(n)}$
Tensor Representations: Multilinear Products (tensor contractions)	
$\mathbf{X} = \underline{\mathbf{G}}^{(1)} \times_3^1 \underline{\mathbf{G}}^{(2)} \times_3^1 \dots \times_3^1 \underline{\mathbf{G}}^{(N-1)} \times_3^1 \underline{\mathbf{G}}^{(N)}$	$\mathbf{Y} = \underline{\mathbf{G}}^{(1)} \times_4^1 \underline{\mathbf{G}}^{(2)} \times_4^1 \dots \times_4^1 \underline{\mathbf{G}}^{(N-1)} \times_4^1 \underline{\mathbf{G}}^{(N)}$
$\underline{\mathbf{G}}^{(n)} \in \mathbb{R}^{R_{n-1} \times I_n \times R_n}, (n = 1, 2, \dots, N)$	$\underline{\mathbf{G}}^{(n)} \in \mathbb{R}^{R_{n-1} \times I_n \times J_n \times R_n}$
Tensor Representations: Outer Products	
$\mathbf{X} = \sum_{r_1, r_2, \dots, r_{N-1}=1}^{R_1, R_2, \dots, R_{N-1}} g_{r_1}^{(1)} \circ g_{r_1, r_2}^{(2)} \circ \dots \circ g_{r_{N-2}, r_{N-1}}^{(N-1)} \circ g_{r_{N-1}}^{(N)}$	$\mathbf{Y} = \sum_{r_1, r_2, \dots, r_{N-1}=1}^{R_1, R_2, \dots, R_{N-1}} \mathbf{G}_{r_1}^{(1)} \circ \mathbf{G}_{r_1, r_2}^{(2)} \circ \dots \circ \mathbf{G}_{r_{N-2}, r_{N-1}}^{(N-1)} \circ \mathbf{G}_{r_{N-1}}^{(N)}$
$g_{r_{n-1}, r_n}^{(n)} \in \mathbb{R}^{I_n}$ blocks of a matrix $\tilde{\mathbf{G}}^{(n)} = (\mathbf{G}_{(3)}^{(n)})^T \in \mathbb{R}^{R_{n-1} I_n \times R_n}$	$\mathbf{G}_{r_{n-1}, r_n}^{(n)} \in \mathbb{R}^{I_n \times J_n}$ blocks of a matrix $\tilde{\mathbf{G}}^{(n)} \in \mathbb{R}^{R_{n-1} I_n \times R_n J_n}$
Vector/Matrix Representations: Strong Kronecker Products	
$\mathbf{x}_{(\overline{i_1 \dots i_N})} = \tilde{\mathbf{G}}^{(1)} \otimes \tilde{\mathbf{G}}^{(2)} \otimes \dots \otimes \tilde{\mathbf{G}}^{(N)} \in \mathbb{R}^{I_1 I_2 \dots I_N}$	$\mathbf{Y}_{(\overline{i_1 \dots i_N}; \overline{j_1 \dots j_N})} = \tilde{\mathbf{G}}^{(1)} \otimes \tilde{\mathbf{G}}^{(2)} \otimes \dots \otimes \tilde{\mathbf{G}}^{(N)} \in \mathbb{R}^{I_1 \dots I_N \times J_1 \dots J_N}$
$\tilde{\mathbf{G}}^{(n)} \in \mathbb{R}^{R_{n-1} I_n \times R_n}$ a block matrix with blocks $g_{r_{n-1}, r_n}^{(n)} \in \mathbb{R}^{I_n}$	$\tilde{\mathbf{G}}^{(n)} \in \mathbb{R}^{R_{n-1} I_n \times R_n J_n}$ a block matrix with blocks $\mathbf{G}_{r_{n-1}, r_n}^{(n)} \in \mathbb{R}^{I_n \times J_n}$

without TT-rounding. The tensor expressed already in TT format is approximated by another TT-tensor with smaller TT-ranks but with prescribed accuracy of approximation ϵ . The most popular TT-rounding algorithm is based on QR/SVD the algorithm which requires $O(NIR^3)$ operations [17], [63]. In practice, we avoid the explicit construction of these matrices and the SVDs when truncating a tensor in TT decomposition to lower TT-rank. Such truncation algorithms for TT are described by Oseledets in [51]. In fact, the method exploits micro-iterations algorithm where the SVD is performed only on relatively small cores at each iteration. Similar approach has been developed by Grasedyck for HT [64]. HT/TT algorithms that avoid the explicit computation of these SVDs when truncating a tensor that is already in tensor network format are discussed in [18], [20], [65].

TT Toolbox developed by Oseledets (http://spring.inm.ras.ru/osel/?page_id=24) is focussed on TT structures, which deals with the curse of dimensionality [63]. The Hierarchical Tucker (HT) toolbox by Kressner and Tobler (http://www.sam.math.ethz.ch/NLAGroup/htucker_toolbox.html) and Calculus library by Hackbusch, Waehnert and Espig, focuss mostly on HT and TT tensor networks [18], [63], [65]. See also recently developed TDALAB (<http://bsp.brain.riken.jp/TDALAB>) and TENSORBOX (<http://www.bsp.brain.riken.jp/~phan>) that provide user-friendly interface and advanced algorithms for selected TD (Tucker, CPD) models [66], [67]. The \langle <http://www.esat.kuleuven.be/sista/tensorlab/> \rangle Tensorlab toolbox builds upon the complex optimization framework and offers efficient numerical algorithms for computing the TDs with various con-

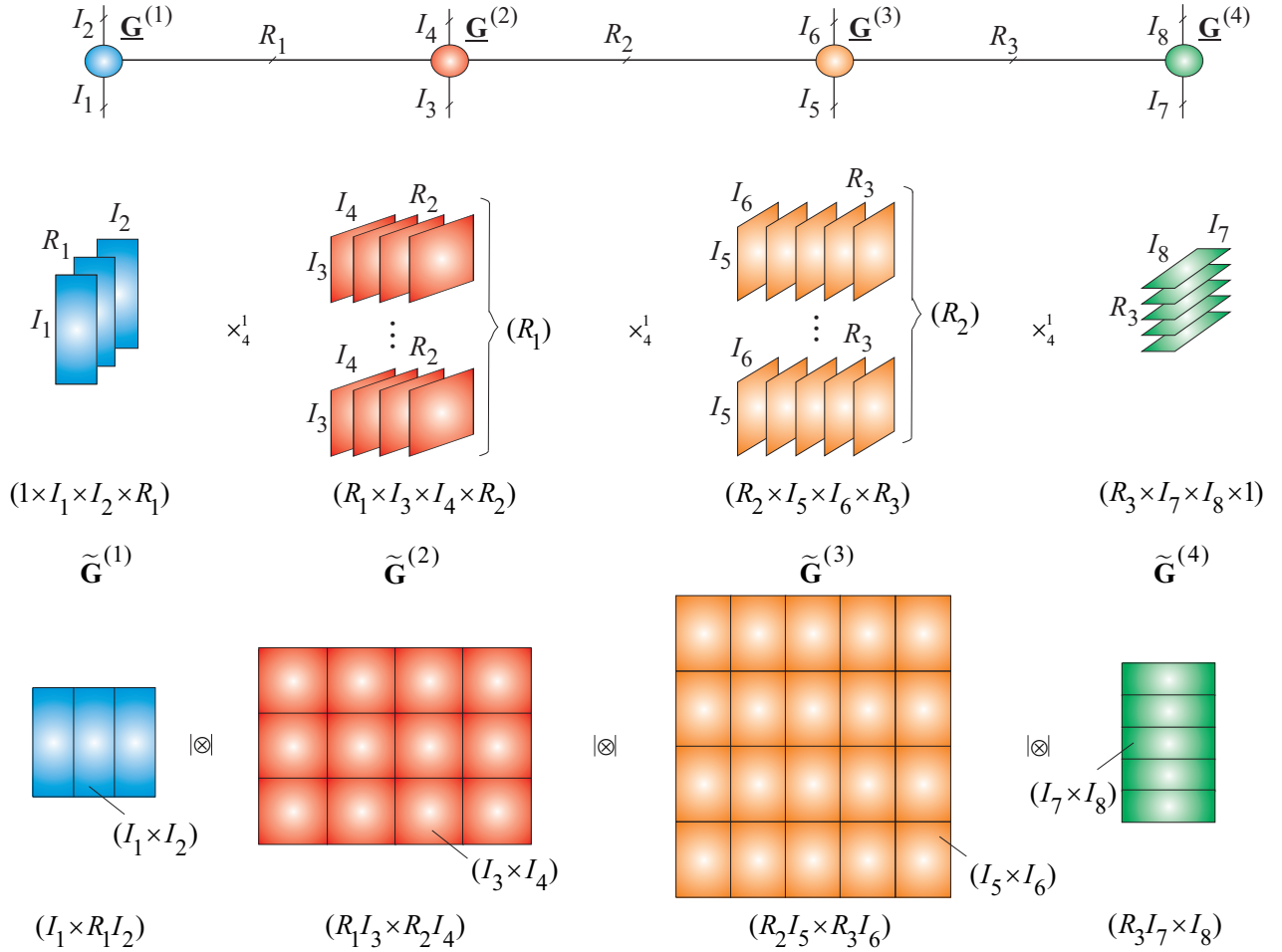


Figure 29: Illustration of tensor train decomposition (TT/MPO) for an 8th-order data tensor or equivalently multidimensional matrix $\mathbf{X} \in \mathbb{R}^{\bar{I}_1 \times \bar{I}_2}$, with $\bar{I}_1 = I_1 I_3 I_5 I_7$ and $\bar{I}_2 = I_2 I_4 I_6 I_8$, expressed by the chain of 4th-order cores as: $\mathbf{X} \cong \mathbf{G}^{(1)} \times_4^1 \mathbf{G}^{(2)} \times_4^1 \mathbf{G}^{(3)} \times_4^1 \mathbf{G}^{(4)} = \llbracket \mathbf{G}^{(1)}, \mathbf{G}^{(2)}, \mathbf{G}^{(3)}, \mathbf{G}^{(4)} \rrbracket$ or in a scalar form as $x_{i_1, i_2, \dots, i_8} \cong \sum_{r_1=1}^{R_1} \sum_{r_2=1}^{R_2} \sum_{r_3=1}^{R_3} g_{i_1, r_1, i_2}^{(1)} g_{r_1, i_2, r_2, i_3}^{(2)} g_{r_2, i_3, r_3, i_4}^{(3)} g_{r_3, i_4, i_5, i_6}^{(4)}$. Alternatively, the TT/MPS decomposition can be expressed in a compact and elegant matrix form as strong Kronecker product of block matrices $\tilde{\mathbf{G}}^{(n)} = \mathbf{G}_{(r_{n-1} i_{2n-1}, r_n i_{2n})}^{(n)} \in \mathbb{R}^{R_{n-1} I_{2n-1} \times R_n I_{2n}}$ (with blocks $\mathbf{G}_{r_{n-1}, r_n}^{(n)} \in \mathbb{R}^{I_{2n-1} \times I_{2n}}$) as: $\mathbf{X}_{(\bar{1}, \bar{3}, \bar{5}, \bar{7}; \bar{2}, \bar{4}, \bar{6}, \bar{8})} \cong \tilde{\mathbf{G}}^{(1)} | \otimes \tilde{\mathbf{G}}^{(2)} | \otimes \tilde{\mathbf{G}}^{(3)} | \otimes \tilde{\mathbf{G}}^{(4)} \in \mathbb{R}^{\bar{I}_1 \times \bar{I}_2}$. For simplicity, we assumed that $R_1 = 3$, $R_2 = 4$ and $R_3 = 5$.

straints (e.g. nonnegativity, orthogonality) and the possibility to combine and jointly factorize dense, sparse and incomplete tensors [68]. The problems related to optimization of existing TN/TD algorithms are active area of research [20], [60], [61].

X. Hierarchical Outer Product Tensor Approximation (HOPTA) and Kronecker Tensor Decompositions

Recent advances in TDs/TNs include, TT/HT [20], [52], [60], PARATREE [69], Block Term Decomposition (BTD) [70], Hierarchical Outer Product Tensor Approximation (HOPTA) and Kronecker Tensor Decomposition (KTD) [71]–[73].

The HOPTA and KTD can be expressed mathematically in simple recursive (hierarchical) forms, respec-

tively (see Fig. 34 and Fig. 35):

$$\underline{\mathbf{X}} \cong \sum_{r=1}^R (\underline{\mathbf{A}}_r \circ \underline{\mathbf{B}}_r), \quad (34)$$

$$\tilde{\mathbf{X}} = \sum_{r=1}^R (\underline{\mathbf{A}}_r \otimes \underline{\mathbf{B}}_r), \quad (35)$$

where each factor tensor can be represented recursively by formulas $\underline{\mathbf{A}}_r \cong \sum_{r_1=1}^{R_1} (\underline{\mathbf{A}}_{r_1}^{(1)} \circ \underline{\mathbf{B}}_{r_1}^{(1)})$ and $\underline{\mathbf{B}}_r \cong \sum_{r_2=1}^{R_2} \underline{\mathbf{A}}_{r_2}^{(2)} \circ \underline{\mathbf{B}}_{r_2}^{(2)}$, etc.

The Kronecker product of two tensors: $\underline{\mathbf{A}} \in \mathbb{R}^{I_1 \times I_2 \times \dots \times I_N}$ and $\underline{\mathbf{B}} \in \mathbb{R}^{J_1 \times J_2 \times \dots \times J_N}$ yields $\underline{\mathbf{C}} = \underline{\mathbf{A}} \otimes \underline{\mathbf{B}} \in \mathbb{R}^{I_1 I_2 \times \dots \times I_N J_N}$ with entries $c_{i_1 \otimes j_1, \dots, i_N \otimes j_N} = a_{i_1, \dots, i_N} b_{j_1, \dots, j_N}$, where the operator \otimes for indices $i_n = 1, 2, \dots, I_n$ and $j_n = 1, 2, \dots, J_n$ is defined as follows $i_n \otimes j_n = j_n + (i_n - 1)J_n$ (see Fig. 34).

Note that the $2N$ th-order sub-tensors $\underline{\mathbf{A}}_r \circ \underline{\mathbf{B}}_r$ and $\underline{\mathbf{A}}_r \otimes \underline{\mathbf{B}}_r$ actually have the same elements, arranged differently. For example, if $\underline{\mathbf{X}} = \underline{\mathbf{A}} \circ \underline{\mathbf{B}}$ and $\underline{\mathbf{X}}' = \underline{\mathbf{A}} \otimes \underline{\mathbf{B}}$,

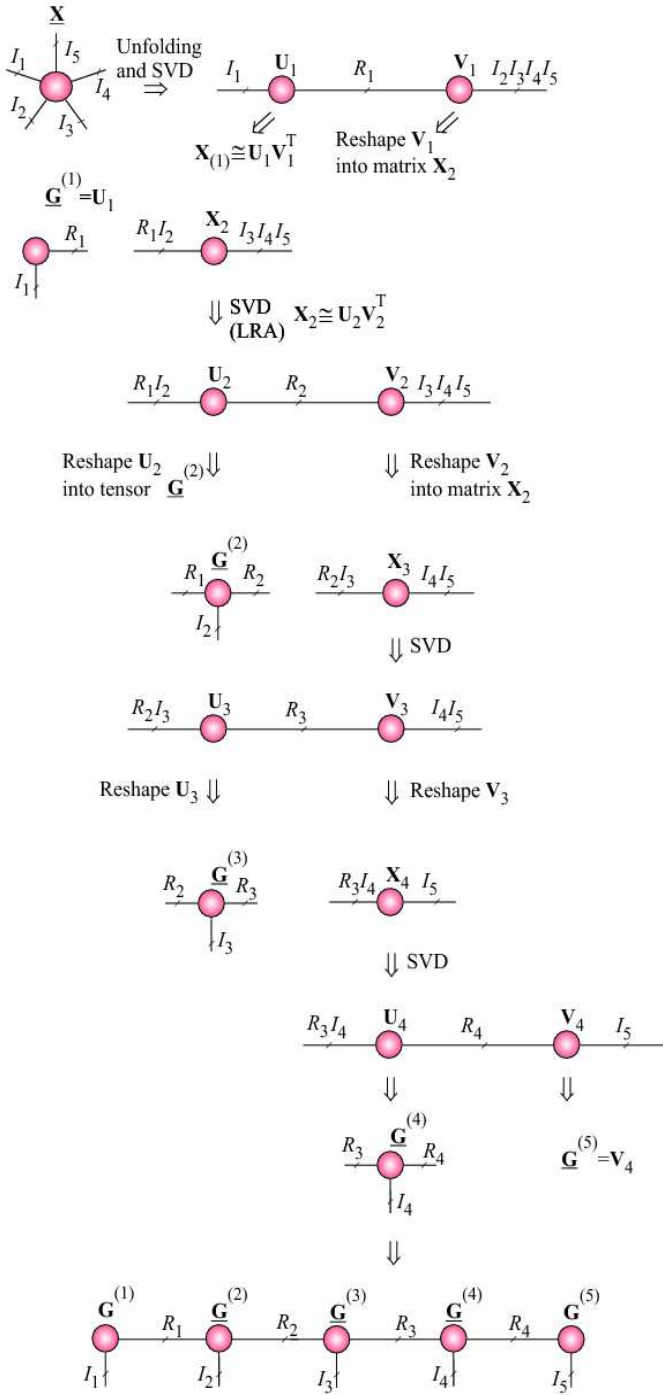


Figure 30: Illustration of the SVD algorithm for TT/MPS for a 5th-order tensor. Instead of the truncated SVD, we can employ any low-rank matrix approximation (LRA), especially QR, CUR, SCA, ICA, NMF.

where $\mathbf{A} \in \mathbb{R}^{I_1 \times I_2 \times \dots \times I_N}$ and $\mathbf{B} \in \mathbb{R}^{K_1 \times K_2 \times \dots \times K_N}$, then $x_{j_1, j_2, \dots, j_N, k_1, k_2, \dots, k_N} = x'_{k_1 + K_1(j_1 - 1), \dots, k_N + K_N(j_N - 1)}$.

It is interesting to note that the KTD and HOPTA can be considered in special cases as a flexible form of Block Term Decomposition (BTD) introduced first by De Lathauwer [30], [70], [74], [75].

The definition of the tensor Kronecker product as-

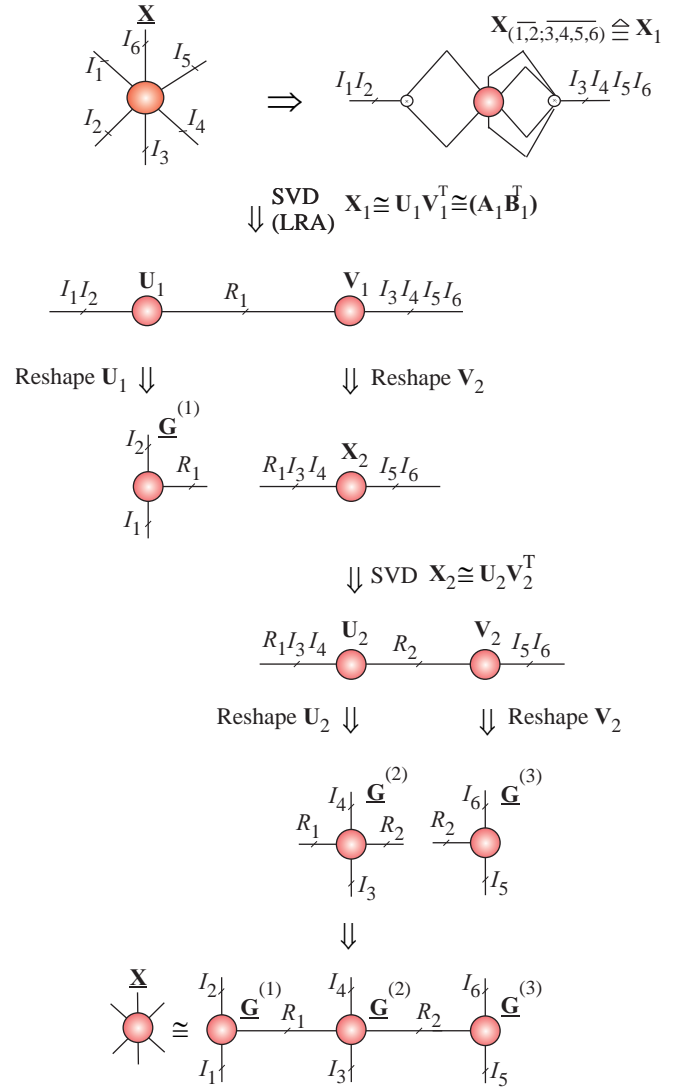


Figure 31: Illustration of SVD algorithm for TT/MPO for a 6th-order tensor. Instead of the SVD we can use alternative Low-Rank Approximation (LRA) (constrained matrix factorizations, e.g., CUR or NMF).

sumes that both core tensors \mathbf{A}_r and \mathbf{B}_r have the same order. It should be noted that vectors and matrices can be treated as tensors, e.g., matrix of dimension $I \times J$ can be treated formally as 3rd-order tensor of dimension $I \times J \times 1$. In fact, from the KTD model, we can generate many existing and emerging TDs by changing structures and orders of factor tensors: \mathbf{A}_r and \mathbf{B}_r , for example:

- If \mathbf{A}_r are rank-1 tensors of size $I_1 \times I_2 \times \dots \times I_N$, and \mathbf{B}_r are scalars, $\forall r$, then (35) expresses the rank- R CPD.
- If \mathbf{A}_r are rank- L_r tensors in the Kruskal (CP) format, of size $I_1 \times I_2 \times \dots \times I_R \times 1 \times \dots \times 1$, and \mathbf{B}_r are rank-1 CP tensor of size $1 \times \dots \times 1 \times I_{R+1} \times \dots \times I_N$, $\forall r$, then (35) expresses the rank- $(L_r \circ 1)$ BTD [70].
- If \mathbf{A}_r and \mathbf{B}_r are expressed by KTDs, we have Nested Kronecker Tensor Decomposition (NKTD), where Tensor Train (TT) decomposition is a particular case [51], [52], [76]. In fact, the model (35) can be used

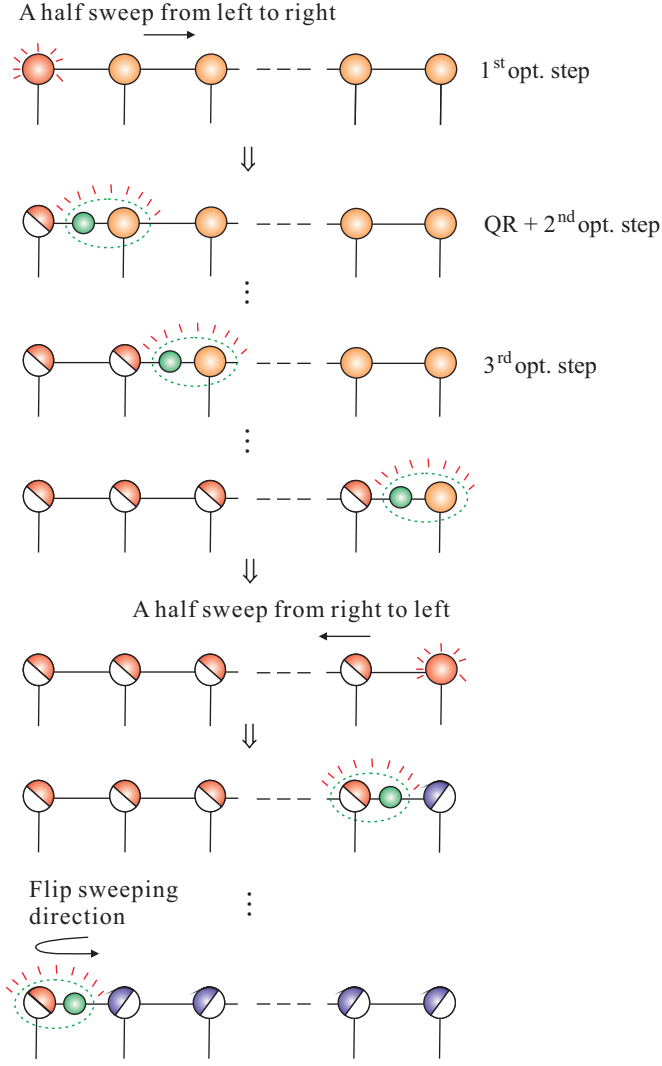


Figure 32: Extension of the ALS algorithm for TT decomposition. The main idea is to optimize only one core tensor at a time (by a minimization of suitable cost function), while fixing the others. Optimization of each core tensor followed by orthogonalization step via the QR or more expensive SVD decomposition. Factor matrices \mathbf{R} are absorbed (incorporated) by the following core.

for) the recursive TT-decompositions [51].

In this way, a large variety of tensor decomposition models can be generated. However, only some of them have unique decompositions and to date only a few have found concrete applications.

The advantage of HOPTA models over BTM and KTD is that they are more flexible and can approximate very high order tensors with a relative small number of cores, and allow us to model more complicated data structures.

XI. Tensorization and Quantization – Blessing of Dimensionality

A. Curse of Dimensionality

The term curse of dimensionality, in the context of tensors, refers to the fact that the number of elements

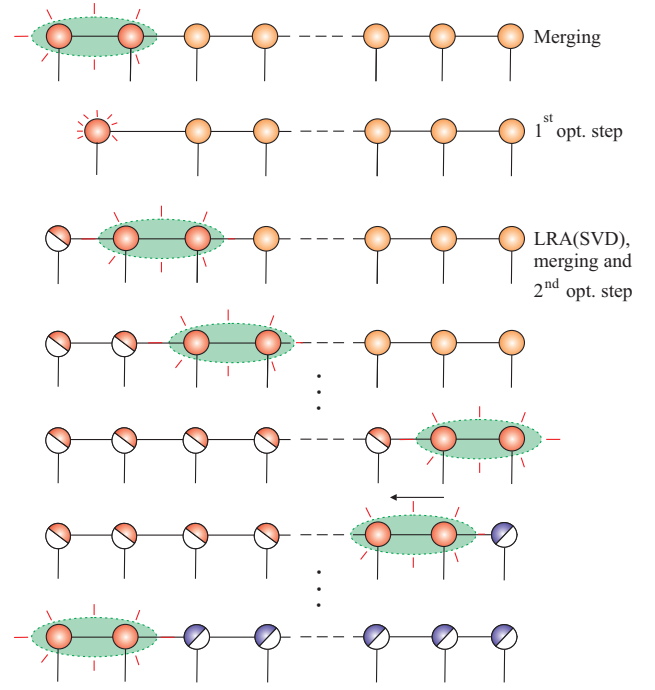


Figure 33: Modified ALS (MALS) algorithm related to the Density Matrix Renormalization Group (DMRG) for TT decomposition. In each optimization step, two neighbor cores are merged. An optimization performed over merged “supercore”. After optimization in the next step we apply truncated SVD or other low-rank matrix factorizations (LRA) to separate the optimized supercore. For example, for nonnegative TT SVD steps can be replaced by a non-negative matrix factorization (NMF) algorithm. Note that each optimization sub-problem is more expensive than the standard ALS and complexity increases but convergence speed may increase dramatically (see also [18], [60]).

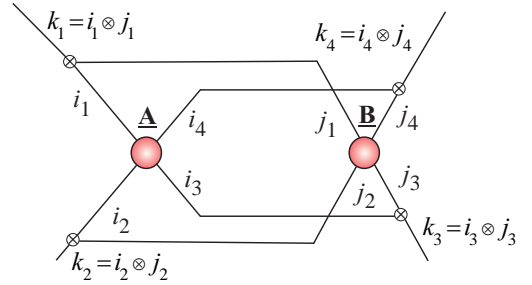


Figure 34: Kronecker product of two 4th-order tensors yields a tensor $\mathbf{C} = \mathbf{A} \otimes \mathbf{B} \in \mathbb{R}^{I_1 J_1 \times \dots \times I_4 J_4}$, with entries $c_{k_1, k_2, \dots, k_4} = a_{i_1, \dots, i_4} b_{j_1, \dots, j_4}$, where $k_n = i_n \otimes j_n = j_n + (i_n - 1)J_n$ ($n = 1, 2, 3, 4$).

of an N th-order $(I \times I \times \dots \times I)$ tensor, I^N , grows exponentially with the tensor order N . Tensors can easily become really big for very high order tensors since the size is exponentially growing with the number of dimensions (ways, or modes). For example, for the Tucker decomposition the number of entries of an original data tensor but also a core tensor scales exponentially in the tensor order, for instance, the number of entries of an N th-order $(R \times R \times \dots \times R)$ core tensor is R^N .

If all computations are performed on a CP tensor

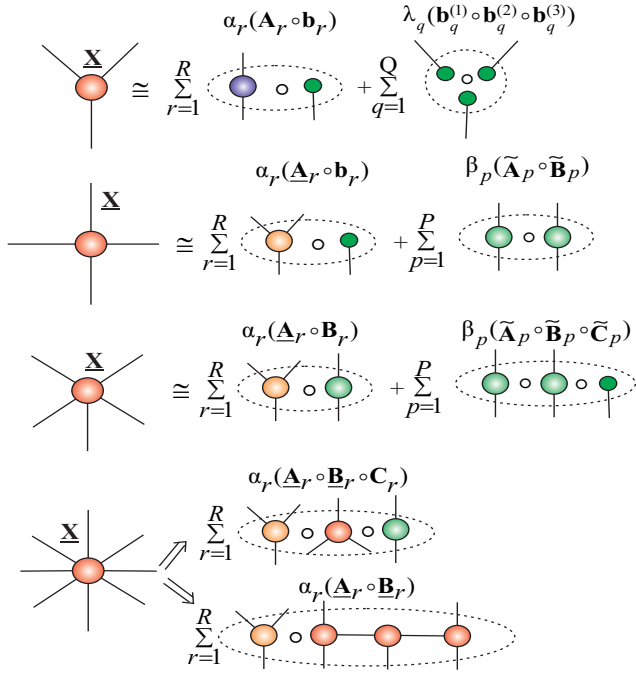


Figure 35: Illustration of Hierarchical Outer Product Tensor Approximation (HOPTA) for higher-order data tensors with different orders. Each component tensor: $\underline{\mathbf{A}}_r$, $\underline{\mathbf{B}}_r$ and/or $\underline{\mathbf{C}}_r$, can be further decomposed using suitable tensor network model. The model can be considered as extension or generalization of the Block Term Decomposition (BTD) model to higher order tensors.

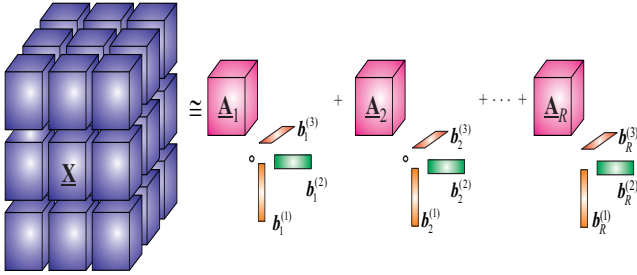


Figure 36: Illustration of decomposition of 6th-order tensor using the BTD of rank- $(L_r, L_r, 1)$ as: $\underline{\mathbf{X}} = \sum_{r=1}^R \underline{\mathbf{A}}_r \circ (\mathbf{b}_r^{(1)} \circ \mathbf{b}_r^{(2)} \circ \mathbf{b}_r^{(3)})$ [30], which can be considered as a special case of the HOPTA.

format and not on the raw data tensor itself, then instead of the original I^N raw data entries, the number of parameters in a CP representation reduces to NRI , which scales linearly in N and I (see Table IV). This effectively bypasses the curse of dimensionality, however the CP approximation may involve numerical problems, since existing algorithms are not stable for high-order tensors.

B. Quantized Tensor Networks

The curse of dimensionality can be overcome through quantized tensor networks, which represents a tensor of possibly very high-order as a set of sparsely interconnected low-order and very low dimensions (typically,

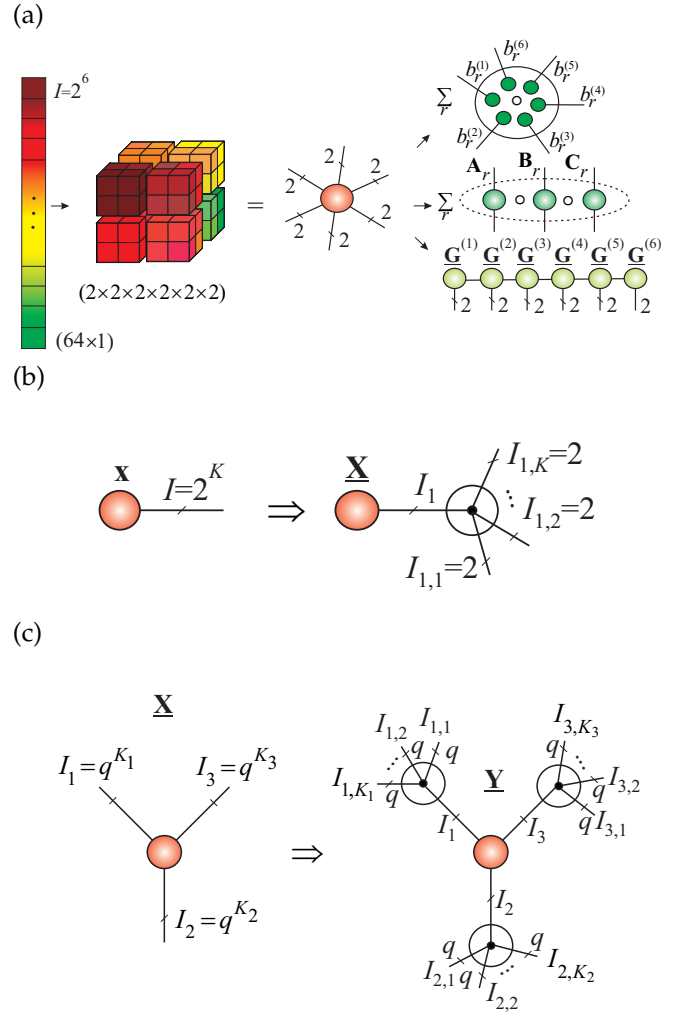


Figure 37: (a) Illustration of the concept of tensorization of a (large-scale) vector ($I = 2^K$) or matrix ($2^L \times 2^L$) into a higher-order tensor. In order to achieve super-compression through a suitable quantized tensor decomposition (e.g., decomposition into rank-1 tensors $\underline{\mathbf{X}} \cong \sum_{r=1}^R \mathbf{b}_r^{(1)} \circ \mathbf{b}_r^{(2)} \circ \dots \circ \mathbf{b}_r^{(6)}$ or rank- q terms using Hierarchical Outer Product Tensor Approximation (HOPTA) as: $\underline{\mathbf{X}} \cong \sum_{r=1}^R \underline{\mathbf{A}}_r \circ \underline{\mathbf{B}}_r \circ \underline{\mathbf{C}}_r$ or Quantized Tensor Train (QTT). (b) Symbolic representation of tensorization of the vector $\mathbf{x} \in \mathbb{R}^I$ into (K) th-order quantized tensor $\underline{\mathbf{X}} \in \mathbb{R}^{2 \times 2 \times \dots \times 2}$. (c) Tensorization of a 3rd-order tensor $\underline{\mathbf{X}} \in \mathbb{R}^{I_1 \times I_2 \times I_3}$ into $(K_1 + K_2 + K_3)$ th-order tensor $\underline{\mathbf{Y}} \in \mathbb{R}^{I_{1,1} \times \dots \times I_{1,K_1} \times I_{2,1} \times \dots \times I_{2,K_2} \times I_{3,1} \times \dots \times I_{3,K_3}}$ with $I_{n,k_n} = q$.

3rd-order) cores [52], [77]. The concept of quantized tensor networks was first proposed by Khoromskij [78] and Oseledets [77]. The low-dimensional cores are interconnected via tensor contractions to provide an efficient, highly compressed low-rank representation of a data tensor. At the same time, existing algorithms for tensor networks, especially TT/HT ensure good numerical properties (in contrast to CPD algorithms), making it possible to control an error and achieve any desired accuracy of approximation [52].

The procedure of creating a data tensor from lower-order original data is referred to as tensorization. In other

words, lower-order data tensors can be also reshaped (reformatted) into high-order tensors. The purpose of a such tensorization or reshaping is to achieve super compression [78]. In general, very large-scale vectors or matrices can be easily tensorized to higher-order tensors, then efficiently compressed by applying a suitable TT decomposition; this is the underlying principle for big data analysis [77], [78]. For example, the quantization and tensorization of a huge vector $x \in \mathbb{R}^I$, $I = 2^K$ can be achieved through reshaping to give an $(2 \times 2 \times \dots \times 2)$ tensor $\underline{\mathbf{X}}$ of order K , as illustrated in Figure 37 (a). Such a quantized tensor $\underline{\mathbf{X}}$ often admits low-rank approximations, so that a good compression of a huge vector x can be achieved by enforcing a maximum possible low-rank structure on the tensor $\underline{\mathbf{X}}$, thus admitting compact representation via a tensor network (see Figure 37 (a) and (b)).

Even more generally, an N th-order tensor $\underline{\mathbf{X}} \in \mathbb{R}^{I_1 \times \dots \times I_N}$, with $I_n = q^{K_n}$, can be quantized in all modes simultaneously to yield a $(q \times q \times \dots \times q)$ quantized tensor $\underline{\mathbf{Y}}$ of higher-order, with small q , (see Fig. 37 (c) and Fig. 38).

In example shown in Fig. 38 the Tensor Train of huge 3rd-order tensor is represented by the strong Kronecker products of block tensor with relatively small 3rd-order blocks.

In general, the strong Kronecker product of two block

$$\text{tensors (cores): } \underline{\mathbf{G}}^{(n)} = \begin{bmatrix} \underline{\mathbf{G}}_{1,1}^{(n)} & \dots & \underline{\mathbf{G}}_{1,R_n}^{(n)} \\ \vdots & \ddots & \vdots \\ \underline{\mathbf{G}}_{R_{n-1},1}^{(n)} & \dots & \underline{\mathbf{G}}_{R_{n-1},R_n}^{(n)} \end{bmatrix} \in \mathbb{R}^{R_{n-1} I_{3n-2} \times R_n I_{3n-1} \times I_{3n}} \text{ and } \underline{\mathbf{G}}^{(n+1)} = \begin{bmatrix} \underline{\mathbf{G}}_{1,1}^{(n+1)} & \dots & \underline{\mathbf{G}}_{1,R_{n+1}}^{(n+1)} \\ \vdots & \ddots & \vdots \\ \underline{\mathbf{G}}_{R_n,1}^{(n+1)} & \dots & \underline{\mathbf{G}}_{R_n,R_{n+1}}^{(n+1)} \end{bmatrix} \in \mathbb{R}^{R_n I_{3n+1} \times R_{n+1} I_{3n+2} \times I_{3n+3}}$$

is defined as a block tensor

$$\underline{\mathbf{C}} = \underline{\mathbf{G}}^{(n)} \mid \otimes \mid \underline{\mathbf{G}}^{(n+1)} = \sum_{r_n=1}^{R_n} \underline{\mathbf{G}}_{r_{n-1},r_n}^{(n)} \otimes \underline{\mathbf{G}}_{r_n,r_{n+1}}^{(n+1)}, \quad (36)$$

where $\underline{\mathbf{G}}_{r_{n-1},r_n}^{(n)} \in \mathbb{R}^{I_{3n-2} \times I_{3n-1} \times I_{3n}}$ and $\underline{\mathbf{G}}_{r_n,r_{n+1}}^{(n+1)} \in \mathbb{R}^{I_{3n+1} \times I_{3n+2} \times I_{3n+3}}$ are block tensors of $\underline{\mathbf{G}}^{(n)}$ and $\underline{\mathbf{G}}^{(n+1)}$, respectively.

In practice, a fine ($q = 2, 3, 4$) quantization is desirable to create as many virtual modes as possible, thus allowing us to implement an efficient low-rank tensor approximations. For example, the binary encoding ($q = 2$) reshapes an N th-order tensor with $(2^{K_1} \times 2^{K_2} \times \dots \times 2^{K_N})$ elements into a tensor of order $(K_1 + K_2 + \dots + K_N)$, with the same number of elements. In other words, the idea of the quantized tensor is quantization of the each n -th physical mode (dimension) by replacing it with K_n virtual modes, provided that the corresponding mode size I_n are factorized as $I_n = I_{n,1} I_{n,2} \dots I_{n,K_n}$. This corresponds to reshaping the n -th mode of size I_n into K_n modes of sizes $I_{n,1}, I_{n,2}, \dots, I_{n,K_n}$.

TABLE IV: Storage complexities of tensor decomposition models for an N th-order tensor $\underline{\mathbf{X}} \in \mathbb{R}^{I_1 \times I_2 \times \dots \times I_N}$, whose original storage complexity is $\mathcal{O}(I^N)$, where $I = \max\{I_1, I_2, \dots, I_N\}$, while R is an upper bound on the ranks of tensor decompositions considered, that is $R = \max\{R_1, R_2, \dots, R_{N-1}\}$ or $R = \max\{R_1, R_2, \dots, R_N\}$.

1. CPD	$\mathcal{O}(NIR)$
2. Tucker	$\mathcal{O}(NIR + R^N)$
3. TT/MPS	$\mathcal{O}(NIR^2)$
4. TT/MPO	$\mathcal{O}(NI^2R^2)$
5. Quantized TT/MPS (QTT)	$\mathcal{O}(NR^2 \log_q(I))$
6. QTT+Tucker	$\mathcal{O}(NR^2 \log_q(I) + NR^3)$
7. Hierarchical Tucker (HT)	$\mathcal{O}(NIR + NR^3)$

The TT decomposition applied to quantized tensors is referred to as the QTT; it was first introduced as a compression scheme for large-scale matrices [77], and also independently for more general settings [62], [78], [79], [81], [82]. The attractive property of QTT is that not only its rank is typically small (below 10) but it is almost independent or at least uniformly bounded by data size (even for $I = 2^{50}$), providing a logarithmic (sub-linear) reduction of storage requirements: $\mathcal{O}(I^N) \rightarrow \mathcal{O}(N \log_q(I))$ – so-called super-compression [78].

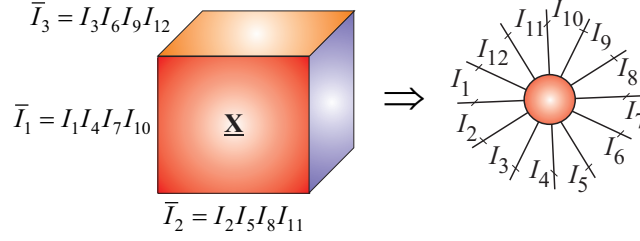
Compared to the TT decomposition (without quantization), the QTT format often represents more deep structure in the data by splitting all the virtual dimensions introduced.

Showing that the TT/QTT ranks are moderate or even low, e.g., constant or growing linearly with respect to N and constant or growing logarithmically with respect to I , is an important issue in the context of big data analytic and has been addressed so far mostly experimentally (see [20], [52], [78] and references therein). The high compressibility of the QTT-approximation is a consequence of the noticeable separability properties in the quantized tensor for suitably structured data. On the other hand, the high efficiency of multilinear algebra in the TT/QTT algorithms based on the well-posedness of the low-rank approximation problems and the fact that such problems are solved quasi-optimally with the use of HOSVD, SVD/PCA and cross-approximation techniques.

In general, tensor networks can be considered as distributed high-dimensional tensors built up from many tensors of low dimension through a few specific tensor contractions. Indeed, tensor networks (TT, MPS, MPO, PEPS and HT) have already been successfully used to solve intractable problems in computational quantum chemistry and in scientific computing [55], [81], [83].

However, in some cases, the ranks of the TT or QTT formats grow quite significantly with the linearly increasing of approximation accuracy. To overcome this

(a)



(b)

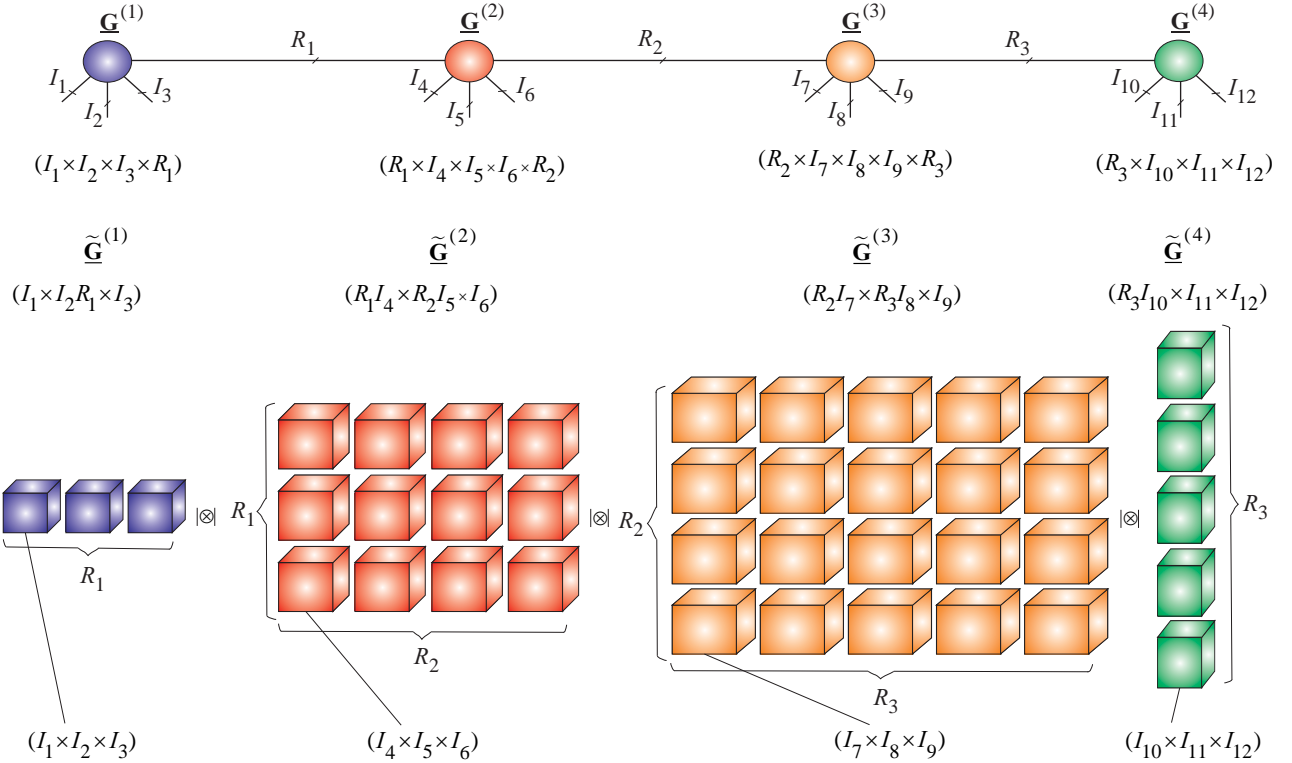


Figure 38: (a) Example of tensorization and decomposition of a large-scale 3rd-order tensor $\mathbf{X} \in \mathbb{R}^{\bar{I}_1 \times \bar{I}_2 \times \bar{I}_3}$ into 12th-order tensor assuming that $\bar{I}_1 = I_1 I_4 I_7 I_{10}$, $\bar{I}_2 = I_2 I_5 I_8 I_{11}$ and $\bar{I}_3 = I_3 I_6 I_9 I_{12}$, (b) representation of the tensor via generalized Tensor Train referred to as the Tensor Product States (TPS). The data tensor can be expressed by strong Kronecker product of block tensors as $\mathbf{X} \cong \tilde{\mathbf{G}}^{(1)} | \otimes | \tilde{\mathbf{G}}^{(2)} | \otimes | \tilde{\mathbf{G}}^{(3)} | \otimes | \tilde{\mathbf{G}}^{(4)} \in \mathbb{R}^{\bar{I}_1 \times \bar{I}_2 \times \bar{I}_3}$, where each block of the core $\tilde{\mathbf{G}}^{(n)} \in \mathbb{R}^{R_{n-1} I_{3n-2} \times R_n I_{3n-1} \times I_{3n}}$ is a 3rd-order tensor of dimensions $(I_{3n-2} \times I_{3n-1} \times I_{3n})$, with $R_0 = R_4 = 1$ for $n = 1, 2, 3, 4$.

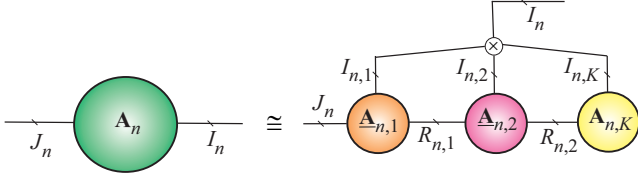
problem, new tensor models of tensor approximation were developed, e.g., Dolgov and Khoromskij, proposed the QTT-Tucker format [62] (see Fig. 39), which exploits the TT approximation not only for the Tucker core tensor, but also QTT for the factor matrices. This model allows distributed computing with bounded ranks and avoid the curse of dimensionality, since the Tucker core tensor is represented in the TT format.

In other words, for very large scale tensors we can make even more advanced approach in which factor matrices are tensorized to higher-order tensors and then represented by TTs as illustrated in Fig. 39 (a).

Modern methods of tensor approximations combine

many TNs and TDs formats including the CPD, BTd, Tucker, TT, HT decompositions and HOPTA (see Fig. 35) low-parametric tensor format. Use of the synthetic tensorization and represent so obtained very high-order tensor in tensor network formats (TT/QTT, HT, QTT-Tucker formats) allows to treat efficiently a very large scale well structured data which admit low rank tensor network approximations. Tensor networks have already found promising applications in very large-scale problems in scientific computing, such as eigenanalysis, super-fast Fourier transforms, and solving huge systems of large linear equations (see [20], [58], [62], [79], [80])

(a)



(b)

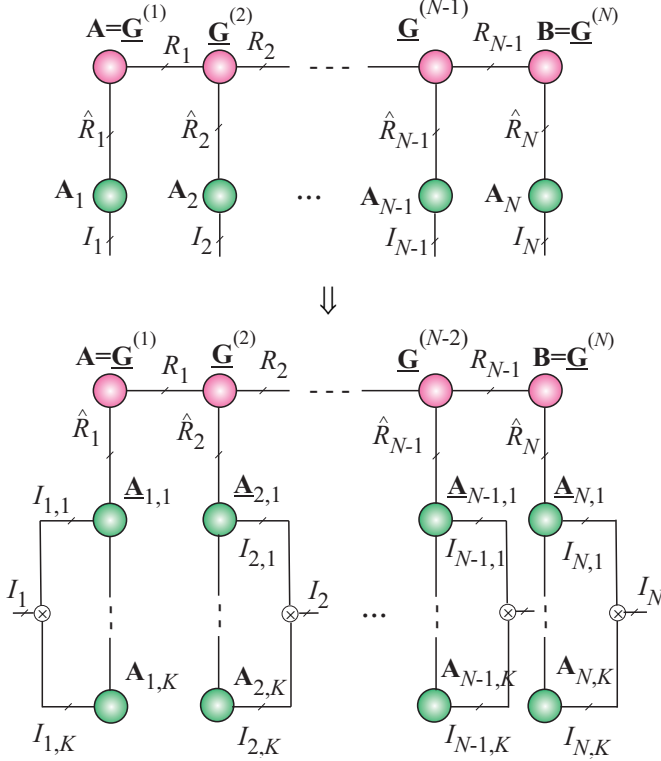


Figure 39: (a) Distributed representation of a large matrix $\mathbf{A}_n \in \mathbb{R}^{I_n \times R_n}$ with large dimension of I_n via QTT by tensorization of the matrix to high-order quantized tensor and next by performing QTT decomposition. (b) Distributed representation of a large-scale N th-order Tucker model via quantized TT model in which core tensor and all large-scale factor matrices \mathbf{A}_n ($n = 1, 2, \dots, N$) are represented by tensor trains. Such representation allows to convert large-scale optimization problems to many interconnected low-scale optimization subproblems, which can be solved iteratively and sequentially.

and references therein).

In summary, the main concept or approach for big data is: a suitable tensorization and quantization of the data and then approximate representation them by a distributed tensor network and performing all tensors/matrix/vectors manipulations in tensor network formats. The employment of the virtual tensorization (QTT, QCPD, Tucker-QTT, formats) allows to treat efficiently even the cases of very large data and it can be a promising tool for big data analytic [84], [85].

XII. Conclusions and Future Directions

Tensor networks, which can be considered as generalization and extension of TDs, are promising tools for analysis of big data due to their extremely good compression abilities and distributed and parallel processing. Moreover, TDs have already found applications in generalized multivariate regression, multi-way blind source separation, sparse representation and coding, feature extraction, classification, clustering and data assimilation. An important and unique advantage of tensor networks include potential abilities of tera- or even petabyte scaling and distributed fault-tolerant computations.

Overall, the benefits of multiway (tensor) analysis methods can be summarized as follows:

- “Super” compression of huge multidimensional data via TNs of high-order tensors by extracting factor matrices and/or core tensors of low-rank and low-order and perform all mathematical manipulations in tensor formats (especially, TT and HT formats).
- A compact and very flexible approximate representation of structurally rich data by accounting for their spatio-temporal and spectral dependencies.
- Opportunity to establish statistical links between cores, factors, components or hidden latent variables for blocks of data.
- Possibility to operate with noisy, incomplete, missing data by using powerful low-rank tensor/matrix approximation techniques.
- A framework to incorporate various diversities or constraints in different modes and thus naturally extend the standard (2-way) CA methods to large-scale multidimensional data.

Many challenging problems related to low-rank tensor approximations remain that need to be addressed.

- A whole new area emerges when several TNs which operate on different datasets are coupled or linked.
- As the complexity of big data increases, this requires more efficient iterative algorithms for their computing, extending beyond the ALS, MALS/DMRG, SVD/QR and CUR/Cross-Approximation class of algorithms.
- Theoretic and methodological approaches are needed to determine what kind of constraints should be imposed on cores in each mode to extract desired hidden (latent) variables with meaningful physical interpretation.
- We need a method to reliably estimate the ranks of TNs, especially for data corrupted by noise and outliers.
- Investigating the uniqueness of various TN models under different constraints need to be investigated.
- Special techniques are needed for distributed computing and to save and process huge ultra large-scale tensors.
- Better visualization tools need to be developed to address large-scale tensor network representations.

In summary, TNs and TDs is a fascinating and perspective area of research with many potential applications in multi-modal analysis of massive big data sets.

Acknowledgments: The author wish to express his appreciation and gratitude to his colleagues and members of the laboratory ABSP, especially: Drs. Namgill LEE, Qibin ZHAO, Cesar CAIAFA, Anh Huy PHAN, Qiang WU, Guoxu ZHOU and Chao LI for hearing his talk, reading the manuscript and giving him comments and suggestions.

REFERENCES

- [1] A. Cichocki, R. Zdunek, A.-H. Phan, and S. Amari, *Nonnegative Matrix and Tensor Factorizations: Applications to Exploratory Multiway Data Analysis and Blind Source Separation*. Chichester: Wiley, 2009.
- [2] A. Cichocki, D. Mandic, C. Caiafa, A.-H. Phan, G. Zhou, Q. Zhao, and L. D. Lathauwer, "Multiway Component Analysis: Tensor Decompositions for Signal Processing Applications," *Signal Processing Magazine (in print)*, 2014.
- [3] A. Cichocki, "Tensors decompositions: New concepts for brain data analysis?" *Journal of Control, Measurement, and System Integration (SICE)*, vol. 47, no. 7, pp. 507–517, 2011.
- [4] T. Kolda and B. Bader, "Tensor decompositions and applications," *SIAM Review*, vol. 51, no. 3, pp. 455–500, September 2009.
- [5] P. Kroonenberg, *Applied Multiway Data Analysis*. New York: John Wiley & Sons Ltd, 2008.
- [6] A. Smilde, R. Bro, and P. Geladi, *Multi-way Analysis: Applications in the Chemical Sciences*. New York: John Wiley & Sons Ltd, 2004.
- [7] W. Hackbusch, *Tensor Spaces and Numerical Tensor Calculus*, ser. Springer series in computational mathematics. Heidelberg: Springer, 2012, vol. 42.
- [8] S. K. Suter, M. Makhynia, and R. Pajarola, "Tamresh - tensor approximation multiresolution hierarchy for interactive volume visualization," *Comput. Graph. Forum*, vol. 32, no. 3, pp. 151–160, 2013.
- [9] H. Wang, Q. Wu, L. Shi, Y. Yu, and N. Ahuja, "Out-of-core tensor approximation of multi-dimensional matrices of visual data," *ACM Trans. Graph.*, vol. 24, no. 3, pp. 527–535, 2005.
- [10] A.-H. Phan and A. Cichocki, "PARAFAC algorithms for large-scale problems," *Neurocomputing*, vol. 74, no. 11, pp. 1970–1984, 2011.
- [11] P. Comon, X. Luciani, and A. L. F. de Almeida, "Tensor decompositions, Alternating Least Squares and other Tales," *Jour. Chemometrics*, vol. 23, pp. 393–405, 2009.
- [12] H. Lu, K. Plataniotis, and A. Venetsanopoulos, "A survey of multilinear subspace learning for tensor data," *Pattern Recognition*, vol. 44, no. 7, pp. 1540–1551, 2011.
- [13] M. Mørup, "Applications of tensor (multiway array) factorizations and decompositions in data mining," *Wiley Interdisc. Rev.: Data Mining and Knowledge Discovery*, vol. 1, no. 1, pp. 24–40, 2011.
- [14] P. Comon and C. Jutten, Eds., *Handbook of Blind Source Separation: Independent Component Analysis and Applications*. Academic Press, 2010.
- [15] F. De la Torre, "A least-squares framework for component analysis," *IEEE Transactions Pattern Analysis and Machine Intelligence (PAMI)*, vol. 34, no. 6, pp. 1041–1055, 2012.
- [16] J. Ballani, L. Grasedyck, and M. Kluge, "Black box approximation of tensors in hierarchical Tucker format," *Linear Algebra and its Applications*, vol. 438, no. 2, pp. 639–657, 2013.
- [17] I. Oseledets and E. Tyrtshnikov, "Breaking the curse of dimensionality, or how to use SVD in many dimensions," *SIAM J. Scientific Computing*, vol. 31, no. 5, pp. 3744–3759, 2009.
- [18] D. Kressner and C. Tobler, "htucker—A MATLAB toolbox for tensors in hierarchical Tucker format," *MATHICSE, EPF Lausanne*, 2012. [Online]. Available: <http://anchp.epfl.ch/htucker>
- [19] L. Grasedyck and W. Hackbusch, "An introduction to hierarchical (h-) rank and tt-rank of tensors with examples," *Comput. Meth. in Appl. Math.*, vol. 11, no. 3, pp. 291–304, 2011.
- [20] L. Grasedyck, D. Kessner, and C. Tobler, "A literature survey of low-rank tensor approximation techniques," *CGAMM-Mitteilungen*, vol. 36, pp. 53–78, 2013.
- [21] A. Cichocki, "Generalized Component Analysis and Blind Source Separation Methods for Analyzing Multichannel Brain Signals," in *Statistical and Process Models for Cognitive Neuroscience and Aging*. Lawrence Erlbaum Associates, 2007, pp. 201–272.
- [22] V. Calhoun, J. Liu, and T. Adali, "A review of group ICA for fMRI data and ICA for joint inference of imaging, genetic, and ERP data," *Neuroimage*, vol. 45, pp. 163–172, 2009.
- [23] G. Zhou, A. Cichocki, and S. Xie, "Fast Nonnegative Matrix/Tensor Factorization Based on Low-Rank Approximation," *IEEE Transactions on Signal Processing*, vol. 60, no. 6, pp. 2928–2940, June 2012.
- [24] F. L. Hitchcock, "Multiple invariants and generalized rank of a p-way matrix or tensor," *Journal of Mathematics and Physics*, vol. 7, pp. 39–79, 1927.
- [25] R. A. Harshman, "Foundations of the PARAFAC procedure: Models and conditions for an explanatory multimodal factor analysis," *UCLA Working Papers in Phonetics*, vol. 16, pp. 1–84, 1970.
- [26] J. Carroll and J.-J. Chang, "Analysis of individual differences in multidimensional scaling via an n-way generalization of 'Eckart-Young' decomposition," *Psychometrika*, vol. 35, no. 3, pp. 283–319, September 1970.
- [27] S. Vorobyov, Y. Rong, N. Sidiropoulos, and A. Gershman, "Robust iterative fitting of multilinear models," *IEEE Transactions Signal Processing*, vol. 53, no. 8, pp. 2678–2689, 2005.
- [28] A. Cichocki and H. A. Phan, "Fast local algorithms for large scale nonnegative matrix and tensor factorizations," *IEICE Transactions on Fundamentals of Electronics, Communications and Computer Sciences*, vol. E92-A, no. 3, pp. 708–721, 2009.
- [29] A.-H. Phan, P. Tichavsky, and A. Cichocki, "Low complexity Damped Gauss-Newton algorithms for CANDECOMP/PARAFAC," *SIAM Journal on Matrix Analysis and Applications (SIMAX)*, vol. 34, no. 1, pp. 126–147, 2013.
- [30] L. Sorber, M. Van Barel, and L. De Lathauwer, "Optimization-based algorithms for tensor decompositions: Canonical Polyadic Decomposition, decomposition in rank- $(L_r, L_r, 1)$ terms and a new generalization," *SIAM J. Optimization*, vol. 23, no. 2, 2013.
- [31] N. Sidiropoulos and R. Bro, "On the uniqueness of multilinear decomposition of N-way arrays," *J. Chemometrics*, vol. 14, no. 3, pp. 229–239, 2000.
- [32] M. Sørensen, L. De Lathauwer, P. Comon, S. Icart, and L. Deneire, "Canonical Polyadic Decomposition with orthogonality constraints," *SIAM J. Matrix Anal. Appl.*, vol. 33, no. 4, pp. 1190–1213, 2012.
- [33] G. Zhou and A. Cichocki, "Canonical Polyadic Decomposition based on a single mode blind source separation," *IEEE Signal Processing Letters*, vol. 19, no. 8, pp. 523–526, 2012.
- [34] L. R. Tucker, "Some mathematical notes on three-mode factor analysis," *Psychometrika*, vol. 31, no. 3, pp. 279–311, September 1966.
- [35] G. Zhou and A. Cichocki, "Fast and unique Tucker decompositions via multiway blind source separation," *Bulletin of Polish Academy of Science*, vol. 60, no. 3, pp. 389–407, 2012.
- [36] L. De Lathauwer, B. De Moor, and J. Vandewalle, "A multilinear singular value decomposition," *SIAM Journal of Matrix Analysis and Applications*, vol. 24, pp. 1253–1278, 2000.
- [37] —, "On the best rank-1 and rank- (R_1, R_2, \dots, R_N) approximation of higher-order tensors," *SIAM J. Matrix Anal. Appl.*, vol. 21, pp. 1324–1342, March 2000.
- [38] Y. Lui, J. Beveridge, and M. Kirby, "Action classification on product manifolds," in *Computer Vision and Pattern Recognition (CVPR), 2010 IEEE Conference on*. IEEE, 2010, pp. 833–839.
- [39] M. Vasilescu and D. Terzopoulos, "Multilinear analysis of image ensembles: Tensorfaces," in *Proc. European Conf. on Computer Vision (ECCV)*, vol. 2350, Copenhagen, Denmark, May 2002, pp. 447–460.
- [40] C. Caiafa and A. Cichocki, "Generalizing the column-row matrix decomposition to multi-way arrays," *Linear Algebra and its Applications*, vol. 433, no. 3, pp. 557–573, 2010.
- [41] E. Acar, D. Dunlavy, T. Kolda, and M. Mørup, "Scalable tensor factorizations for incomplete data," *Chemometrics and Intelligent Laboratory Systems*, vol. 106 (1), pp. 41–56, 2011. [Online]. Available: <http://www2.imm.dtu.dk/pubdb/p.php?5923>

- [42] S. Gandy, B. Recht, and I. Yamada, "Tensor completion and low-rank tensor recovery via convex optimization," *Inverse Problems*, vol. 27, no. 2, 2011.
- [43] M. W. Mahoney, M. Maggioni, and P. Drineas, "Tensor-CUR decompositions for tensor-based data," *SIAM Journal on Matrix Analysis and Applications*, vol. 30, no. 3, pp. 957–987, 2008.
- [44] S. A. Goreinov, N. L. Zamarashkin, and E. E. Tyrtshnikov, "Pseudo-skeleton approximations by matrices of maximum volume," *Mathematical Notes*, vol. 62, no. 4, pp. 515–519, 1997.
- [45] S. A. Goreinov, E. E. Tyrtshnikov, and N. L. Zamarashkin, "A theory of pseudo-skeleton approximations," *Linear Algebra Appl.*, vol. 261, pp. 1–21, 1997.
- [46] I. Oseledets and E. Tyrtshnikov, "TT-cross approximation for multidimensional arrays," *Linear Algebra and its Applications*, vol. 432, no. 1, pp. 70–88, 2010.
- [47] M. Mahoney and P. Drineas, "CUR matrix decompositions for improved data analysis," *Proc. National Academy of Science*, vol. 106, pp. 697–702, 2009.
- [48] A. Phan and A. Cichocki, "Tensor decompositions for feature extraction and classification of high dimensional datasets," *Nonlinear Theory and Its Applications, IEICE*, vol. 1, no. 1, pp. 37–68, 2010.
- [49] G. Zhou, A. Cichocki, S. Xie, and D. Mandic, "Beyond Canonical Correlation Analysis: Common and individual features analysis," *IEEE Transactions on PAMI*, 2013. [Online]. Available: <http://arxiv.org/abs/1212.3913>, 2012
- [50] Q. Zhao, C. Caiafa, D. Mandic, Z. Chao, Y. Nagasaka, N. Fujii, L. Zhang, and A. Cichocki, "Higher-order partial least squares (HOPLS): A generalized multi-linear regression method," *IEEE Trans on Pattern Analysis and machine Intelligence (PAMI)*, vol. 35, no. 7, pp. 1660–1673, 2013.
- [51] I. V. Oseledets, "Tensor-train decomposition," *SIAM J. Scientific Computing*, vol. 33, no. 5, pp. 2295–2317, 2011.
- [52] B. Khoromskij, "Tensors-structured numerical methods in scientific computing: Survey on recent advances," *Chemometrics and Intelligent Laboratory Systems*, vol. 110, no. 1, pp. 1–19, 2011.
- [53] D. Perez-Garcia, F. Verstraete, M. M. Wolf, and J. I. Cirac, "Matrix product state representations," *Quantum Info. Comput.*, vol. 7, no. 5, pp. 401–430, Jul. 2007. [Online]. Available: <http://dl.acm.org/citation.cfm?id=2011832.2011833>
- [54] F. Verstraete, V. Murg, and J. Cirac, "Matrix product states, projected entangled pair states, and variational renormalization group methods for quantum spin systems," *Advances in Physics*, vol. 57, no. 2, pp. 143–224, 2008.
- [55] R. Orus, "A Practical Introduction to Tensor Networks: Matrix Product States and Projected Entangled Pair States," *The Journal of Chemical Physics*, 2013.
- [56] U. Schollwöck, "Matrix product state algorithms: Dmrg, tebd and relatives," in *Strongly Correlated Systems*. Springer, 2013, pp. 67–98.
- [57] —, "The density-matrix renormalization group in the age of matrix product states," *Annals of Physics*, vol. 326, no. 1, pp. 96–192, 2011.
- [58] T. Huckle, K. Waldherr, and T. Schulte-Herbrigg, "Computations in quantum tensor networks," *Linear Algebra and its Applications*, vol. 438, no. 2, pp. 750 – 781, 2013.
- [59] G. Vidal, "Efficient classical simulation of slightly entangled quantum computations," *Physical Review Letters*, vol. 91, no. 14, p. 147902, 2003.
- [60] S. Holtz, T. Rohwedder, and R. Schneider, "The alternating linear scheme for tensor optimization in the tensor train format," *SIAM J. Scientific Computing*, vol. 34, no. 2, pp. 683–713, 2012.
- [61] T. Rohwedder and A. Uschmajew, "On local convergence of alternating schemes for optimization of convex problems in the tensor train format," *SIAM Journal on Numerical Analysis*, vol. 51, no. 2, pp. 1134–1162, 2013.
- [62] S. Dolgov and B. Khoromskij, "Two-level QTT-Tucker format for optimized tensor calculus," *SIAM J. Matrix Analysis Applications*, vol. 34, no. 2, pp. 593–623, 2013.
- [63] I. Oseledets, "TT-toolbox 2.2," 2012. [Online]. Available: <https://github.com/oseledets/TT-Toolbox>
- [64] L. Grasedyck, "Hierarchical Singular Value Decomposition of tensors," *SIAM J. Matrix Analysis Applications*, vol. 31, no. 4, pp. 2029–2054, 2010.
- [65] M. Espig, M. Schuster, A. Killaitis, N. Waldren, P. Wähnert, S. Handschuh, and H. Auer, "Tensor Calculus library," 2012. [Online]. Available: <http://gitorious.org/tensorcalculus>
- [66] G. Zhou and A. Cichocki, "TDALAB: Tensor Decomposition Laboratory," LABSP, Wako-shi, Japan, 2013. [Online]. Available: <http://bsp.brain.riken.jp/TDALAB/>
- [67] A.-H. Phan, P. Tichavský, and A. Cichocki, "Tensorbox: a matlab package for tensor decomposition," LABSP, RIKEN, Japan, 2012. [Online]. Available: <http://www.bsp.brain.riken.jp/~phan/tensorbox.php>
- [68] L. Sorber, M. Van Barel, and L. De Lathauwer, "Tensorlab v1.0," Feb. 2013. [Online]. Available: <http://esat.kuleuven.be/sista/tensorlab/>
- [69] J. Salmi, A. Richter, and V. Koivunen, "Sequential unfolding SVD for tensors with applications in array signal processing," *IEEE Transactions on Signal Processing*, vol. 57, pp. 4719–4733, 2009.
- [70] L. De Lathauwer, "Decompositions of a higher-order tensor in block terms – Part I and II," *SIAM Journal on Matrix Analysis and Applications (SIMAX)*, vol. 30, no. 3, pp. 1022–1066, 2008, special Issue on Tensor Decompositions and Applications. [Online]. Available: <http://publi-etis.ensea.fr/2008/De08e>
- [71] A. H. Phan, A. Cichocki, P. Tichavský, D. Mandic, and K. Matsuoaka, "On Revealing Replicating Structures in Multiway Data: A Novel Tensor Decomposition Approach," in *Proc. 10th International Conf. LVA/ICA, Tel Aviv, March 12-15,, 2012*, pp. 297–305.
- [72] S. Ragnarsson, "Structured tensor computations: Blocking, symmetries and Kronecker factorizations," PhD Dissertation, Cornell University, Department of Applied Mathematics, 2012.
- [73] A.-H. Phan, A. Cichocki, P. Tichavský, R. Zdunek, and S. Lehky, "From basis components to complex structural patterns," in *Proc. of the IEEE International Conference on Acoustics, Speech, and Signal Processing (ICASSP 2013)*, Vancouver, Canada, 2013.
- [74] L. De Lathauwer, "Blind separation of exponential polynomials and the decomposition of a tensor in rank- $(L_r, L_r, 1)$ terms," *SIAM J. Matrix Analysis Applications*, vol. 32, no. 4, pp. 1451–1474, 2011.
- [75] L. De Lathauwer and D. Nion, "Decompositions of a higher-order tensor in block terms – Part III: Alternating least squares algorithms," *SIAM Journal on Matrix Analysis and Applications (SIMAX)*, vol. 30, no. 3, pp. 1067–1083, 2008.
- [76] I. V. Oseledets and E. E. Tyrtshnikov, "Algebraic wavelet transform via quantics tensor train decomposition," *SIAM J. Scientific Computing*, vol. 33, no. 3, pp. 1315–1328, 2011.
- [77] I. Oseledets, "Approximation of $2^d \times 2^d$ matrices using tensor decomposition," *SIAM J. Matrix Analysis Applications*, vol. 31, no. 4, pp. 2130–2145, 2010.
- [78] B. Khoromskij, " $O(d \log N)$ -quantics approximation of N -d tensors in high-dimensional numerical modeling," *Constructive Approximation*, vol. 34, no. 2, pp. 257–280, 2011.
- [79] S. Dolgov, B. Khoromskij, I. Oseledets, and D. Savostyanov, "Computation of extreme eigenvalues in higher dimensions using block tensor train format," *Computer Physics Communications*, vol. 185, no. 4, pp. 12071216, 2014.
- [80] D. Kressner, M. Steinlechner, and A. Uschmajew, "Low-rank tensor methods with subspace correction for symmetric eigenvalue problems," (submitted), 2014.
- [81] V. Kazeev and B. Khoromskij, "Low-rank explicit QTT representation of the Laplace operator and its inverse," *SIAM J. Matrix Analysis Applications*, vol. 33, no. 3, pp. 742–758, 2012.
- [82] V. Kazeev, O. Reichmann, and C. Schwab, "Low-rank tensor structure of linear diffusion operators in the TT and QTT formats," *Linear Algebra and its Applications*, vol. 438, no. 11, pp. 4204–4221, 2013.
- [83] N. Nakatani and G. Chan, "Efficient tree tensor network states (TTNS) for quantum chemistry: Generalizations of the density matrix renormalization group algorithm," *The Journal of Chemical Physics*, 2013.
- [84] N. Lee and A. Cichocki, "An overview of low-rank tensor methods for high dimensional problems," RIKEN, Brain Science Institute, LABSP, Tech. Rep., 2013. [Online]. Available: <http://www.bsp.brain.riken.jp/>
- [85] Q. Wu and A. Cichocki, "Algorithms for tensor train networks," RIKEN, Brain Science Institute, LABSP, Tech. Rep., 2013. [Online]. Available: <http://www.bsp.brain.riken.jp/>